

# **An Investigation on the Impact Fatigue Characteristics of Compressor Valve Leaves**

by

**Abdullah Can Altunlu**

**A Thesis Submitted to the  
Graduate School of Engineering  
in Partial Fulfillment of the Requirements for  
the Degree of**

**Master of Science**

**in**

**Mechanical Engineering**

**Koc University**

**August 2009**

Koc University  
Graduate School of Sciences and Engineering

This is to certify that I have examined this copy of a master's thesis by

Abdullah Can Altunlu

and have found that it is complete and satisfactory in all respects,  
and that any and all revisions required by the final  
examining committee have been made.

Committee Members:

---

İsmail Lazođlu, Ph.D. (Advisor)

---

Murat Sözer, Ph.D.

---

Erdem Alaca, Ph.D.

---

Mustafa Bakkal, Ph.D.  
(Istanbul Technical University)

---

Emre Ođuz, Ph.D.  
(Arcelik A.S.)

Date: \_\_\_\_\_

*“Whoever has once seen a dissection of the human body will understand and remember the relative position of its parts with far greater certainty than if he had read the most exhaustive treatises on anatomy, but had never actually seen a dissection performed.”*

**Comenius, The Great Didactic, 1641**

## **Abstract**

A unique automated impact fatigue test system has been designed and produced, which enables to carry out impact fatigue tests of the compressor valve leaves under the desired impact velocities. The non-contact actuation test system serves investigations on the impact fatigue characteristics with the ability of crack detection and as the subsequent step of terminating the test system. The crack detection technique incorporates a microphone and a data acquisition system. The impact fatigue experiments were performed on hardened and tempered carbon flapper valve strip steel, martensitic stainless chromium steel alloyed with molybdenum and new stainless steel grade.

The impact fatigue life of compressor valve leaves was determined for various impact velocities. The influence of the working temperature on the impact fatigue life of carbon steel was investigated in the designed temperature control cabin. Cold-worked edges of the valve leaves were sharpened due to the blanking operation of the valve leaves. Therefore, a tumbling operation is performed in order to round the sharp edges, remove the small manufacturing defects and introduce compressive residual stresses. The edge radius of the specimens was characterized and tumbling duration was correlated with the impact fatigue life. In addition, asymmetrical impact behavior due to the variation in working condition of compressor and the designs of other components were examined. Microscopic and metallographic observations were performed on the specimens. It was observed that the impact fatigue failure originated at the edge of the valve leaves on the contact surface of valve leaf and valve plate. The crack propagation results were presented. The introduced test system and methodology guides the design optimization process of valve leaves in terms of compressor performance due to energy consumption and lifetime of the valve leaf.

## Özet

Kompresör valf yaprakların istenilen çarpma hızlarında darbe yorulması testlerinin yapılabilmesi için, özgün otomatik darbe yorulması test sistemi tasarlandı ve üretildi. Darbe yorulması karakteristiklerinin incelenmesini için tasarlanan temassız tahrikli otomatik test sistemi çatlak algılama ve sistemi otomatik olarak durdurabilmektedir. Çatlak algılama tekniği mikrofon ve veri toplama sistemi ile beraber çalışmaktadır. Darbe yorulması deneylerinde sertleştirilmiş ve temperlenmiş karbon valf yaprağı çeliği, molibden ile alaşımlanmış martensit paslanmaz krom çeliği ve yeni paslanmaz çeliği olarak üç farklı numune kullanılmıştır.

Kompresör valf yapraklarının darbe yorulması ömrü çeşitli çarpma hızları için elde edilmiştir. Tasarlanan sıcaklık kontrol kabiniinde, çalışma sıcaklığın karbon çeliği numunesinin darbe yorulması ömrüne olan etkisi incelenmiştir. Valf yapraklarının preslenme operasyonu sonucunda soğuk şekil vermeden dolayı yaprak kenarları keskin formdadır. Bu sebepten dolayı, keskin köşeleri yuvarlatmak, üretimden dolayı oluşan küçük kusurları ortadan kaldırmak ve basma artık gerilme oluşturmak için tamburlama operasyonu uygulanmaktadır. Test numunelerinin kenar radyüsü karakterize edilmiştir ve tamburlama süresi darbe yorulması ömrü ile ilişkilendirilmiştir. Buna ek olarak, kompresörün çalışma şartlarındaki değişiklikler ve diğer elemanların tasarımına bağlı olarak oluşan asimetrik çarpma davranışı incelenmiştir. Numuneler üzerinde mikroskopik ve metalografik gözlemler yapılmıştır. Darbe yorulması kusuru valf yapraklarının kenarında, valf yaprağı ve valf tablası temas yüzeyinde başladığı görülmektedir. Çatlak ilerleme sonuçları sunulmuştur. Tanıtılan test sistemi ve metodoloji, enerji tüketimi ve valf yapraklarının ömrünü göz önüne alınarak belirlenen kompresör performansı anlamında valf yapraklarının tasarım optimizasyonu sürecine yol gösterecektir.

## **Acknowledgements**

Foremost, I would like to express my gratitude to my advisor, Assoc. Prof. İsmail Lazođlu for the continuous support to my research. His patience, guidance and supervision with his extensive knowledge led me to provide the work.

I would like to thank Dr. Emre Ođuz from Thermodynamic Technologies Department in Arcelik A.S. R&D Center, Istanbul, Turkey and Serkan Kara from Product Development Department in Compressor Plant Arcelik A.S., Eskisehir, Turkey for their knowledge and experiences that enhance my insight through the research. I would like to thank Dr. Feriha Sertçelik Birol, Sibel Odabaş and Turgay Gönül from Materials Technologies Department in Arcelik A.S. R&D Center, Istanbul Turkey for their support along my research.

I would like to thank Assist. Prof. Erdem Alaca and Assist. Prof. Demircan Canadinc for their valuable guidance and Selim Ölçer for his support.

I would like to acknowledge the Ministry of Industry and Trade of Turkey and Arcelik A.S. (SANTEZ Project No.: 2.STZ.2006- 1) for its support on the project. I would like to thank my research group, MARC at Koc University for the times of sharing. And I would like to acknowledge Koc University (MSc.) and Istanbul Technical University (BSc.) where I was brought up.

Finally I would like to express my gratefulness, appreciation and passion to my family and the one who I called the life. The existence of their spirit provides me the perseverance, diligence and the power for dealing with intricacies and challenges and to enjoy the wind.

## Table of Contents

Abstract .....	v
Özet .....	vi
Acknowledgements.....	vii
List of Tables.....	xi
List of Figures.....	xii
Nomenclature.....	xvii
Chapter 1: Introduction .....	1
Chapter 2: Literature Review .....	5
Chapter 3: Materials and Methods.....	13
3.1. Introduction.....	13
3.2. Materials .....	14
3.3. Electromagnetic Experimental Setup:.....	15
3.4. Pneumatic Experimental Setup:.....	25
3.5. Crack Detection Method:.....	30
3.6. Experimental procedure .....	33
3.7. Temperature Control Cabin: .....	35
3.8. Multi - Station Experimental Setup: .....	38
3.9. Reciprocating Setup:.....	39
3.10. Specimen Preparation Procedure for Scanning Electron Microscope (SEM): .....	41
3.10.1. Ultrasonic Cleaning:.....	41

3.10.2. Mounting: .....	42
3.10.3. Grinding and Polishing:.....	43
3.10.4. Etching:.....	45
3.11. Valve Plate Prototype: .....	45
3.11.1. Computer Aided Design (CAD):.....	46
3.11.2. Computer Aided Manufacturing (CAM):.....	47
3.11.3. Surface Quality:.....	50
Chapter 4: Results and Discussions: .....	52
4.1. Introduction:.....	52
4.2. Valve Leaf Characterization: .....	53
4.2.1. CAD:.....	53
4.2.2. Resonance Frequency:.....	54
4.2.3. Stiffness: .....	57
4.2.4. Valve Leaf Impact Velocity Mapping:.....	59
4.2.5. Stroboscopic Display of Impact: .....	62
4.2.6. Microstructure Observation:.....	64
4.3. Strip Carbon Steel Impact Fatigue Life: .....	65
4.4. Edge Radius Characterization and Correlation to Impact Fatigue Life.....	67
4.5. Asymmetrical Impacts .....	70
4.6. The Influence of Temperature on the Impact Fatigue Life:.....	71
4.7. Crack Length and Crack Growth Rate:.....	73

4.8. Comparison of Impact Fatigue Life (Carbon Steel, Stainless Steel, New Stainless Steel Grade): .....	77
4.9. Microscopic Surface and Fractographic Observations .....	79
4.10. Wear Mark Evolution Microscopic Observation (Electromagnetic Setup):.....	85
4.11. Scanning Electron Microscope (SEM) and Optical Microscope Observations:.....	89
4.12. Metallographic Observations:.....	95
4.13. High Speed Camera Observations: .....	97
4.14. Finite Element Transient Impact Analysis:.....	99
4.15. Finite Element Crack Propagation Modeling Analysis: .....	102
Chapter 5: Conclusions .....	105
Bibliography... ..	109
VITA.....	112

## **List of Tables**

Table 1: Chemical composition of Sandvik strip steels.....	14
Table 2: Mechanical properties of Sandvik strip steels .....	14
Table 3: Grinding and polishing procedure .....	44
Table 4: Roughness Average (Ra) of valve plate surface after machining.....	51

## List of Figures

Figure 3.1. (a) Valve leaf (reed valve), (b) valve plate, (c) valve leaf & plate assembly ....	13
Figure 3.2. Experimental Setup Devices.....	15
Figure 3.3. Electromagnetic Experimental Setup .....	16
Figure 3.4. Electromagnet.....	17
Figure 3.5. Transistor Circuit.....	18
Figure 3.6. Temperature Measurements .....	19
Figure 3.7. Temperature Measurements (filtered) .....	19
Figure 3.8. Free vibration of valve leaf at resonance (displacement vs. time) .....	20
Figure 3.9. Velocity measurement with an additional neodymium magnet .....	22
Figure 3.10 Velocity measurement with an additional neodymium magnet (zoomed view) ...	22
Figure 3.11. Electromagnet B-Field.....	23
Figure 3.12. Attached permanent neodymium magnet B-Field.....	24
Figure 3.13. Total B-Field .....	24
Figure 3.14. Schematic display of test system.....	25
Figure 3.15. Pneumatic Experimental Setup Components .....	26
Figure 3.16. Solenoid valve and pressure regulator.....	27
Figure 3.17. Valve Plate Fixture Solid Model .....	28
Figure 3.18. (a) Printed Circuit Board (PCB).....	29
Figure 3.19. (a) Proteus (Isis) circuit schematic drawing (b) Proteus (Ares) pcb drawing (c) LPKF S62 PCB Machine .....	29
Figure 3.20. Pneumatic Experimental Setup maximum velocity measurement .....	30
Figure 3.21. Crack detection system.....	31
Figure 3.22. Isolation method .....	32

Figure 3.23. Flowchart of the system.....	34
Figure 3.24. Temperature control cabin heaters .....	36
Figure 3.25. Temperature control cabin components .....	37
Figure 3.26. Temperature control cabin zoomed view .....	37
Figure 3.27. Multi-station experimental setup.....	38
Figure 3.28. Multi-station experimental setup detail .....	38
Figure 3.29. Basic shape of exhaust valve [32] .....	40
Figure 3.30. Reciprocating setup .....	40
Figure 3.31. Specimens with mounting technique.....	42
Figure 3.32. Mechanical preparation machine.....	44
Figure 3.33. Valve plate solid model (a) Top view (b) Bottom view (c) CAM model .....	46
Figure 3.34. CAM (a) Tool path generation (b) Tool Path Verification.....	48
Figure 3.35. Machining process simulation.....	48
Figure 3.36. Valve plate machining operation.....	49
Figure 3.37. Mazak FJV\$200 UHS Vertical Machining Center.....	49
Figure 3.38. Surface roughness measurement directions.....	50
Figure 3.39. Surface roughness measurement .....	51
Figure 3.40. Valve plate surface profile after machining .....	51
Figure 4.1. (a) Valve leaf solid model (b) Valve leaf & plate assembly .....	53
Figure 4.2. Experimental resonance frequency.....	54
Figure 4.3. Solid model for CAE.....	55
Figure 4.4. Solid model meshing with element size 0.1 mm .....	55
Figure 4.5. Simulated resonance frequency .....	56
Figure 4.6. Modes and corresponding frequencies .....	56
Figure 4.7. Experimental stiffness calculation.....	58
Figure 4.8. Simulation stiffness calculation.....	58

Figure 4.9 Valve Leaf impact region .....	59
Figure 4.10. Valve Leaf (a) Impact region nodal representation (b) Measurement nodes (coordinates in [mm]) .....	60
Figure 4.11. Impact velocity measurement on the valve leaf .....	60
Figure 4.12. Valve leaf mapping - velocity profile.....	61
Figure 4.13. Valve leaf impact velocity mapping.....	61
Figure 4.14. Stroboscopic image frames part (1).....	63
Figure 4.15. Stroboscopic image frames part (2).....	64
Figure 4.16. Microstructure of strip carbon steel.....	65
Figure 4.17. Endurance curve of strip carbon steel. ....	66
Figure 4.18. Edge radius characterization of carbon and stainless steel.....	68
Figure 4.19. The effect of tumbling duration on impact fatigue life of carbon steel.....	69
Figure 4.20. The effect of tumbling duration on impact fatigue life of stainless steel .....	69
Figure 4.21. Valve leaf asymmetrical impact generation .....	70
Figure 4.22. Asymmetrical and smooth impact comparison .....	71
Figure 4.23. Temperature effect on the impact fatigue life of carbon steel.....	72
Figure 4.24. Temperature versus Lifetime for carbon steel.....	73
Figure 4.25. Crack length microscopic observation (50X).....	74
Figure 4.26. Microscopic observation of final fracture at the edge (100X). ....	75
Figure 4.27. Crack length measurements for $a_1$ , $a_2$ , $a_3$ .....	76
Figure 4.28. Crack propagation rates of $a_1$ , $a_2$ , $a_3$ .....	76
Figure 4.29. Comparison of impact fatigue life.....	77
Figure 4.30. Comparison of Stainless Steel and New Stainless Steel Grade.....	78
Figure 4.31. Difference in lifetime (Stainless Steel and New Stainless Steel Grade) .....	78
Figure 4.32. Valve leaf & plate assembly solid model and drawing .....	79
Figure 4.33. Critical regions on the valve plate .....	80

Figure 4.34. Valve plate critical regions.....	80
Figure 4.35. Valve leaf contact diameters on the valve plate .....	81
Figure 4.36. Valve leaf microscopic observation .....	82
Figure 4.37. Valve leaf tip wear mark radius.....	82
Figure 4.38. Valve leaf fractographic observation case (1) .....	83
Figure 4.39. Valve leaf fractographic observation case (2) .....	84
Figure 4.40. Fractographic Observation case (2).....	84
Figure 4.41. Microscopic observation setup .....	85
Figure 4.42. Microscopic observations (a) $14 \times 10^7$ cycles and (b) $22 \times 10^7$ cycles .....	86
Figure 4.43. Microscopic observations: (a) $25 \times 10^7$ cycles and (b) $32 \times 10^7$ cycles .....	86
Figure 4.44. Microscopic observations: (a) $37 \times 10^7$ cycles and (b) $40 \times 10^7$ cycles .....	87
Figure 4.45. Microscopic observations: (a) $47 \times 10^7$ cycles and (b) $69 \times 10^7$ cycles .....	87
Figure 4.46. Microscopic observation: wear marks $32 \times 10^7$ cycles .....	88
Figure 4.47. Scanning Electron Microscope (SEM).....	89
Figure 4.48. Valve leaf double crack origin (a) stroboscopic image of top face and (b) microscopic display of impact face.....	90
Figure 4.49. Microscopic observation: wear marks of symmetrical regions (a) and (b) .....	91
Figure 4.50. Microscopic and SEM observation .....	92
Figure 4.51. SEM observation: north crack.....	93
Figure 4.52. SEM observation: north crack origin .....	93
Figure 4.53. SEM observation: south crack.....	94
Figure 4.54. SEM observation: south crack origin .....	94
Figure 4.55. SEM observation: Fractography.....	95
Figure 4.56. Regional microstructure by SEM (a) crack origin, (b) branching point, (c) original microstructure.....	96
Figure 4.57. Branching along the crack path by SEM, Region (c).....	97

Figure 4.58. High speed camera display at 10000fps .....	98
Figure 4.59. High speed camera display at 16000fps .....	98
Figure 4.60. High speed camera display at 40000fps .....	99
Figure 4.61. Simulation applied pressure .....	100
Figure 4.62. ANSYS (a) fixed support and (b) applied pressure region.....	100
Figure 4.63. ANSYS analysis node selection .....	101
Figure 4.64. Stress along z-direction .....	101
Figure 4.65. Stress along x-direction .....	102
Figure 4.66. ANSYS crack propagation analysis procedure .....	103
Figure 4.67. ANSYS (a) meshing and (b) mesh refinement of selected region .....	104
Figure 4.68. Crack propagation steps along the pre-defined crack path.....	104

## Nomenclature

*COP* Coefficient of Performance

*IF* Impact Fatigue

*NIF* Non Impact Fatigue

*CAD* Computer Aided Design

*CAM* Computer Aided Manufacturing

*CAE* Computer Aided Engineering

*SEM* Scanning Electron Microscope

$\rho$  Electrical resistivity of copper ( $1.72 * 10^{-8}$  ohm.m)

$L$  Length of wire (40 m for the case)

$A$  Cross-sectional area of wire ( $((0.5 * 10^{-3})^2 * \pi) = 0.785 * 10^{-6}$  m<sup>2</sup>)

$R_a$  The arithmetic average deviation from the mean line

$L_s$  The sampling length

$Y$  The ordinate of the profile curve

$m_a$  Added weight (kg)

$g$  Gravity (9.81 m/s<sup>2</sup>)

$\delta$  Displacement of valve leaf (m)

- Valve leaf impact region outer radius:  $R_v$

- Valve plate diameters:  $D_{t1}$  –  $D_{t2}$  –  $D_{t3}$

- Distance from tip to fixing region of valve leaf:  $d_1$

- Temperature levels:  $T_1$ ,  $T_2$ ,  $T_3$

- Tumbling duration levels:  $T/2$ ,  $3T/4$ ,  $T$ ,  $5T/4$ ,  $3T/2$

- Impact velocity main levels:  $V_1$ ,  $V_2$ ,  $V_3$ ,  $V_4$ ,  $V_5$ ,  $V_6$ ,  $V_7$ ,  $V_8$

- Impact velocity levels (between the main levels):  $V_{12}$ ,  $V_{23}$ ,  $V_{34}$ ,  $V_{45}$ ,  $V_{56}$ ,  $V_{67}$ ,  $V_{78}$

## Chapter 1: Introduction

Hermetic reciprocating compressors are used in especially heat, ventilation and air conditioning (HVAC) applications and other applications. Since environment friendliness and the energy consumption becomes a momentous issue, improving the performance of the compressor, which covers the main part of energy consumption, became a crucial important subject. The parameters that affect the compressor performance include; valve leaf dynamics, re-expansion volume, heat transfer, flow resistance, friction loss, the leakage caused by the piston and cylinder clearance [1]. The valve leaf, which is the heart of the compressor, controls the suction and discharge phases of the reciprocating compressors. Therefore, valve leaf characteristic plays one of the determinative roles on the compressor performance.

Vapor compressor cycle system consist of four main parts; compressor, high pressure heat exchanger, low pressure heat exchanger, expansion valve. Compressor is the key component for refrigeration system performance and the maintaining the refrigeration system. In this regard, designing high performance and reliable compressors is essential for improving the refrigeration system performance. In a reciprocating compressor, whose nominal working frequency is 50 Hz, the complete cycle consists of four stages; expansion of the gas in the dead volume, suction of fresh to the cylinder from the plenum, compression of the gas in the plenum and the last stage, the discharge to the discharge plenum. Hermetic reciprocating compressors are used in refrigerators and consist of five main groups; compressor main body (cylinder, suction and exhaust silencer, valve plate & leaf), mechanic system (crankshaft a combination of connecting rod and piston), spring

system (vibration damper springs), electric motor: (rotor and stator), casing (metal casing for the other parts and oil tank for lubricating the system).

In the hermetic reciprocating compressors; cylinder, where the compression process is occurred, was machined into the compressor main body. The stroke volume varies between 3 -12 cm<sup>3</sup> due to the desired capacity and refrigerant type. Cylinder is enclosed by valve plate and piston. Suction and exhaust ports, which provide inlet and outlet of the refrigerant into the cylinder occupy on the valve plate. The electrical power is converted to the mechanical power by electric motor consisted of rotor and stator. Crank and connecting rod mechanism is used in compressors. The rotation motion of crank is translated to the transition motion of piston with the aid of connecting rod.

Three main parameters that affect the performance of hermetic refrigeration compressors include; electric motor efficiency, mechanical efficiency which is defined as the activity of the conversion of mechanic energy to compression energy and volumetric efficiency that is related to the decrease in the refrigeration capacity [2].

During suction and exhaust phases, the valve leaf vibration depending on the crank angle causes the pressure oscillations. The pressure oscillations significantly influence the energy efficiency (coefficient of performance, COP) and the sound power level of the reciprocating compressors, hence designing optimum valve leaf and processes after production is very critical.

Valve leaves must maintain proper working properties in the lifetime of the compressor without failure. During working in the compressors, valve leaves are experienced especially bending stresses and impact stresses, therefore bending fatigue strength and

impact fatigue strength of the reed valve plays a deterministic role. In this regard, the parameters, which affect the bending fatigue life and impact fatigue life, are needed to be investigated.

In the design process, valve leaf parameters conflict each other. For instance, more valve leaf yields more efficient compressor because of lower flow losses through the port and valve. On the other hand, more valve lift causes more impact stresses and valve leaf flutter which induces additional vibrations in addition to impact motion of the valve leaf. The undesired flutter vibration results a decreased COP, an increase in the sound level and a shortening in the life of the valve leaves. In addition, the valve leaves inertia are decreased in order to improve the performance of the reciprocating compressors in where the energy loss minimum level at the opening and closure stage of the valve leaves. On the other hand, the reduction in the inertia results higher stress concentrations due to higher impact velocities of the valve leaf at the closure stage of the suction phase. As a conclusion, the valve leaves are tend to failure due to the impact fatigue stresses.

The thesis presents an investigation on the impact fatigue characteristics of compressor valve leaves. Therefore four experimental setups and a crack detection method were developed in order to define the parameters that affect the impact fatigue life of valve leaves and crack initiation & propagation mechanism.

The second chapter provides a literature review on the investigations of the compressor valve leaves. The experimental and computational studies were introduced and the parameters related to the fatigue strength, were presented.

The third chapter outlines the experimental techniques and setup designs in order to investigate the impact fatigue characteristics of the valve leaves. Experimental setups include pneumatic and electromagnetic actuated experimental setup, temperature control cabin, multi-station experimental setup and reciprocating setup. A crack detection method which is implemented to the experimental setup introduces. In addition specimen preparation details for metallographic observation and valve plate prototype manufacturing is exhibited.

The fourth chapter, the results of the investigations and observations on the impact fatigue life are presented. The valve leaf was characterized in terms of resonance frequency, stiffness, impact velocity profile and microstructure. Three types of material were investigated, carbon steel, and martensitic stainless chromium grades, stainless steel and new stainless steel grade in terms various impact velocities. Working conditions; asymmetrical impacts and temperature effects on the impact fatigue life were investigated. The edge radius of the valve leaves was characterized and correlated with the impact fatigue life. The reasons of crack initiation and propagation of the valve leaf caused by impact fatigue was investigated. The valve leaves were subjected to fractographic, Scanning Electron Microscopy, microscope and metallographic observations. Besides, the explanations and explications through the results were presented as the discussion. Finally, the fifth chapter concludes the thesis.

## Chapter 2: Literature Review

Valve leaves must maintain proper working properties in the lifetime of the compressor without failure. During working in the compressors, valve leaves are experienced especially bending stresses and impact stresses, therefore bending fatigue strength and impact fatigue strength of the reed valve plays a deterministic role. On the other hand, bending fatigue failure could be prevented by choosing high bending fatigue strength strip steel for valve leaves. In addition, bending fatigue strength could be examined in commercial fatigue testing devices. In this regard, the parameters, which affect the impact fatigue life, are needed to be investigated in special impact fatigue testing apparatus.

A review of the studies in literature shows that the impact fatigue phenomenon and experiments have been investigated from various viewpoints. Nakayama and Tanaka carried out impact fatigue experiments on plain and notched carbon steel, aluminum and duralumin specimens in push-pull type pulsating impact load applier test machine [3-5], Iguchi et al. [6] performed impact fatigue experiments on smooth and notched low carbon steel in a forced falling hammer type testing machine [7], Futakawa et al. investigated impact bending of fine-grained isotropic graphite material in pendulum type repeated impact bending machine [8], Dumitru et al. introduced a guided hammer with cam mechanism apparatus for testing torsional impact fatigue of carbon steel shafts [9].

The response of surfaces for repeated impact loads was examined in terms of free falling particle on the metallic material specimen surfaces [10], bullet-shaped projectiles impact using magnetic fields [11], solid particle streams on the specimen surface [12-14], creating repetitive impulsive loading with hammers driven by electric motors [15, 16],

impact of steel particles with a rotating arm apparatus [17], electromagnetically forced cantilever beam which had a ball-bearing hammer on the tip for studying repeated impact wear [18].

Impact fatigue investigation and testing is possible with the novel automated impact fatigue test system presented in this thesis. The impact fatigue test apparatus is unique in terms of non-contact actuation; crack detection technique and system trigger mechanism. Suction valves in refrigerators provide an example of an engineering component where the effects of impact fatigue, bending fatigue, wear pose a considerably challenge for a successful design. Some critical issues on the lifetime of the compressor suction valve leaves for refrigerators were considered in the thesis.

The automated test apparatus for impact fatigue presented here is a unique test system that allows investigating impact fatigue characteristics of thin strip specimens such as compressor valve leaves subjected to repeated impact loads and the system simulates the real working behavior of valve leaves during lifetime.

Impact fatigue fracture mechanism in the compressor valve leaves was “edge chipping”. Small segments were broken out from the edge of the valve leaves during the repeated impact loading [19, 20]. Highest stress concentration exists on the tip of the broken segments where the crack initiates.

The failure mechanisms of reed valves used in reciprocation compressors is described by Glaeser, W.A. (1999). In refrigeration systems, the valve leaves, which controls the flow of inlet and outlet gas through the cylinder, mostly produced by a thickness of 0.15 – 0.20 mm steel plate. The pressure difference, that is required for valve opening and closure,

directly affects the compressor performance. Therefore, a low inertia is desired for the valve leaves. Especially in the compressors which work at high frequencies, the valve leaves, that open and close at least one time in every cycle, are exposed to fatigue failure. In addition to bending fatigue; since the valve leaf impacts the valve plate at high velocities, stress concentration exists in particular regions and for that reason impact fatigue failure occurs. The failure mechanism of four kind of valve leaves used in refrigeration systems is investigated. After 20 h of operation,  $10^7$  cycles, of the compressor, a premature failure observed and several crack origins are observed in the analysis of Scanning Electron Microscope (SEM). The crack origins of the valve leaf occupies on the impact area, is formed by the contact of valve plate during closure, thus the failure is described as impact fatigue. A strip steel of higher impact fatigue strength material grades and tumbling is recommended for preventing failures. In an another investigation of a valve leaf – valve plate couple; the sharp stress raisers observed that are formed after manufacturing operation on valve plate, cause crack initiations on the valve leaf. A controlled cleaning process after machining of the valve plates is recommended in order to remove the stress raisers. Two different kind of valve leaf failure caused by bending fatigue and wear is investigated by Glaeser [21]. The impact fatigue failure on the compressor valve leaves observed and various diagnoses are outlined, however a controlled test ring was not formed in order to investigate the parameters which affect the impact fatigue life. In addition, crack initiation and propagation mechanisms were not clearly observed.

An experimental study was introduced to study the impact fatigue of suction valve leaves of refrigeration compressors. The test system can achieve 1000 Hz working frequency with an opposite pulsating air flow on the valve leaf. The carbon steel valve plate (HV 100) is compared with nitrated valve plate (HV 500) and concluded that increasing the hardness of the valve plate decreases the surviving probability of the valve

leaves. The test system had a limited impact velocity range and a crack detection technique was not described through the system [22].

Experimental studies were made on the differences of impact fatigue and non-impact fatigue by Iguchi, H., et al. (1979). Smooth and notched specimens are used in the experiments. Investigations were performed with various tensile loads, and the numbers of cycles the specimen can resist throughout different crack formations are shown. After the tests, microstructure and macrostructure deformations, crack lengths were observed. Smooth specimen's life was shorter in non-impact fatigue than impact fatigue. As a conclusion, it was stated that the fatigue life of smooth specimen could be predicted best with the plastic strain range parameter than stress parameters, both in impact and non-impact fatigue. Also, the material was more susceptible to fracture under impact fatigue if cracks or flaws occupies. In addition, the notched specimen lives were short in impact fatigue than non-impact fatigue [6].

Tekeli, S. (2002) studied on the improvement of SAE 9245 in terms of fatigue strength. Shot peening method was proposed in the valve leaf, valve spring and spring steel products in order to form compressive residual stresses. The article mainly focused on the fatigue strength investigation of SAE 9245 steel which used in helical spring production. The prepared standard specimens were subjected to shot peening process with various pressurized air amplitudes and duration. As a conclusion, it was reported that the bending fatigue strength of SAE 9245 steel was increased 30% [23]. There was no research on the impact fatigue and parameters which affect the lifetime.

The article about suction and exhaust valves produced by ceramic material was presented by Sonsino, C. M. (2003). The research focused on  $Al_2O_3$  and  $Si_3N_4$  ceramic

materials on the bending fatigue strengths. Since the lesser slopes of the S-N Curves of the investigated ceramic materials, a methodology is formed by the author [24]. The research was carried out fatigue of ceramic materials beside the valve leaf strip steel material and impact fatigue was not studied.

Sobiecki, J. R., et al. (2004) presented a study for improving the valve steel properties. The effects of the nitriding process at between the temperatures 450 °C and 650 °C on the valve steel properties are investigated. The research is mainly focused in 0.35-0.45 C, 0.7 Mn, 2 Si, 8-10 Cr, 0.6 Ni composition content of H9S3 steel. The micro-hardness, corrosion strength and wear resistance is carried out[25]. The research subjects were not related with the impact fatigue.

Yu, Z. W. and Xu, X. L. (2006) researched the diesel engine exhaust valves in failure analysis under the normal service conditions. 5Cr21Mn9Ni4N (21-4) steel, which was used as the diesel engine plate material, was mentioned as a good heat-resistant and PbO-corrosion resistant material. Three exhaust valves, which were with a six cylinder diesel engine, was investigated by SEM and visual observation in terms of metallurgical investigation and fractographic analysis. As a consequence, fatigue dominant failure mechanism was observed in two plate material. On the other hand, the parameters or characteristics result in fatigue failure was not studied [26].

Reed, J., et al. (2005) studied the development of a compressor using reed valves for a satellite borne J-T cryocooler. Three significant failure mechanisms were determined on the lifetime of the reed valves, bending fatigue of reeds, impact fatigue fracture of the reed and the impact fatigue fracture of the reed valve seat. Stainless steel reed valve and plastic seat combination eliminated debris, which locally increases the stress, was not formed on

the valve seat. In this regard, the bending fatigue failure was focused rather than impact fatigue failure. The reed valves were tested for  $10^8$  cycles on a vibration generator. The reed valve manufacturer carried out the tests and the amplitude was set ten times of the normal working conditions. Steel/plastic combination used in the compressor was proper for long life operation with a bending failure probability less than 0.0001%. Steel/steel reed valve and seat combination was not investigated in the paper [27].

Improving bending and impact fatigue properties of flapper valve steels were studied by Chai, G., et al. (2004). The inertia of the compressor exhaust and suction valves were reduced by thinning the valves that results an increase in the compressor performance. Since the valve lift was increased, the flapper valves were needed to be tested in terms of bending and impact fatigue strengths. Hiflex<sup>TM</sup> material, which was manufactured by Sandvik, was mentioned suitable for high pressure applications due to higher bending and impact fatigue properties compare to AISI 420 steel. Increase in tensile strength did not mean increase in the fatigue strength in high strength steels such as flapper valve steels. Increasing tensile strength, ductility and damping capacity was beneficial for impact fatigue strength. Oblique impact of the flapper valve resulted longitudinal direction propagation of the cracks and new crack initiation occurs due to Rayleigh waves. Subsequently, the crack propagated depending on the tension and shear stress wave conditions. The crack initiated near the impact area or between the impact area and the specimen edge, eventually final fracture occurred as the crack reaches the specimen edge where edge chipping occurs. As a conclusion, in impact fatigue conditions, increasing the resistance of the material to crack initiation and propagation and increasing the stress decay rate results in higher impact fatigue strength. In addition high compressive residual stress with a low stress relaxation rate and good surface finish were crucial parameters in impact

fatigue life. However valve leaf geometry, working conditions in compressor and tumbling effect were not studied in article [28].

Johnson, A. A. and R. J. Storey (2007) reviewed articles related to the impact fatigue properties of irons and steels. The testing equipment and the materials studied through the articles were examined. The characteristics of the impact fatigue were analyzed. In heat treatment, it was observed that the impact fatigue strength increased when the materials austenite and the nickel content was increased. It was examined that crack nucleation and growth in impact was similar to that in tensile tests. Fractography and surface modifications were investigated. The effects of environment were researched and it was understood that the overall endurance of the steel is better when the temperature was decreased. As conclusion, the authors stated that, since the reviewed articles were carried out various types of materials, it was hard to compare the results indeed[29].

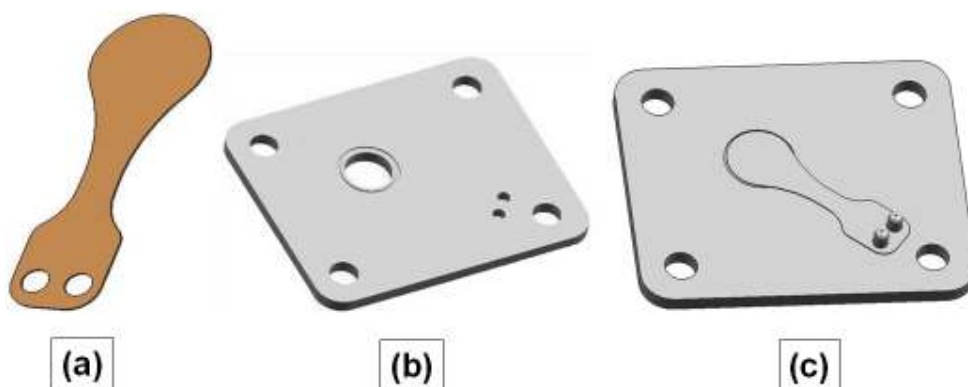
Jin, S. H., et al. (2001), examined the shape of stress wave propagation of three dimensional stress field, produced in the process of time increment. A finite element program about 3-dimensional stress wave propagation was formed in order to explore how the material changes shape under the stress of the impact load. Three important points indicated. First, the thickness could be insignificant by dividing the element of thickness direction into more than the layers in analyzing the code in order to have the most accurate results while applying the magnitude of the stress field. Second, there was an order that the middle, the upper and the opposite layers' tensile and compressive stress become larger and an order the upper, middle and the opposite layers' sheer stress become larger when the impact load was applied [30].

De los Santos et al. (1991), outlined a simulation model for reciprocating hermetic compressors. Admission and discharge circuits' acoustical behavior is examined applying the discrete element model. Ducts were thought-out as rigid elements with inertia and cavities as elastic elements. Reed valves were designed as systems of three degrees of freedom, and they are studied with modal analysis. As conclusion, there were four important points. First, there was a great similarity between experimental and theoretical curves of pressure and there was an excellent matching of plenum discharge pressure. Second, their frequencies of the oscillations were similar. Briefly, two types of results, experimental and theoretical matched adequately; the model represents the global behavior of hermetic compressors in a satisfactory way [31].

## Chapter 3: Materials and Methods

### 3.1. Introduction

Materials and methods chapter includes information about the tools and materials utilized in investigating the impact fatigue characteristics of compressor valve leaves shown in Figure 3.1. In this regard; electromagnetic and pneumatic experimental setups were introduced, in addition implemented crack initiation detection system was described. Moreover, the chapter includes temperature control cabin for observing the influence of temperature on impact fatigue life, accelerated experiments via multi-station experimental setup, reciprocating experimental setup for exhaust valves. Finally, specimen preparation method for metallographic observation of valve leaves failure on Scanning Electron Microscope (SEM) and the procedure followed in manufacturing was introduced. In addition to that the tools and materials applied within the procedure Computer Aided Manufacturing (CAM) were reported in detail.



**Figure 3.1. (a) Valve leaf (reed valve), (b) valve plate, (c) valve leaf & plate assembly**

### 3.2. Materials

The materials used in the tests were hardened and tempered carbon flapper valve strip steel, martensitic stainless chromium steel alloyed with molybdenum and new stainless steel grade. Chemical composition of the materials was presented in Table 1, and mechanical properties were listed in Table 2. The structure of the specimen is tempered martensite. Grain of material was longitudinal oriented in manufacturing. Valve leaves used in the compressors for refrigeration were investigated.

**Table 1: Chemical composition of strip steels**

Material	Chemical composition (nominal) %						
	C	Si	Mn	P	S	Cr	Mo
Carbon Steel	1.00	0.30	0.40	0.008	0.0070	-	-
Stainless Steel	0.38	0.38	0.50	0.018	0.0027	13.45	0.94
New Stainless Steel	0.38	0.35	0.60	0.015	0.0035	13.58	1.01

**Table 2: Mechanical properties of strip steels**

Material	Mechanical properties (at 20 °C)	
	Min Tensile Strength $R_{\min}$ (MPa)	Max Tensile Strength $R_{\max}$ (MPa)
Carbon Steel	1990	2030
Stainless Steel	1770	1830
New Stainless Steel	1860	1940

### 3.3. Electromagnetic Experimental Setup:

Electromagnetic experimental setup was designed for investigating the impact fatigue life characteristics of the valve leaf by a non-contact actuation. Electromagnetic setup simulated the real working behavior of valve leaves in the compressor. Since the valve leaf was a ferromagnetic material, an electromagnet was build-up in order to achieve high electromagnetic field, thus high impact velocity amplitude. The experiment setup included electromagnet, DC power supply, cycle counter, oscilloscope, PC & data acquisition system, Laser Doppler Vibrometer (LDV), LCD Screen as shown in Figure 3.2; and signal input/out (I/O) terminal box, transistor circuit, electromagnet and aluminum platform shown in Figure 3.3.

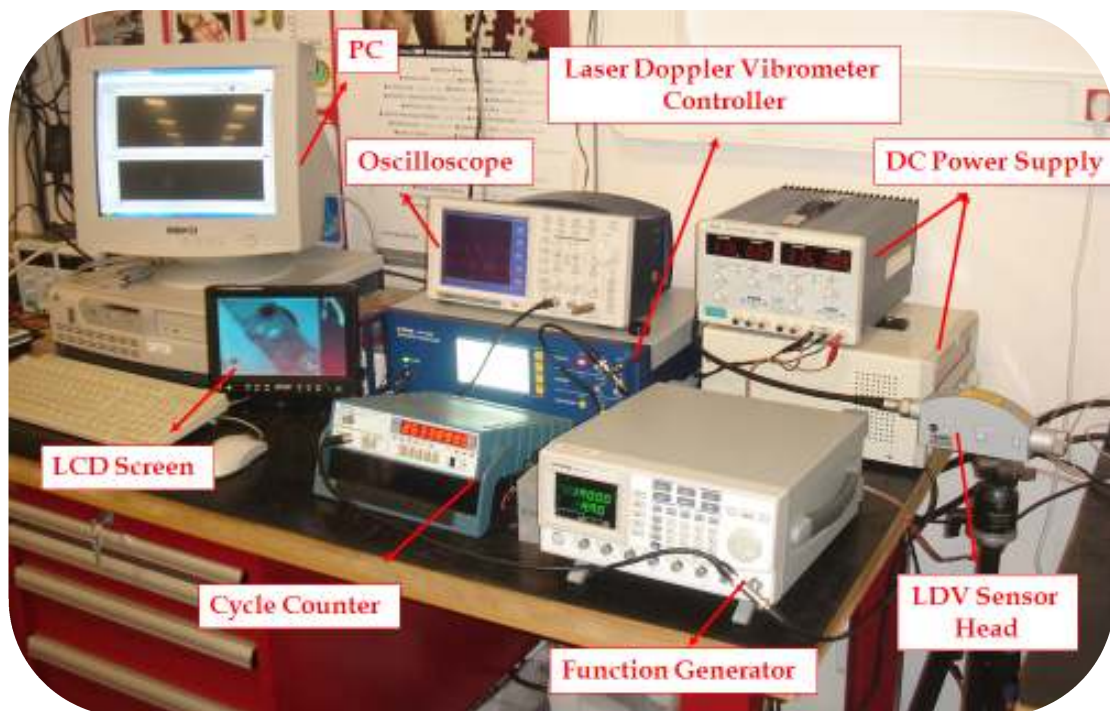
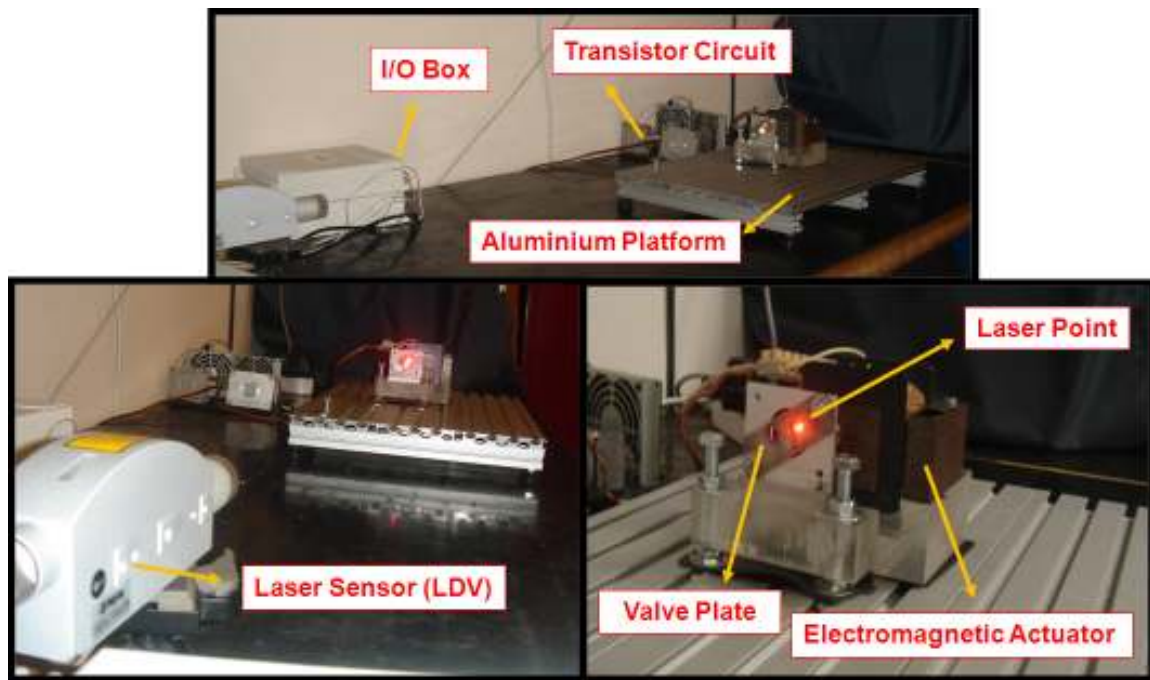


Figure 3.2. Experimental Setup Devices

Valve leaf was actuated in the desired frequency via function generator; displacement and velocity of the valve leaf was measured simultaneously via LDV in order to form frequency response function of the valve leaf and natural frequency, stiffness were determined.



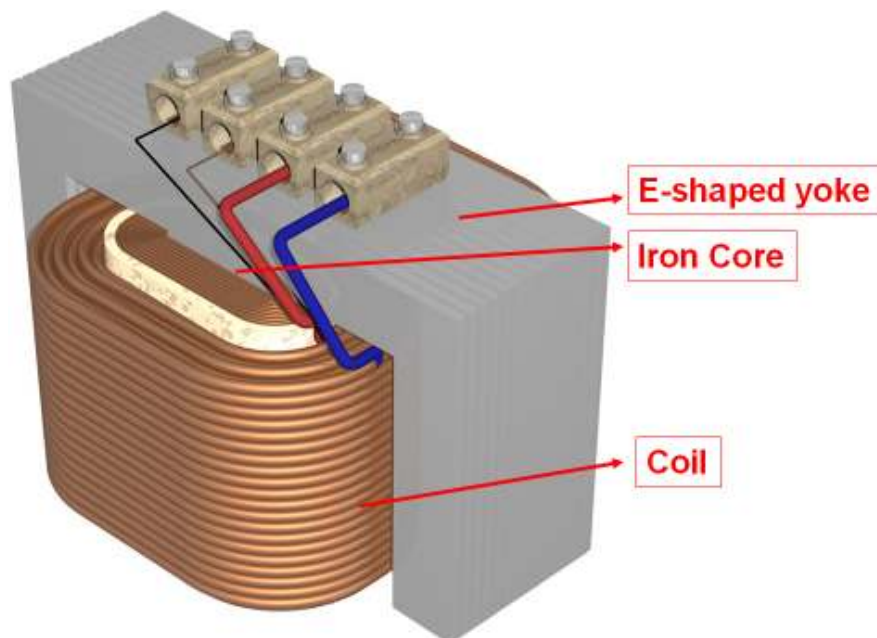
**Figure 3.3. Electromagnetic Experimental Setup**

Electromagnet was designed of transformer steel layers as an E-shaped yoke was used with 180 turns of coil (Figure 3.4). 40 meters length and 1 mm diameter galvanized copper wire was used to wound the E-shaped yoke. The winding number was selected as 180 turns in order to have enough strength of magnetic field. The resistance of the electromagnet with 180 turns was measured as 0.9 ohm.

The resistance of the coil can be calculated theoretically by the formula:

$$R = \rho * L / A \quad (3.1)$$

The calculated resistance of the wiring was 0.876 ohm which was close to the measured resistance of the copper wire used in winding of the coil.



**Figure 3.4. Electromagnet**

The circuit, shown in Figure 3.5, used in the experimental setup consists of mosfet (metal–oxide–semiconductor field-effect transistor) which was used for fostering the input was used in the setup. The circuit was connected to two aluminum cooler plates which



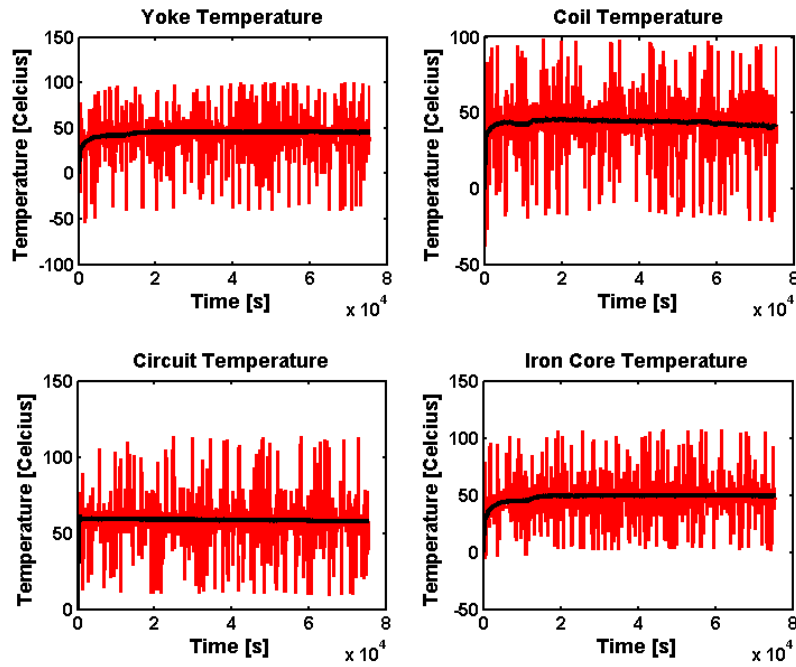


Figure 3.6. Temperature Measurements

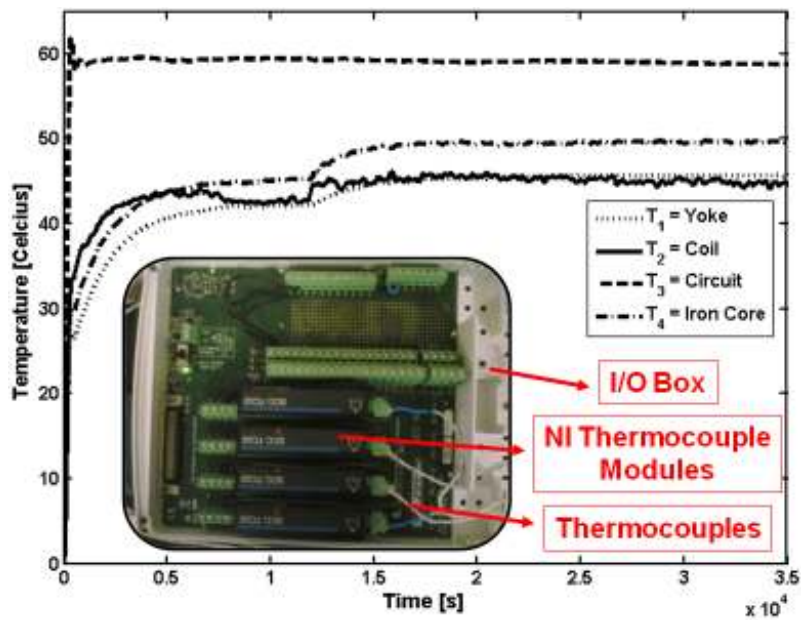


Figure 3.7. Temperature Measurements (filtered)

The displacement of the reed valve could reach 3 mm and the velocity 3.4 m/s without a valve plate stop. On the other hand in the valve plate condition the displacement amplitude became 0.22 mm and velocity was very small compared to without valve plate condition. A significant difference in displacement value occurred because of the extra inertial energy gain of the reed valve. In Figure 3.8, it was showed how the amplitudes were increasing by the time. While the valve leaf was fixed 27.20 mm distance from the tip, initial displacement amplitude was 0.14 mm (Figure 3.8) that was similar to the valve plate condition.

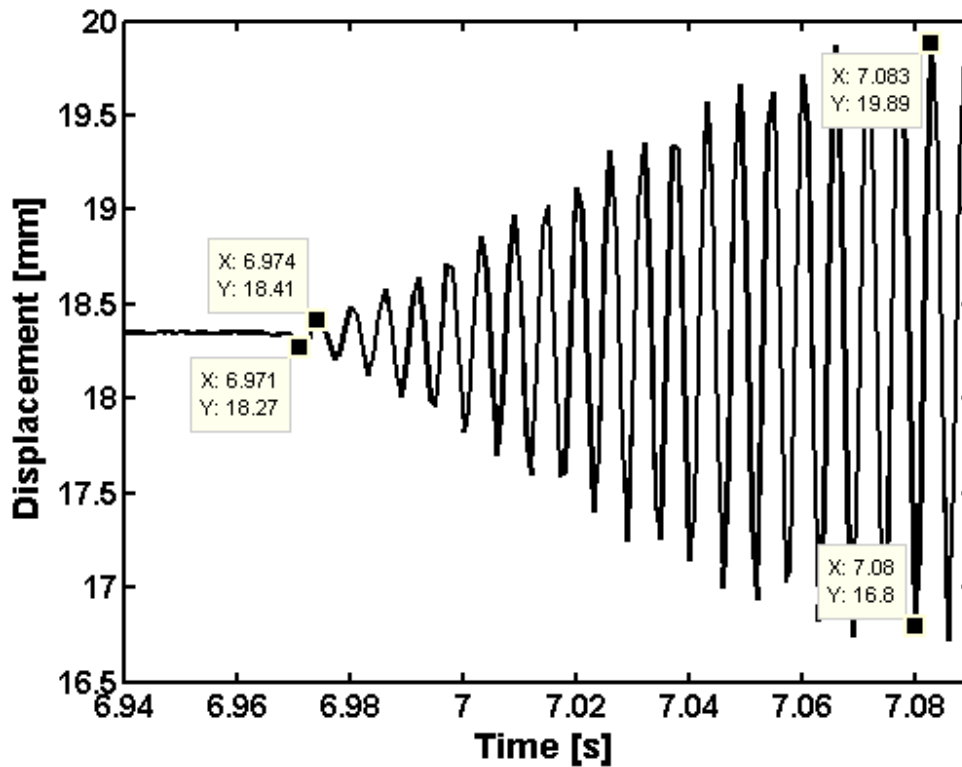
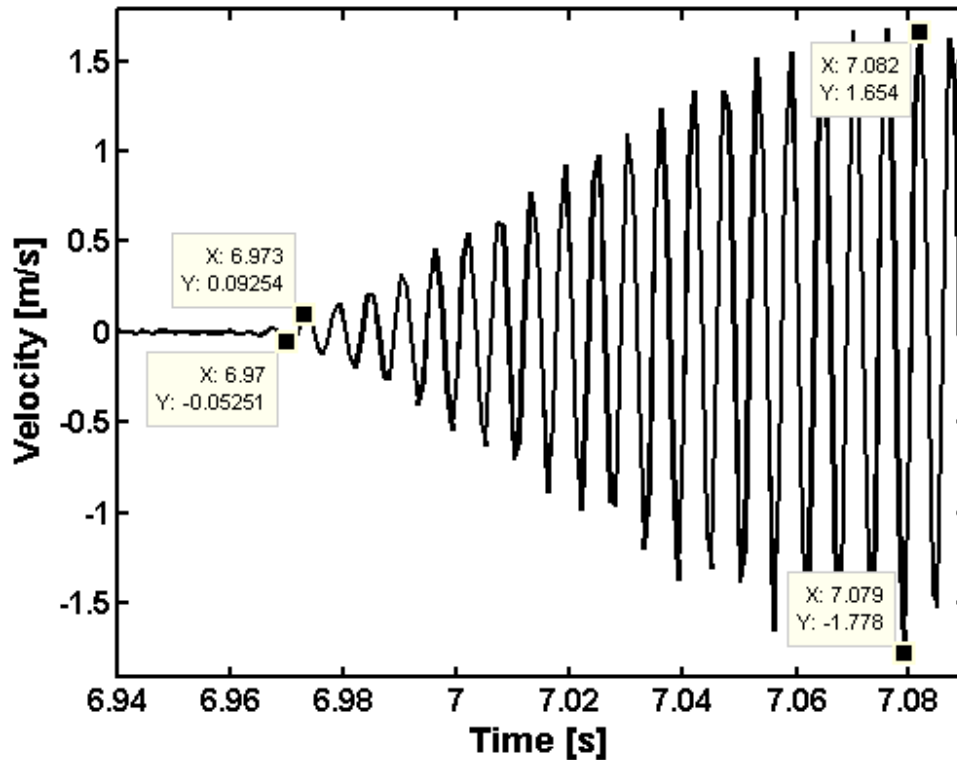


Figure 3.8. Free vibration of valve leaf at resonance (displacement vs. time)



**Free vibration of valve leaf at resonance (velocity vs. time)**

After the measurements, the steel valve plate was replaced with the aluminum valve plate; the maximum displacement value increased to 0.45 mm. It could be concluded that the electromagnetic force was shared between the reed valve, steel valve plate and bolts-nuts.

Therefore, the steel valve plate volume was decreased by machining (Figure 3.3) in order to remain only the impact zone and fixing part to hold the reed valve. In addition, two permanent neodymium magnets were attached to the iron core in order to strengthen the electromagnetic force. The displacement of the reed valve velocity increased to 5 m/s with the attachment of permanent magnet to the iron core.

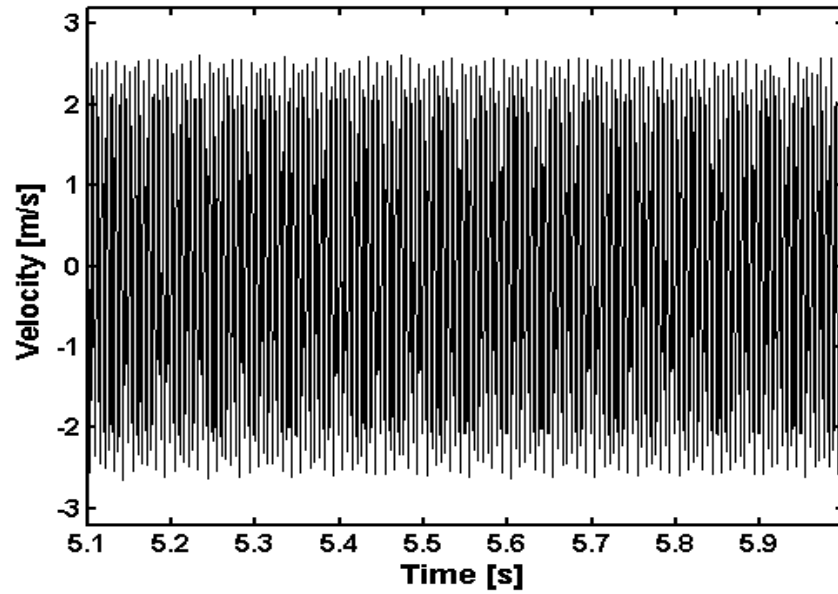


Figure 3.9. Velocity measurement with an additional neodymium magnet

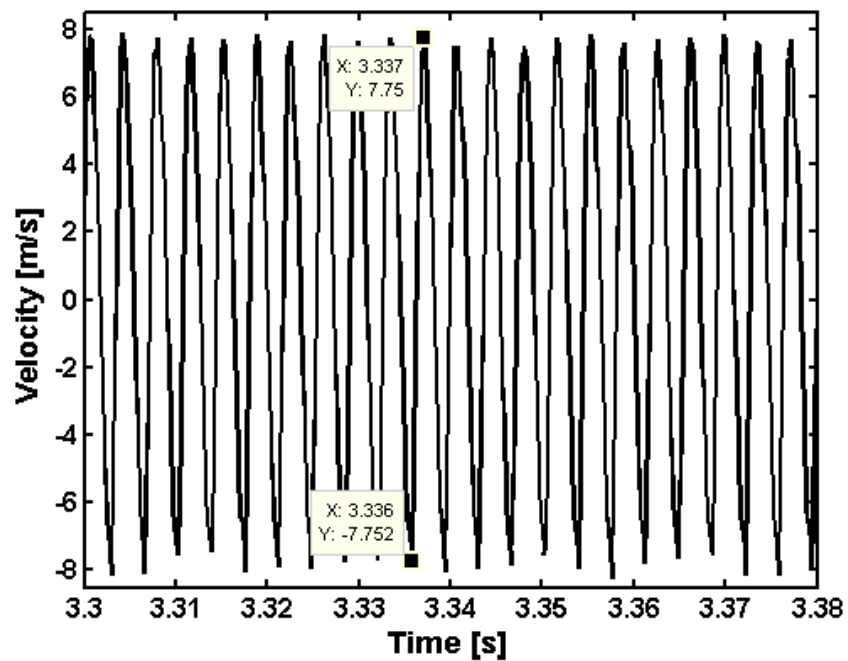
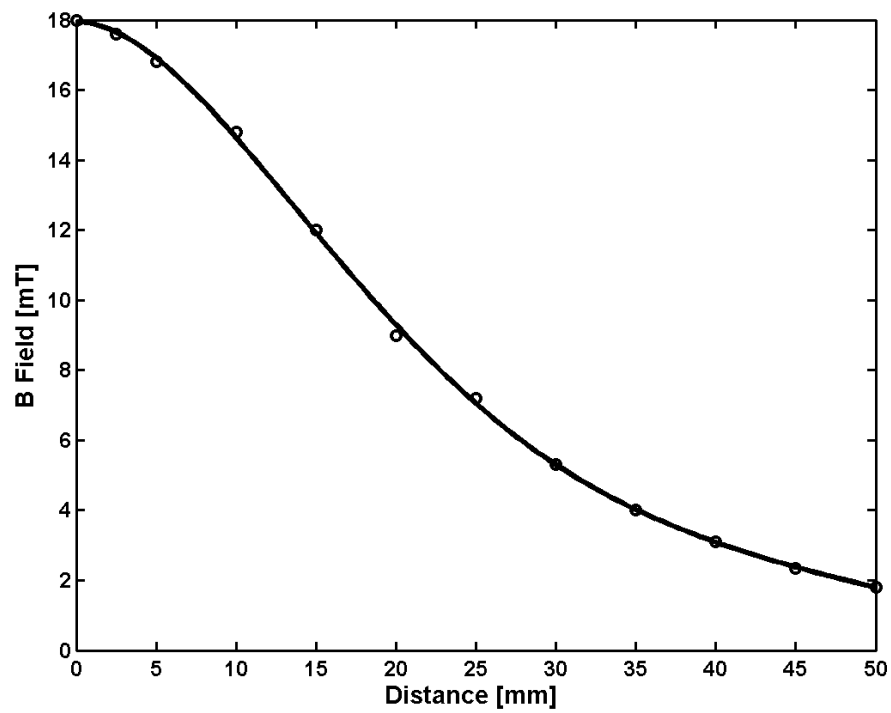


Figure 3.10 Velocity measurement with an additional neodymium magnet (zoomed view)

The electromagnetic field was measured via the Magnet-Physik magnetic field strength meter Teslameter FH 54 and the results were presented in Figure 3.11 for electromagnet, in Figure 3.12 for attached permanent neodium magnets, in Figure 3.13 for total system.



**Figure 3.11. Electromagnet B-Field**

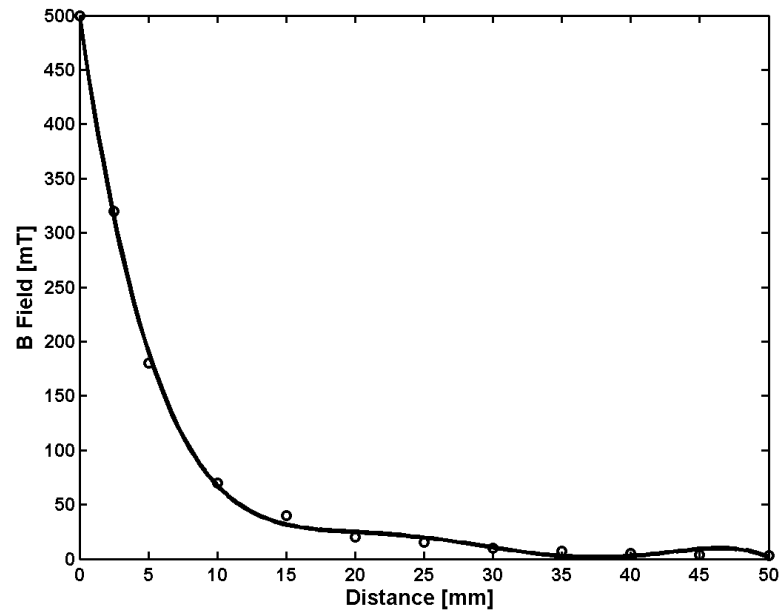


Figure 3.12. Attached permanent neodymium magnet B-Field

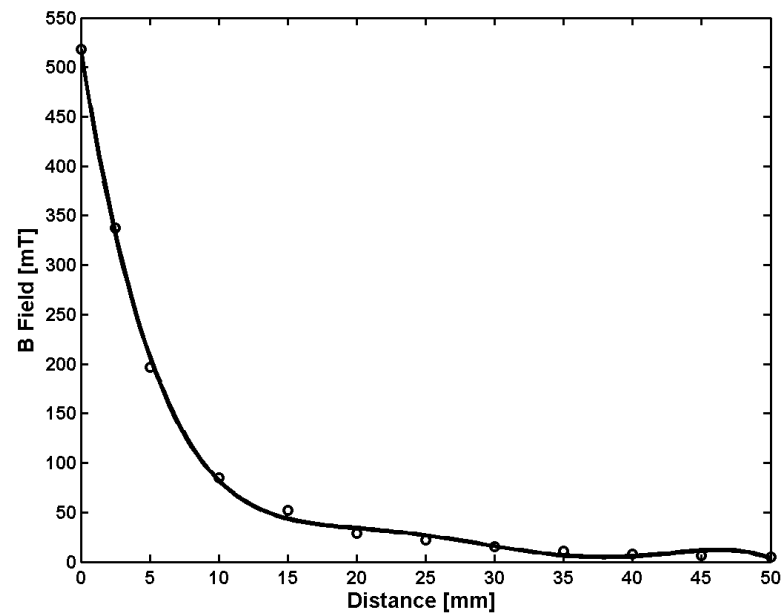


Figure 3.13. Total B-Field

### 3.4. Pneumatic Experimental Setup:

The test system was designed in such a way that the impact fatigue life characteristics of the compressor valve leaves could be investigated. In addition, crack initiation detector based on a microphone was implemented in the system. Extensive impact fatigue tests were performed in the test system which was schematically shown in Figure 3.14.

The real working behavior of valve leaves in the compressor was simulated with a non-contact actuation. The test system included compressor valve plate and fixture, solenoid valve, pressure regulator, filter, pressure sensor, function generator, DC power supply, cycle counter, PC & data acquisition system, microphone, signal input/out (I/O) connector block, transistor circuit, Laser Doppler Vibrometer (LDV), LCD Screen for CCD camera in LDV.

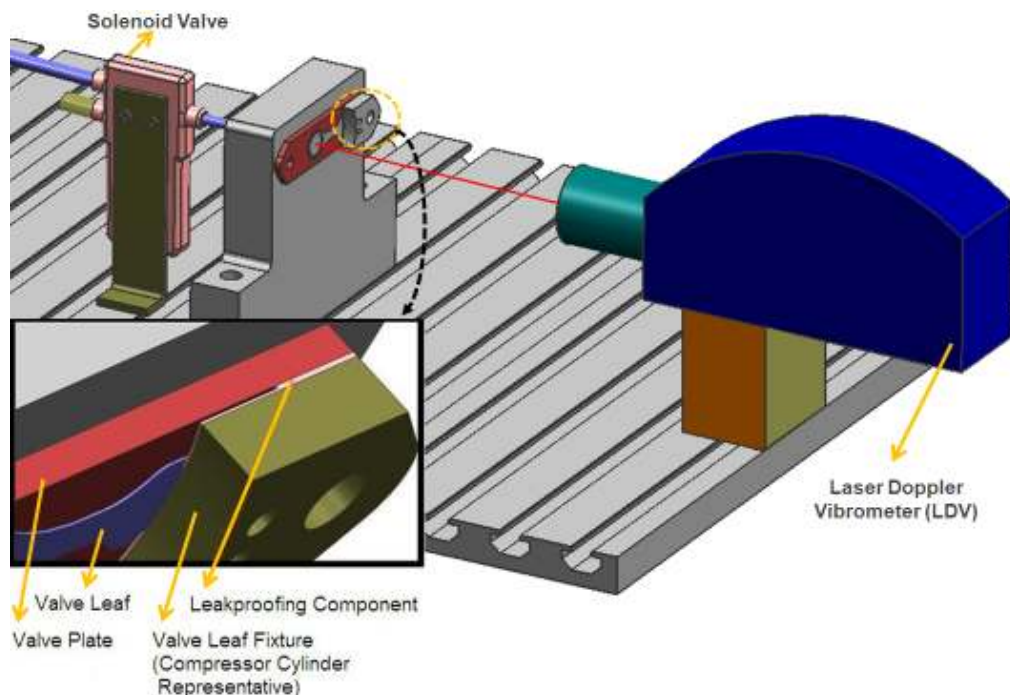
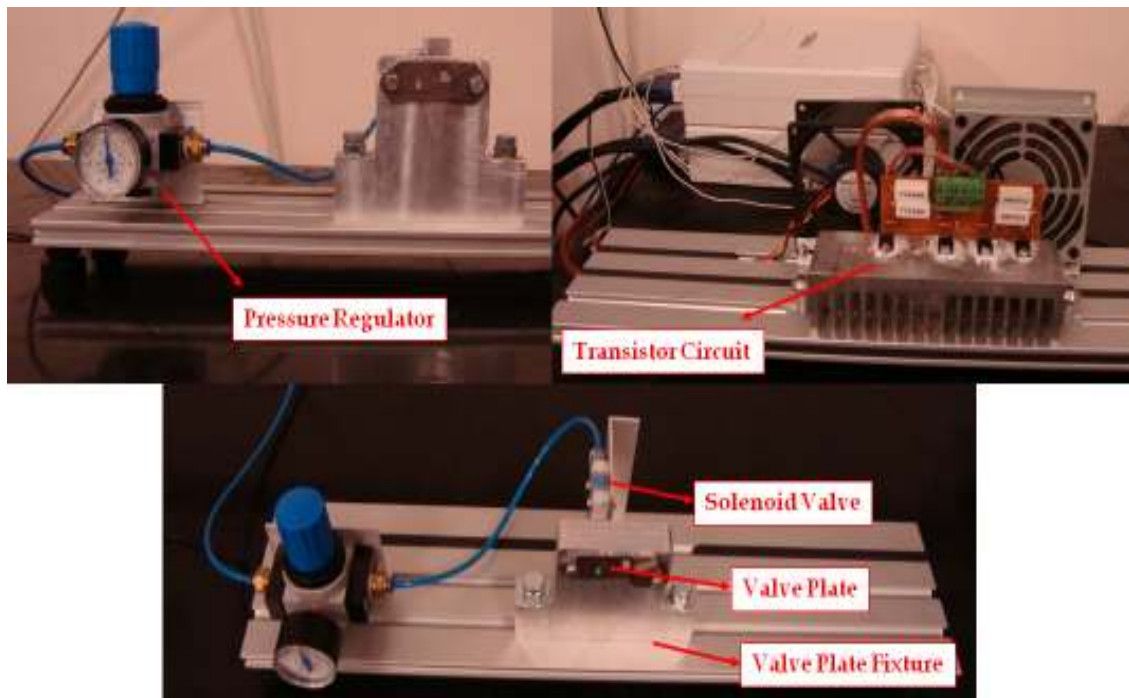
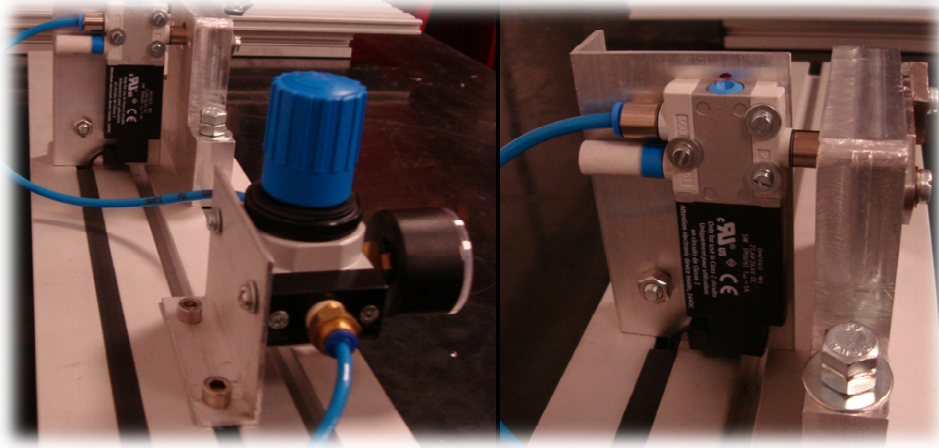


Figure 3.14. Schematic display of test system

Pneumatic experimental setup was designed for investigating the impact fatigue characteristics of impact fatigue in order to reach higher impact velocity to shorten the experiment duration and testing the valve leaf in a wide impact velocity spectrum compared with electromagnetic setup. Pneumatic experimental circuit, shown in Figure 3.15, consisted of a pressure regulator, transistor circuit, solenoid valve, valve plate and fixture. Solenoid valve is a fast-switching 3/2-way valve with a maximum switching frequency of 330 Hz. The power consumption of the solenoid valve is 5 W which is well below the electromagnetic setup.



**Figure 3.15. Pneumatic Experimental Setup Components**

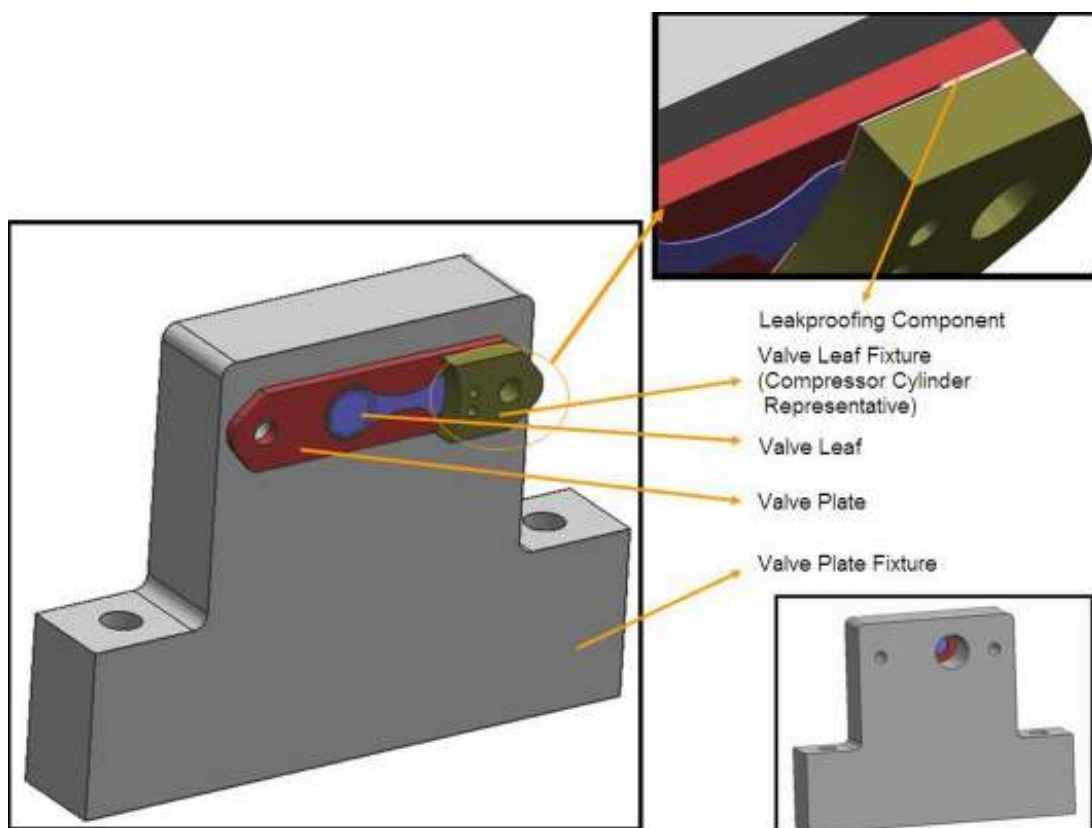


**Figure 3.16. Solenoid valve and pressure regulator**

In the experimental setup, the valve leaf and plate assembly was simulated as the real components in the compressor (Figure 3.17). The solenoid valve was actuated in the desired frequency with a generation of square signals via signal generator. Transistor circuit connected to DC power supply, function generator and solenoid valve. Semiconductor circuit, shown in Figure 3.18, was schematically designed by PROTEUS (Isis), after that PCB drawing was accomplished with PROTEUS (Ares) and finally manufactured with LPKF S62 PCB Machine (Figure 3.19). Pneumatic experimental setup allows impact velocity up to 15 m/s which was sufficient to examine the impact fatigue characteristics with different valve leaf designs.

In the test system, original valve plate and valve leaf couple was utilized through the experimentation in order to simulate the real behavior in the compressor. A fixture was designed to mount the valve plate. The main principle of the system is creating pulsating air flow through the solenoid valve. The inlet pressure air supplied from the main compressed air source is filtered with a good particle separation and regulated with

minimal hysteresis in order to avoid pressure oscillations. The solenoid valve is actuated in the desired frequency with generation of reference square signals with the aid of function generator in order to simulate opening and closing movement of the valve leaf. The numbers of impacts are displayed by an electronic cycle counter which is connected to the function generator. The inlet pressure is measured and displayed by a pressure sensor. When a failure of the specimen due to impact fatigue occurs, the failure detector based on a microphone, terminates the experimentation. Graphical programming environment was created with LabVIEW software for data acquisition, signal processing and triggering mechanism. The impact fatigue experimental setup provides an automation system for controllable impact fatigue tests.



**Figure 3.17. Valve Plate Fixture Solid Model**

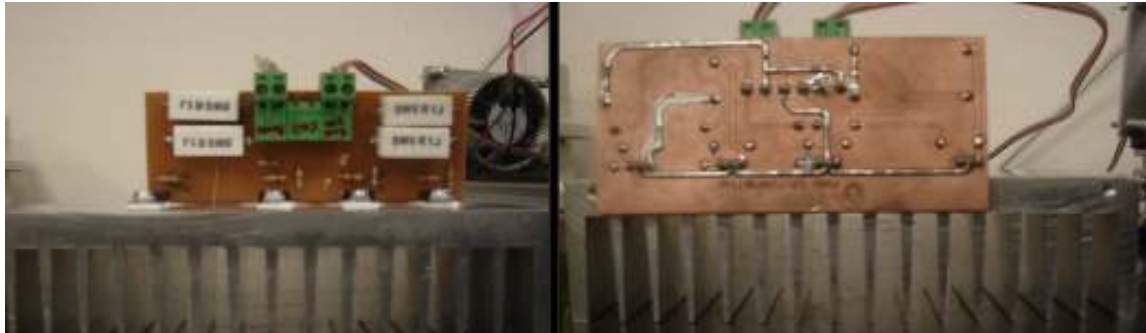


Figure 3.18. (a) Printed Circuit Board (PCB)

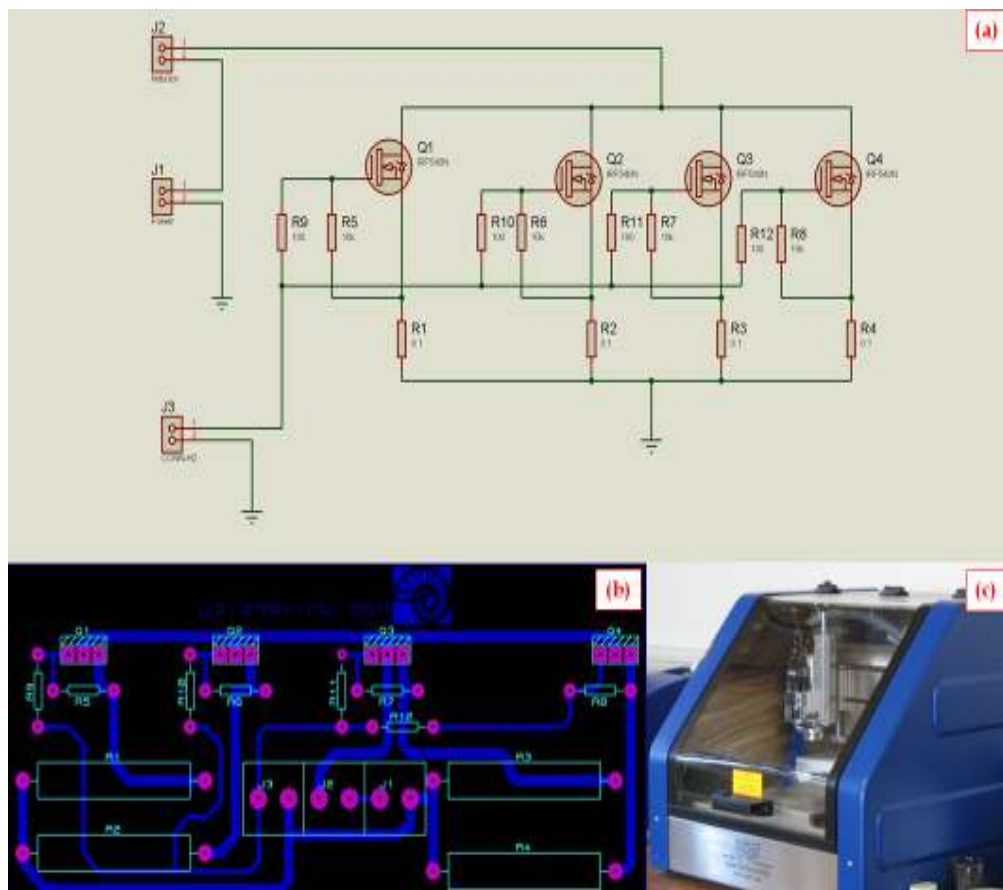


Figure 3.19. (a) Proteus (Isis) circuit schematic drawing (b) Proteus (Ares) pcb drawing (c) LPKF S62 PCB Machine

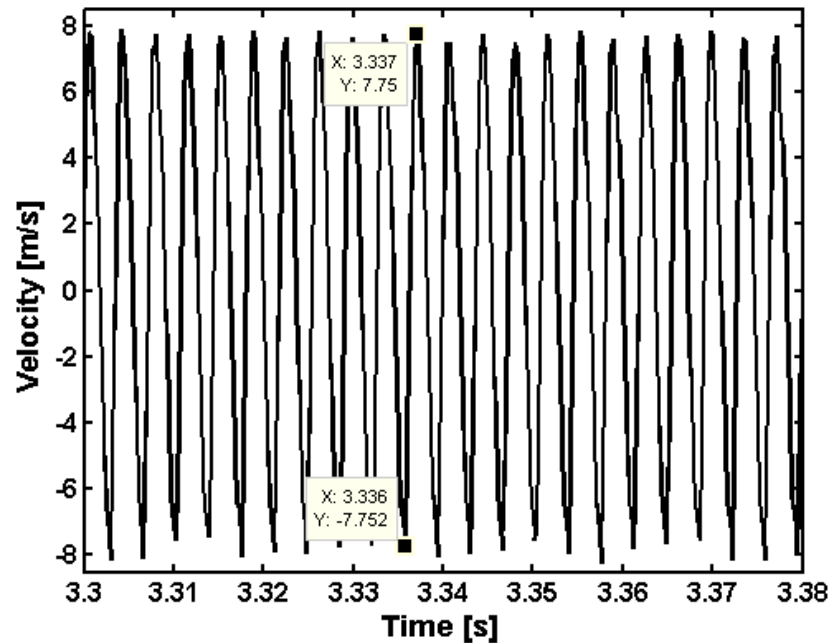
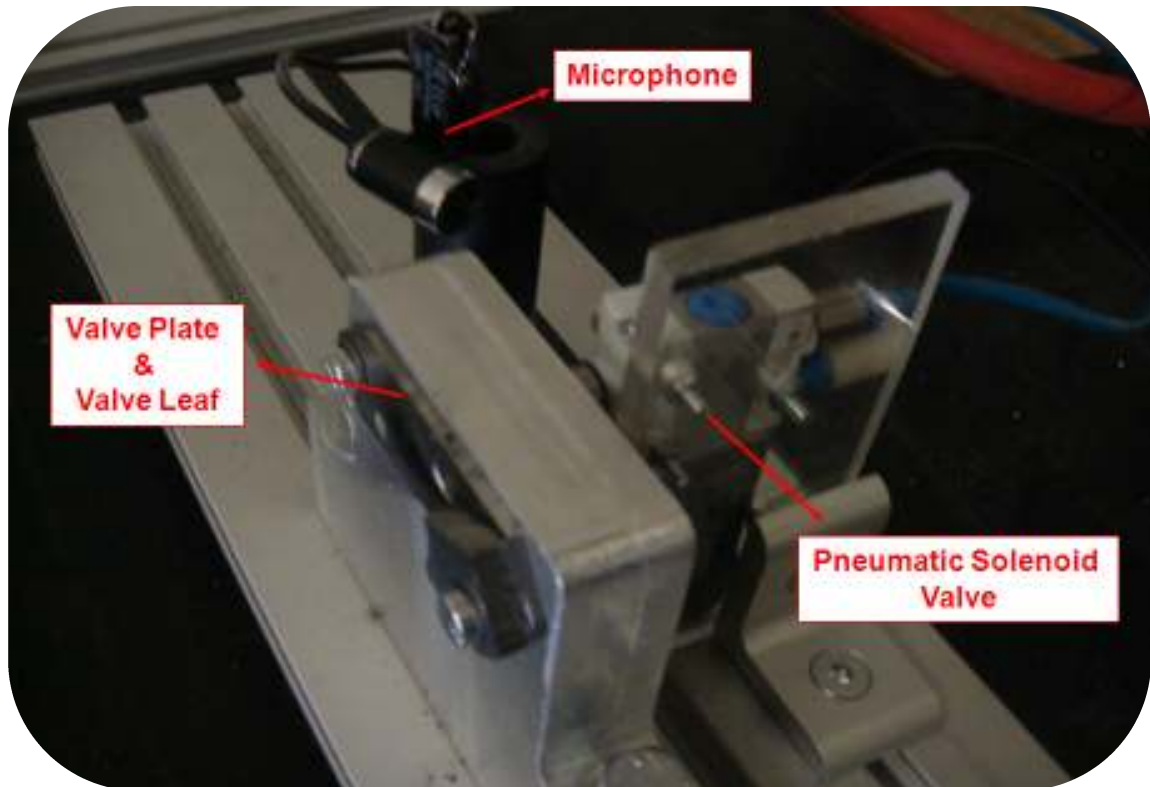


Figure 3.20. Pneumatic Experimental Setup maximum velocity measurement

### 3.5. Crack Detection Method:

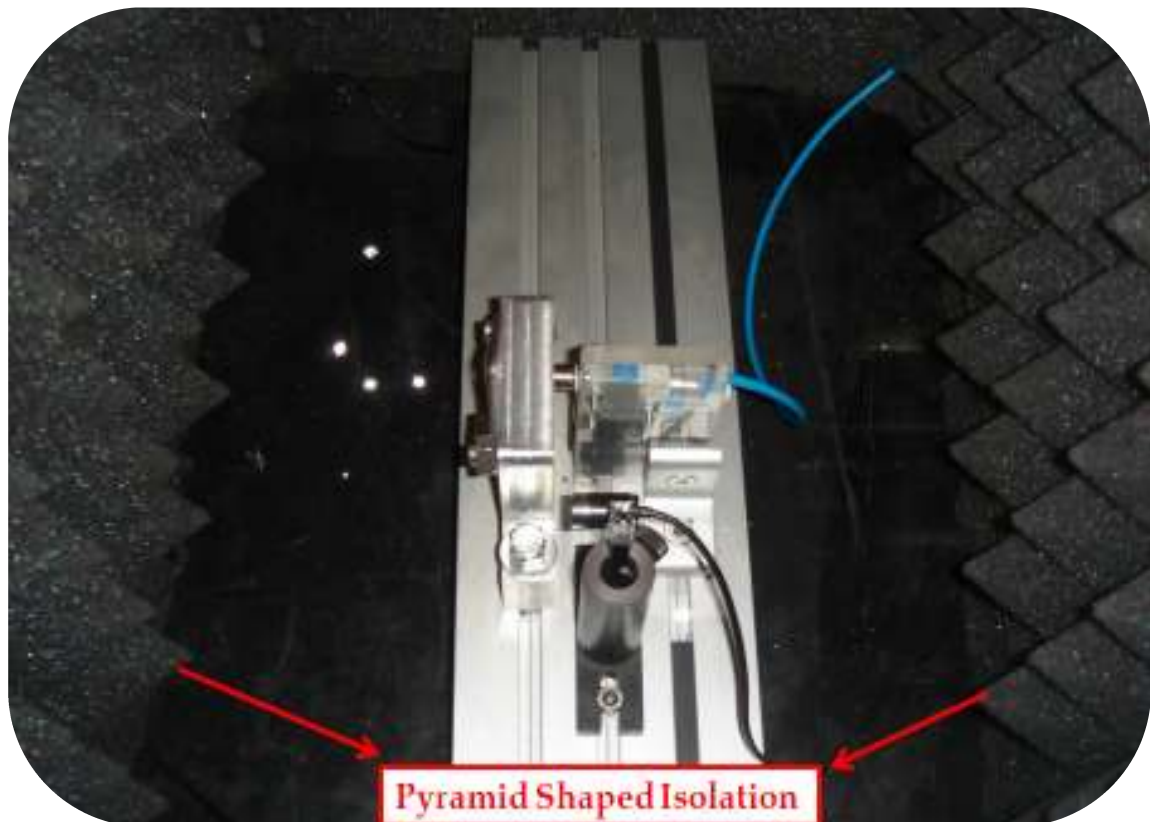
A crack detection technique was developed in order to discern the crack initiation during the experimentation process. Crack detection method based on a microphone which is acquiring the sound pressure generated by valve leaf impacts as shown in Figure 3.21. Microphone sound pressure input which is collected from the valve leaf repeated impacts on the valve plate, acquired and processed by LabVIEW software. The microphone sound level signal is proportional with the impact energy of the valve leaf. Acquired sound pressure in the time domain converted to the frequency domain by Fast Fourier Transform (FFT) in LabVIEW. The LabVIEW program detects the maximum amplitude at the actuation frequency.



**Figure 3.21. Crack detection system**

Since the sound pressure amplitudes tend to change as the crack initiates, the sound input data is compared with the following acquired input data at the actuation frequency. If the desired difference is obtained between the data, the program terminates the data acquisition and the impact fatigue lifetime of the specimen, corresponding date & time is displayed on the computer. Through the DAQ device a signal is generated automatically as the failure occurs and I/O connector block is used for signal connection from DAQ device. A transistor circuit connected to I/O connector block terminates the experimentation when a failure occurs.

The system is surrounded by a pyramid shaped isolation material shown in Figure 3.22 in order to isolate the system cabin from the external noise. As a consequence, the crack propagation stage could be set by controlling the sound pressure data difference in addition to that the impact fatigue life is obtained for the specimens precisely and further crack propagation is prevented by terminating the program. During the experiments, the data difference was set to 15% which was optimum value due to the experimental trials.



**Figure 3.22. Isolation method**

### **3.6. Experimental procedure**

The experiments were performed at room temperature in dry environment conditions. The impact velocity and displacement of the specimens, which characterize impact fatigue lifetime, were measured simultaneously with LDV. LDV measurements were performed on the center of the valve leaf impact region. The tests were performed at 250 Hz. When a fracture occurs at the edge of the specimen, the failure is detected by a microphone. The automated system prevents further damage on the specimen by terminating the test and the impact fatigue life of the specimen is recorded. Stroboscopic motion of the valve leaves during tests is displayed on the LCD screen with a CCD camera mounted in the LDV. The flowchart of the system is shown in Figure 3.23.

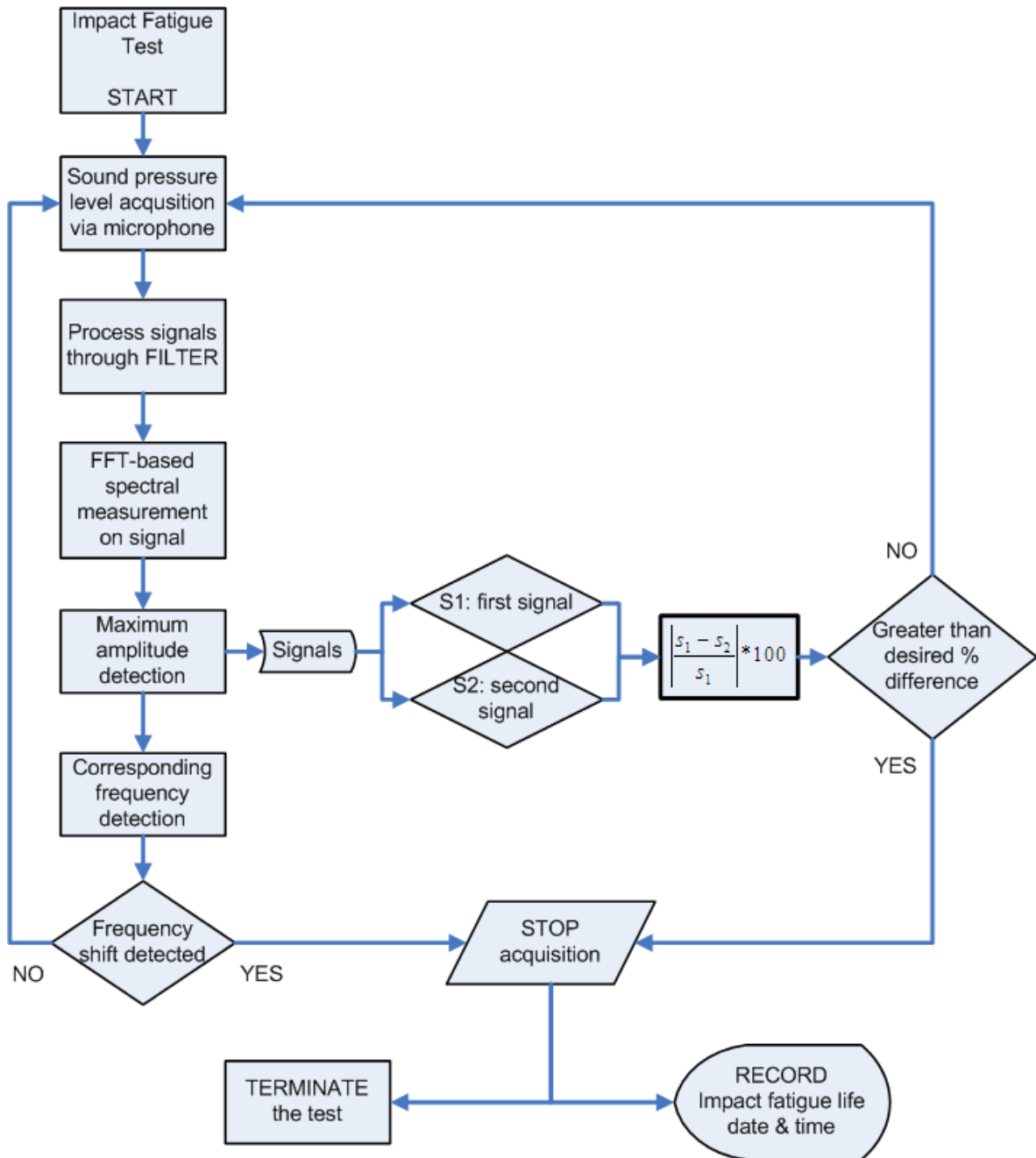


Figure 3.23. Flowchart of the system

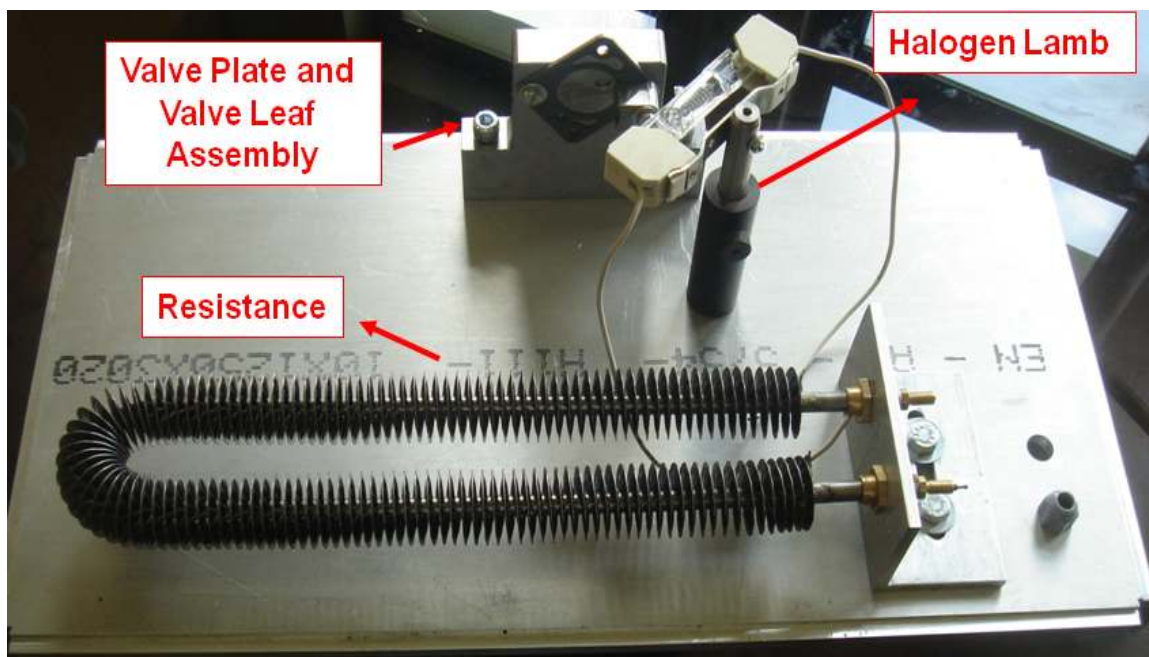
### 3.7. Temperature Control Cabin:

A temperature control cabin was designed to investigate the influence of the working temperature on the impact fatigue life of the compressor valve leaves. Beside the utilized tests at ambient temperature, the effect of working temperature at which the valve leaves are experienced in the compressor and were examined. Therefore, the experimental setup was placed in a cabin that was isolated from the environment in order to investigate the impact fatigue life in various temperatures. In the temperature control cabin, the impact fatigue life tests were performed at T1, T2 and T3 temperature levels.

Temperature control cabin includes an electrical resistance, halogen lamp, tempered glass windows, fuzzy logic temperature PID controller and K-type thermocouple (Figure 3.24, Figure 3.25 and Figure 3.26). Temperature control procedure includes a thermocouple which is in contact with the valve leaf, simultaneously measures the temperature of valve leaf and a temperature PID controller connected to the thermocouple. Electrical resistance and halogen lamp are adjusted due to the controlling action of the PID controller in order to reach the desired experiment temperature.

Since the operating fluid temperature range of the solenoid valve is between  $-5\text{ }^{\circ}\text{C}$  and  $60\text{ }^{\circ}\text{C}$ , the inlet air could not be preheated, so that the inlet air through the solenoid valve was at ambient temperature. Besides the electrical resistance, a powerful instant heating was directly exposed on the valve leaf by a 500 W halogen lamp. In addition, the thermocouple was hidden behind the valve leaf fixture (Figure 3.17) in order to prevent the halogen lamp instant heat exposure. In the temperature control cabin, a special tubing and push-in fitting combination was used in order not to avoid softening by the high temperature, in addition to that the equipments were located behind the steel valve plate

fixture in order to prevent instant heat exposure created by halogen lamp. Experimental cabin was surrounded by tempered glass which was impact resistant and resistant to thermal stresses. Applied stresses must first overcome the compression of the tempered glass, which was created by the tempering production technique, before any possible fracture. As a consequence, a reliable test system was provided.



**Figure 3.24. Temperature control cabin heaters**

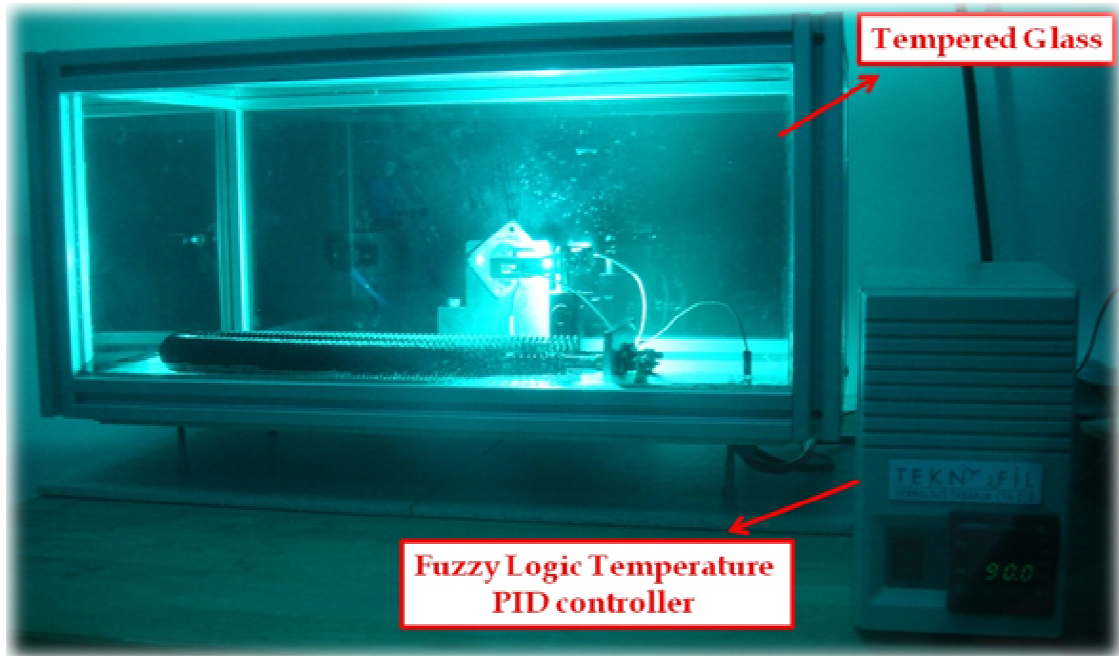


Figure 3.25. Temperature control cabin components

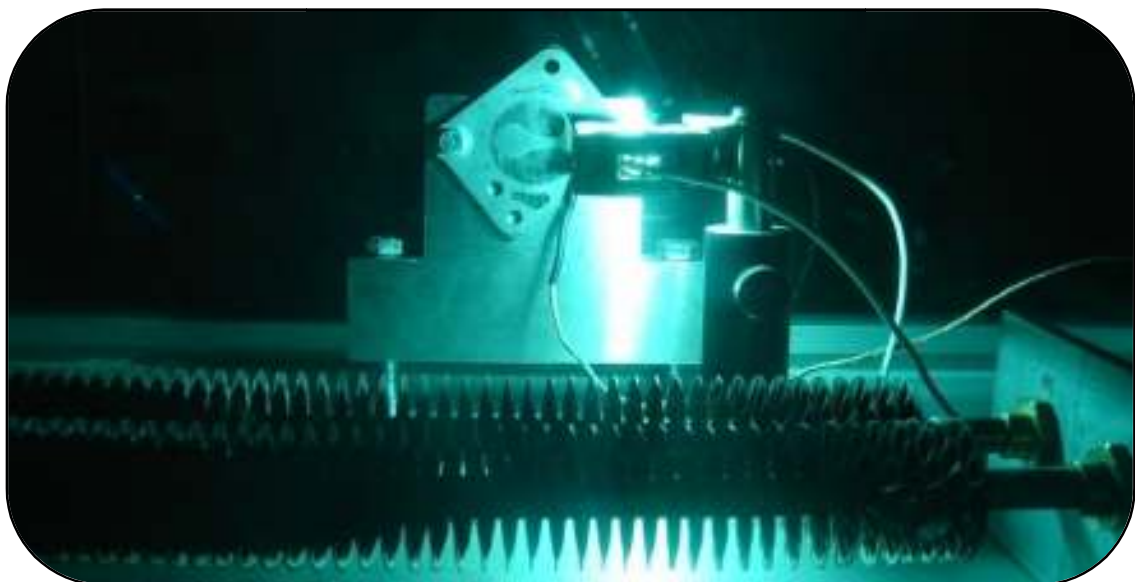
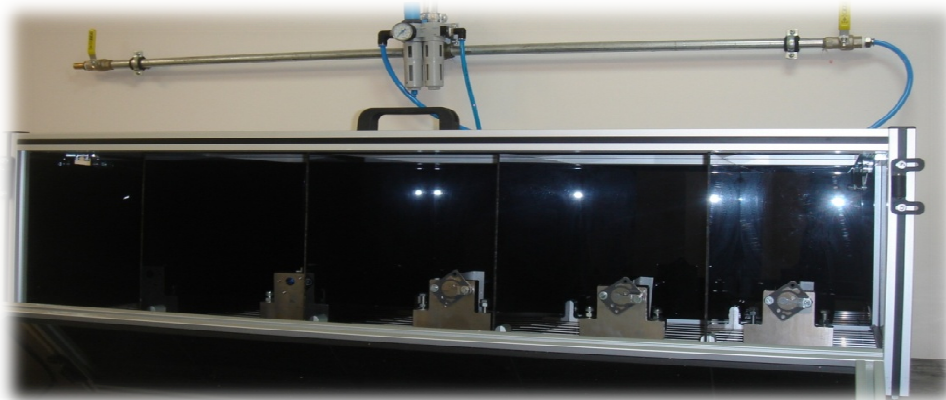


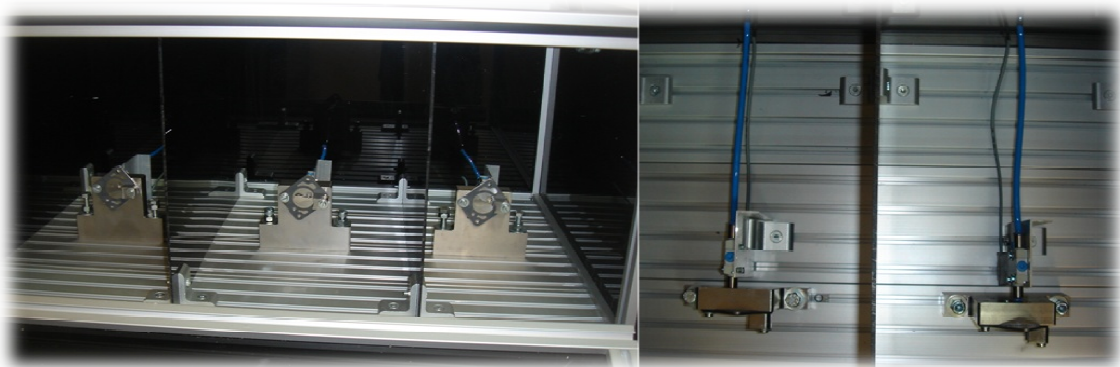
Figure 3.26 Temperature control cabin zoomed view

### 3.8. Multi - Station Experimental Setup:

A multi-station experimental setup is designed in order to test five specimens simultaneously and decrease the experiment duration. Main inlet air is divided five parts with multiple distributor fittings. Inside the setup, each test ring is separated with a window to prevent the air vibrations created by the solenoid valve air waves. Thus, each section is treated as an individual volume. The multi-station experimental setup is showed in Figure 3.27.



**Figure 3.27. Multi-station experimental setup**



**Figure 3.28. Multi-station experimental setup detail**

### 3.9. Reciprocating Setup:

In the reciprocating compressor cycle, after the piston reaches the final position, piston started to move inverse direction. The suction valve closes in order to avoid the refrigerant travel inside the cylinder. Pressure of the refrigerant is increased by the compression which is created by the piston. The pressure applied by the refrigerant forces make the exhaust valve open at a certain point and the compressed refrigerant flows out of the cylinder. As the piston reaches its final position on the suction valve, piston moves reversely and the cycle repeated.

A reciprocating test system was introduced for investigating the exhaust valve leaves. In contrast to the suction valve leaf occupied in the low pressure side of the refrigeration cycle, exhaust valves occupied in the high pressure side exposed to high pressure differences and high stresses. A valve stopper called retainer is mounted on the valve plate in order to maintain the closing of the exhaust valve leaf in time and prevent back leakage and over opening of the valve leaf. On the other hand, retainer is not used in the suction valves to prevent a death volume inside the cylinder. In the exhaust valve experiments, retainer creates a constraint for reaching high impact velocities because the stopper obstructs free opening of the valve leaf.

Reciprocating experimental setup was designed to overcome the restriction. The valve impact region of the retainer was drilled to provide a hole where second solenoid outlet tubing can be placed, so that two solenoid valves were working synchronous. As seen in Figure 3.30, a solenoid valve, located at the valve plate orifice, was responsible for opening the exhaust valve, and in opposite side second solenoid valve was responsible for increasing closing impact velocity of the valve leaf. Designed experimental setup formed a

reciprocal work. Synchronous working was obtained with a transistor circuit located between the solenoid valves.

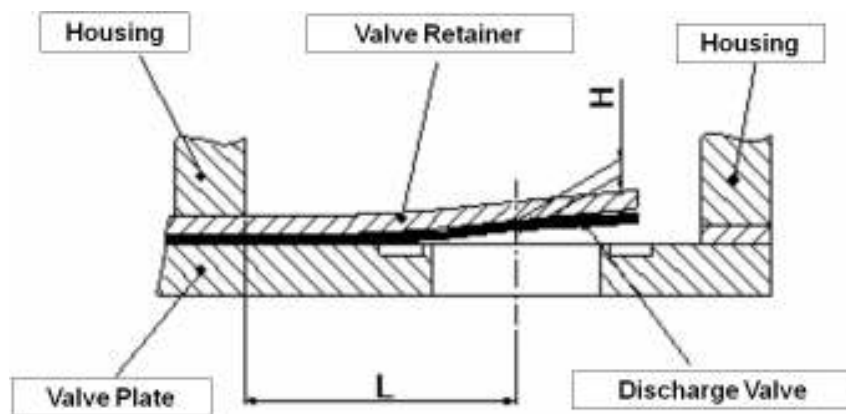


Figure 3.29. Basic shape of exhaust valve [32]

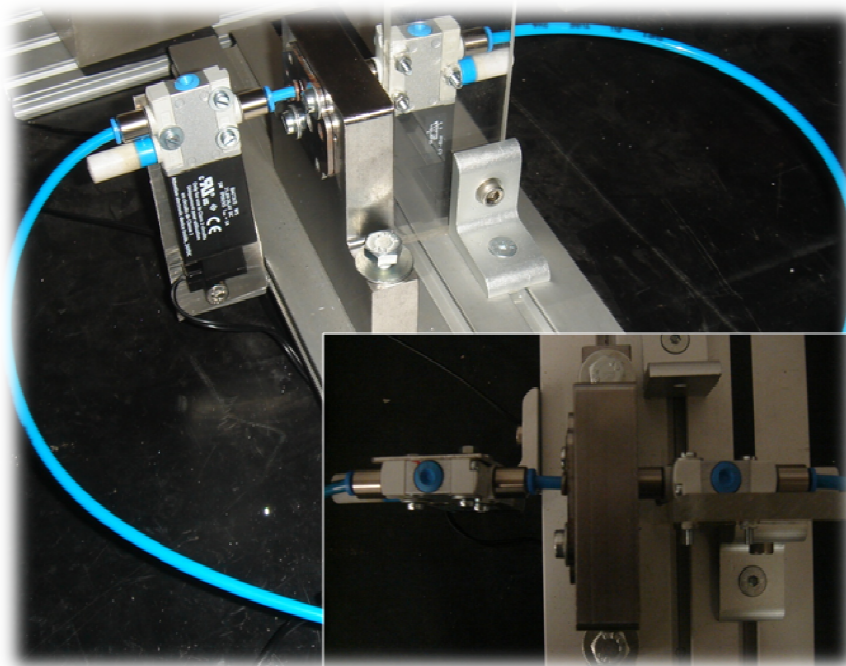


Figure 3.30. Reciprocating setup

### **3.10. Specimen Preparation Procedure for Scanning Electron Microscope (SEM):**

Specimen preparation procedure is important in SEM observations in order to define the microstructure near the crack tip and original valve leaf. Specimen preparation should satisfy conditions for metallographic observations, which are;

- The prepared specimen must be representative of the main body,
- Structural elements must be remained on the specimen,
- The prepared surface must be purified from scratches, no deformation,
- Specimen surface must be lack of foreign matters,
- The flatness and reflectiveness of the specimen must be provided [33].

The procedure for metallographic specimen preparation includes: ultrasonic cleaning, mounting, planar grinding, rough polishing, final polishing, etching and SEM analysis.

#### **3.10.1. Ultrasonic Cleaning:**

The first step of the preparation procedure is ultrasonic cleaning. The cleaner machine is integrated with ultrasonic generator and cleaning tank in an enclosure. Ultrasonic pre-cleaning operation removes the residual dirt on the specimen surface as a non-destructive method. Specimens are cleaned in 15 minutes prior to mounting which is the second step of preparation. The valve leaf surface is cleaned from grease and other contaminants, which lead to the best adhesion of mounting material to sample. Specimens are washed with alcohol as a final operation.

### 3.10.2. Mounting:

Valve leaf specimens were embedded in resin, mounting powder to facilitate handling during preparation process. Since the entire part of the valve leaf was investigated and specimens were needed protection of layers, hot mounting was applied. Hot mounting (also called hot compression mounting) provided a uniform distribution of mounting material, high quality and short process time.

Mounting operation was done in Struers / Prontopress-2 machine. Hot compression of bakelite powder is done at 25 kN. The total process duration was 21 minutes. The first stage duration was 13 minutes for heating the bakelite powder and the second stage duration was 8 minutes for cooling.



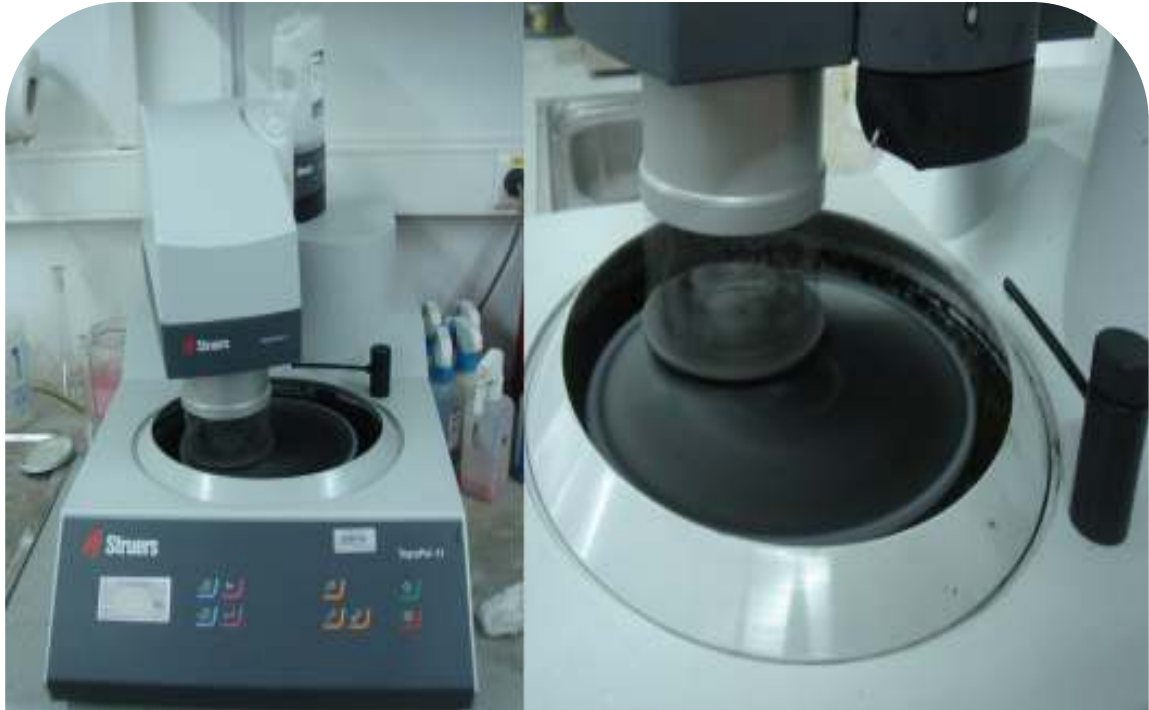
**Figure 3.31. Specimens with mounting technique**

### 3.10.3. Grinding and Polishing:

Planar grinding is the third step of metallographic specimen preparation. The grinding operation performed with a fixed abrasive which is bonded physically to a special cloth. Removing plastic deformation which is induced into the specimen surface after the experiments is the main goal of the grinding. Maintaining the plane surface of the specimen is mandatory for subsequent operations and SEM observation. Plastic deformation, which is created by the grinding operation, forms scratches on the specimen surface. The scratches must be cleaned by the subsequent polishing steps.

During the plane grinding operation with MD-Piano<sup>TM</sup>, water is used as a coolant. The purpose of the coolant is to carry away debris caused by grinding and prevent heating of the specimen to a point where the microstructure is altered. In grinding operation, using water as a coolant minimize the alteration of microstructure and extend the life of the grinding belt [34]. The second step was fine grinding with MD-Allegro<sup>TM</sup> and DiaPro as diamond suspension.

The last step of the mechanical preparation step is polishing. The polishing was performed with MD-Plus<sup>TM</sup> and DiaPro Plus as diamond suspension. The main objective is to remove any scratches on the interest area and provide a flat surface. The most important point is to retain the crack regions after polishing to observe microstructure after the experiments. Optimum operation speed, duration and force must be applied in order to maintain the specimen edge retention.



**Figure 3.32. Mechanical preparation machine**

The grinding and polishing operation is carried out by Struers TegraPol-11 & TegraForce-1 grinding/polishing machine (Figure 3.32). The details of the mechanical preparation procedure are shown in Table 3.

**Table 3: Grinding and polishing procedure**

Operation	Speed [rpm]	Duration [min]	Force [N]	Coolant
Plane Grinding	150	10	20	Water
Fine Grinding	200	3	25	-
Final Polishing	250	12	25	-

#### **3.10.4. Etching:**

In the etching stage of specimen preparation, the main purpose is to reveal the microstructure of the specimen with a selective chemical interaction by using an etchant. Etching method enhances the microstructure features such as grain size and phase features, in addition to that microstructure features based on the composition, crystal structure is altered by selectively etching.

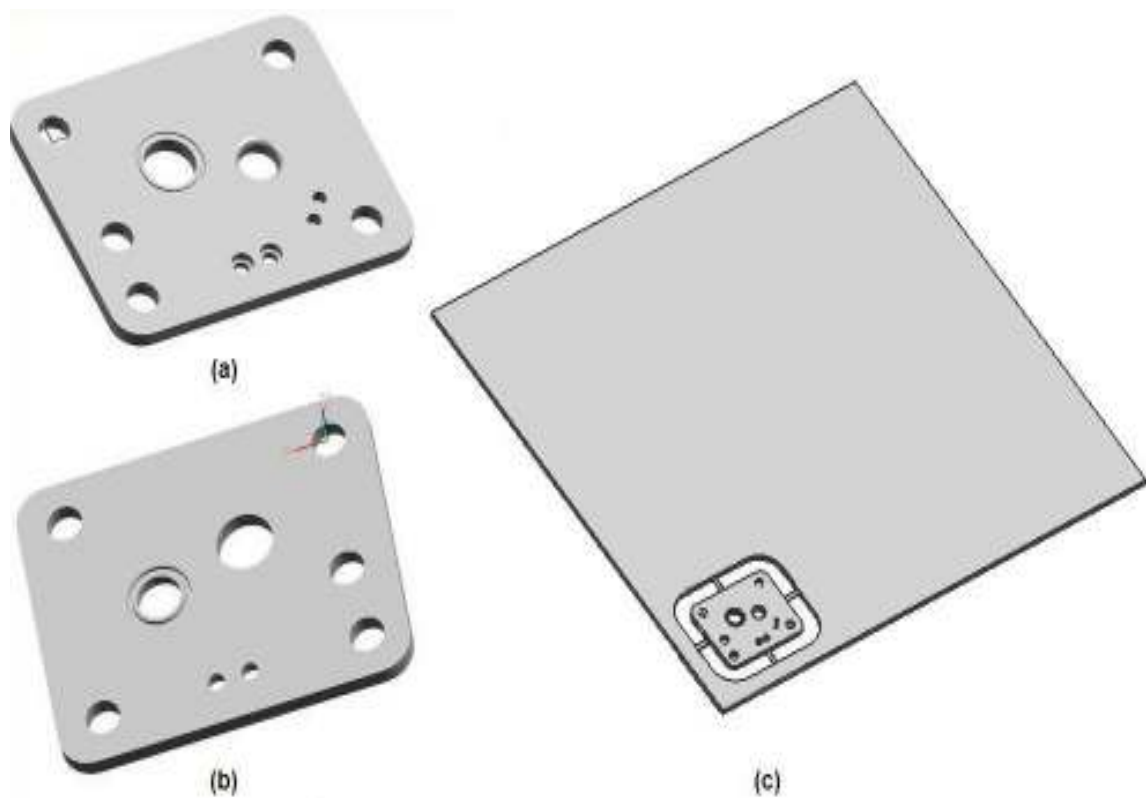
Etchant choice and the application duration is the most important point of the etching operation. In the SEM observations, Carbon Strip Steel is investigated in terms of microstructure. 2 % Nital (a mixture of nitric acid and ethanol, methanol, methylated spirits) etchant is applied for 10 seconds for observation on optical microscope and 30 seconds for SEM. After application of etching, the specimen must immediately be washed in alcohol and dried with a pressurized air.

#### **3.11. Valve Plate Prototype:**

Beside investigations of the parameters directly related with the compressor valve leaf, the design parameters of valve plate have an influence in valve leaf impact fatigue life. Main design parameters of the valve plate, which influence the impact fatigue life of the valve leaf, are cylinder orifice diameter, groove region inner diameter and corresponding blend radiuses. The valve plate prototype is produced. In this chapter, manufacturing process of the valve plate prototype is presented.

### 3.11.1. Computer Aided Design (CAD):

The valve plate solid model is formed by CAD software Unigraphics® (UG) in order to perform the Computer Aided Manufacturing (CAM) procedure (Figure 3.33 a and b). The valve plate model was implemented into 30 x 30 x 2.5 mm plate as seen from Figure 3.33 (c) and the valve plate features were created by UG NX feature modeling in order to prepare the solid model to the following step, CAM.



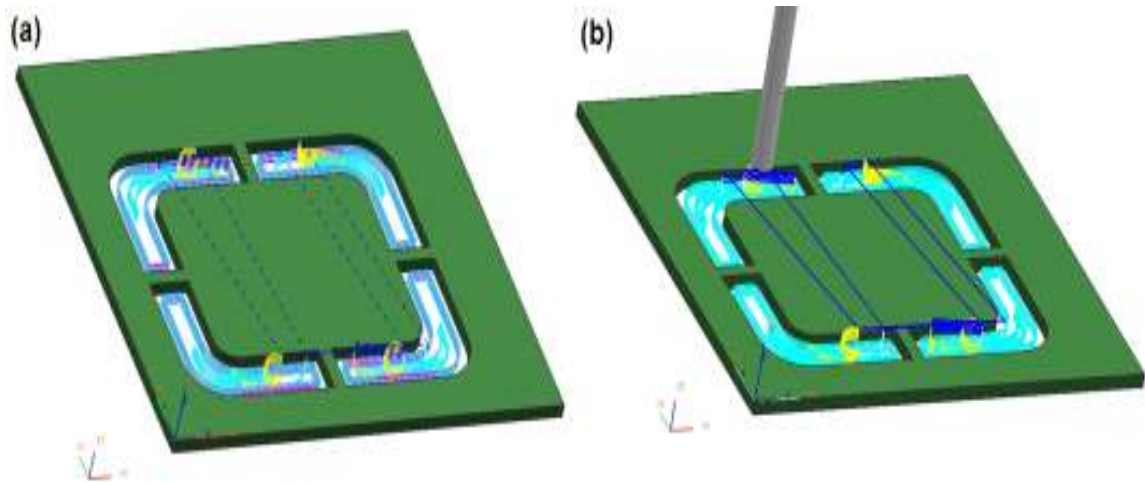
**Figure 3.33. Valve plate solid model (a) Top view (b) Bottom view (c) CAM model**

### 3.11.2. Computer Aided Manufacturing (CAM):

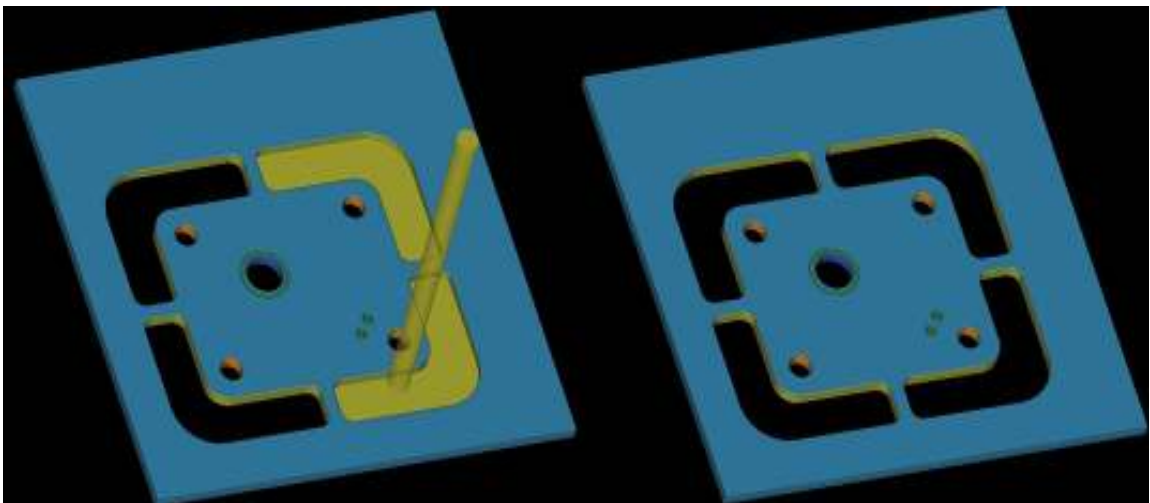
Computer-Aided Manufacturing (CAM) is programming tool in the translation of computer-aided design models into manufacturing instructions for numerical controlled machine tools. CAM system converts the 3D designs into the computer controlled process.

A text file, called G-Code, is generated by the CAM software as an output and is transferred to the numerical controlled machine tool in order to perform the machining operation. Unigraphics® CAM module is used to generate G-Code text file. In the manufacturing module, first the workpiece, cut regions and tool path were defined as seen in Figure 3.34, after that the road map of machining is formed by selecting type of the tool and diameter, tool path, machining process and stage. The parameters are implemented into the G Code generated by the software. The G-codes were simulated in Unigraphics® CAM module. G-Code text file is controlled due to prevent any malpractice of the CAM tool. The simulation of the machining process is demonstrated in Figure 3.35.

Valve plate prototype is manufactured by Mazak FJV-200 UHS Vertical Machining Center (VMC) with 25000 rpm spindle motor (Figure 3.37). The valve plate, which is machined from 2.5 mm cold drawn steel plate, includes two manufacturing stages roughing and finishing.



**Figure 3.34. CAM (a) Tool path generation (b) Tool Path Verification**



**Figure 3.35. Machining process simulation**

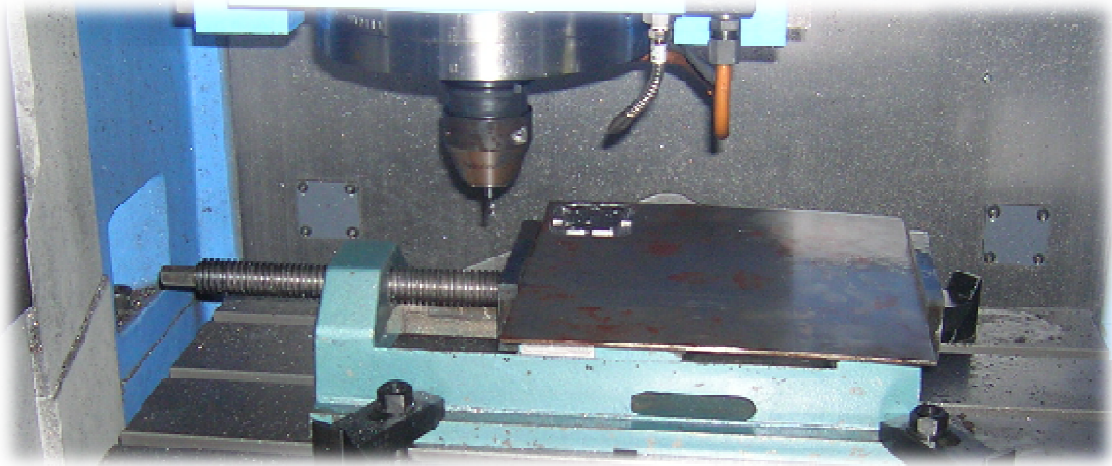


Figure 3.36. Valve plate machining operation



Figure 3.37. Mazak FJV\$200 UHS Vertical Machining Center

### 3.11.3. Surface Quality:

After the machining operation, surface roughness must be satisfied with the upper limit in the technical drawing of the valve plate. The surface roughness is quantified by the vertical fluctuations of the machined surface compared to the ideal part surface. The surface roughness, which is the measure of the machined part texture, is undesirable. Measurements were carried out by Mitutoyo SJ-301 surface roughness machine, as seen in Figure 3.39, in both machining direction and perpendicular to the machining direction (Figure 3.38).

Roughness average (Ra) is an international parameter for surface roughness and Ra is also known as the arithmetic mean roughness value, AA (arithmetic average). In the figure Figure 3.40, the surface profile of the part after machining is presented and roughness average value (Ra) is calculated (Table 4).

$$R_a = \frac{1}{L_s} \int_0^L |Y(x)| dx$$

(3.2)

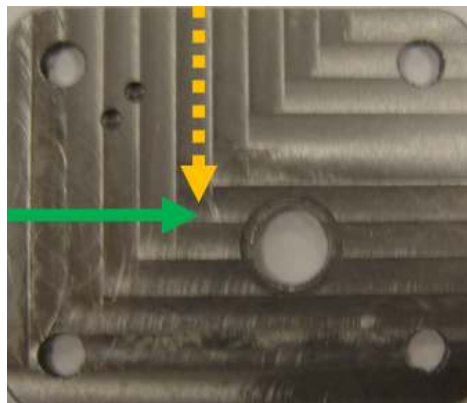
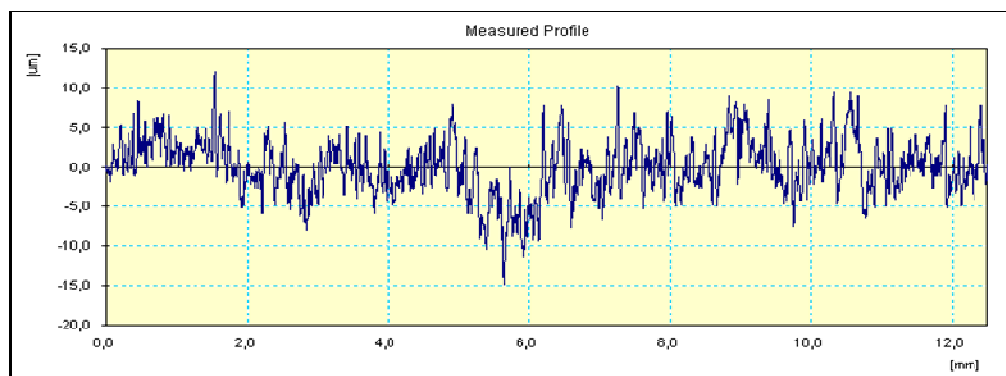


Figure 3.38. Surface roughness measurement directions


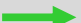


**Figure 3.39. Surface roughness measurement**



**Figure 3.40. Valve plate surface profile after machining**

**Table 4: Roughness Average (Ra) of valve plate surface after machining**

<u>Valve Plate Surface Roughness</u>		
 Machining Direction	Ra	2.32 µm
 Perpendicular to Machining Direction	Ra	2.98 µm

## **Chapter 4: Results and Discussions:**

### **4.1. Introduction:**

The chapter includes the results of the investigations on the impact fatigue characteristics of the compressor valve leaves. First, the valve was characterized in terms of resonance frequency and stiffness both experimental and simulation. After that the valve leaf impact velocity is mapped and the valve leaf impact motion is stroboscopic displayed with frames. In addition to that the original microstructure of the carbon strip steel used in compressors is visualized.

After the valve leaf characterization section, the parameters which influence the impact fatigue life of the compressor valve leaves presented. The impact velocity, asymmetrical impacts, temperature effect and manufacturing process effect on the impact fatigue life of valve leaves are investigated. The impact fatigue lives of three different materials were compared and the crack propagation was microscopically observed.

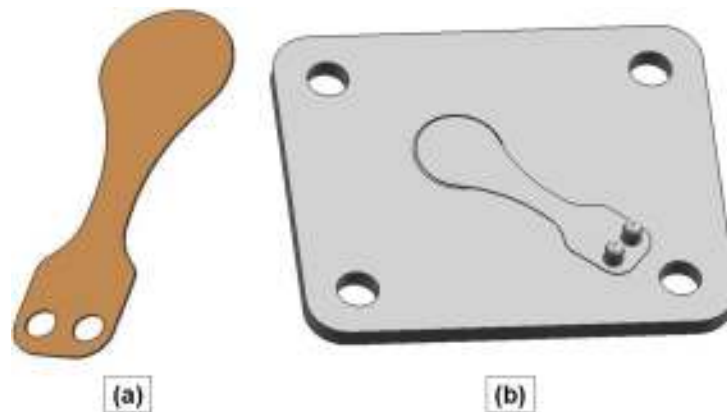
Finally fractographic, Scanning Electron Microscope (SEM) and metallographic observations are presented in order to define the crack initiation and propagation mechanism caused by impact fatigue.

## 4.2. Valve Leaf Characterization:

The compressor valve leaf was characterized due to the investigations on the impact fatigue properties. The solid model of the valve leaf was drawn for the Computer Aided Engineering (CAE) stage. The average values of dimensions, which were come from the tolerances, were used in solid model drawing and further simulations. Stiffness and resonance frequency of the valve leaf is determined experimentally and satisfied via simulation. Finally, impact velocity mapping and microstructure of the valve leaf is presented.

### 4.2.1. CAD:

The compressor valve leaf was modeled by CAD software Unigraphics® (UG) in order to apply the Computer Aided Engineering (CAE) procedure. The solid model of the valve leaf was implemented into the Finite Element Analysis (FEA) software, ANSYS. The solid model of the valve leaf and valve leaf – plate assembly are shown in Figure 4.1.



**Figure 4.1. (a) Valve leaf solid model (b) Valve leaf & plate assembly**

#### 4.2.2. Resonance Frequency:

The resonance frequency of the valve leaf was determined experimentally by sweeping valve leaf frequency and the observed maximum amplitude was defined as the resonance frequency (Figure 4.2). In addition, the resonance frequency was calculated via simulation in FEA software, ANSYS (Figure 4.5). As a conclusion, both results were close to each other.

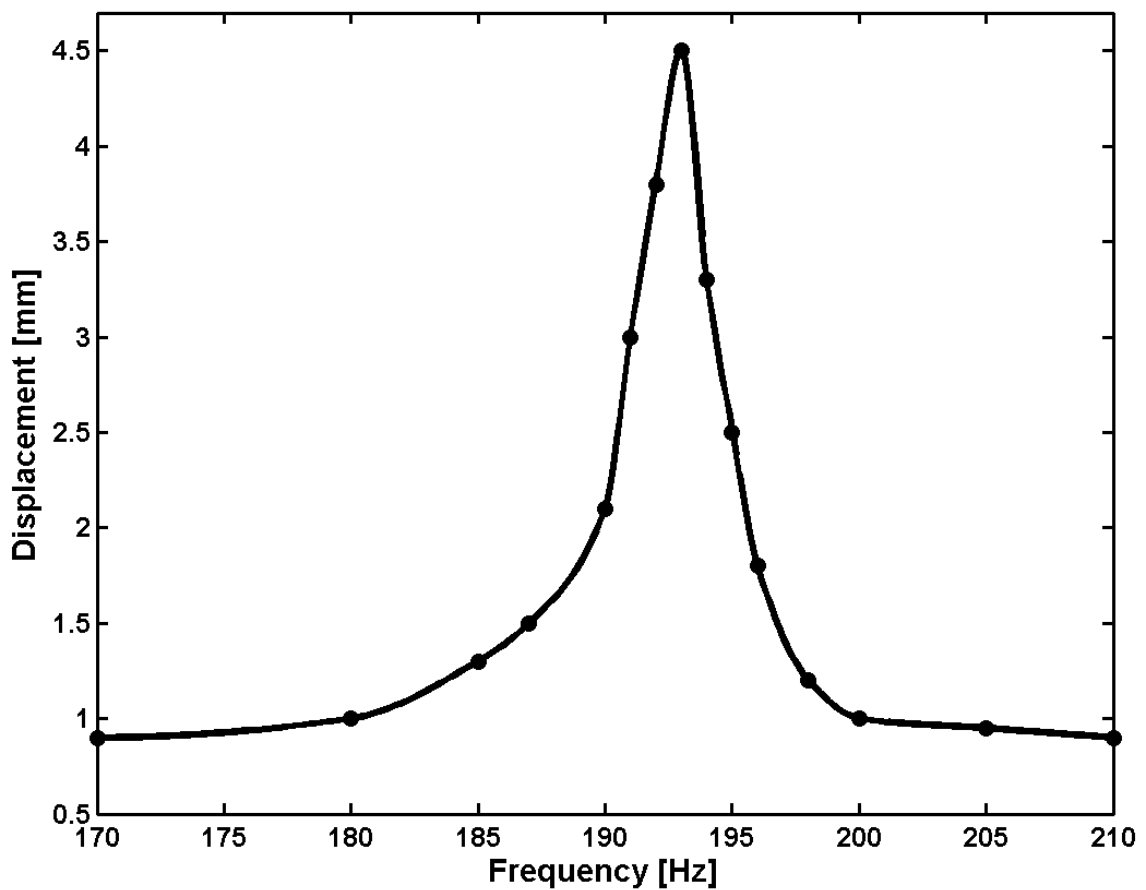


Figure 4.2. Experimental resonance frequency

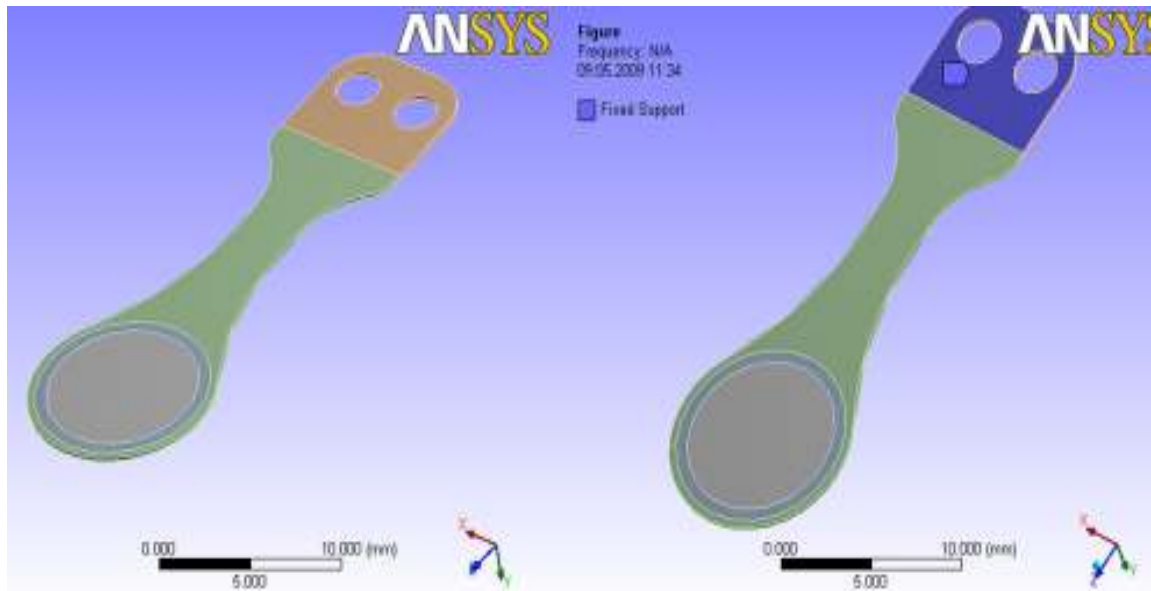


Figure 4.3. Solid model for CAE

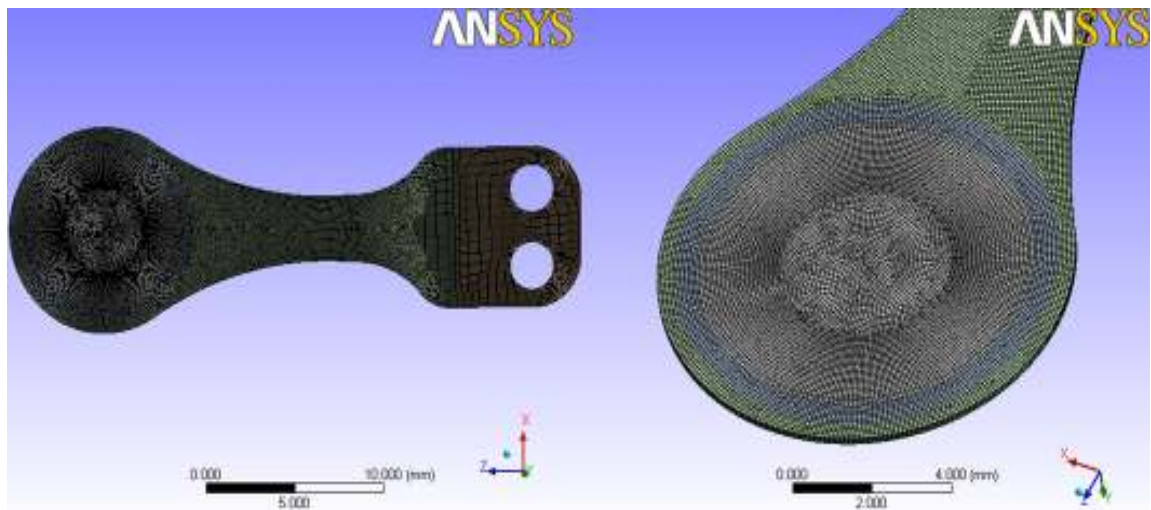


Figure 4.4. Solid model meshing with element size 0.1 mm

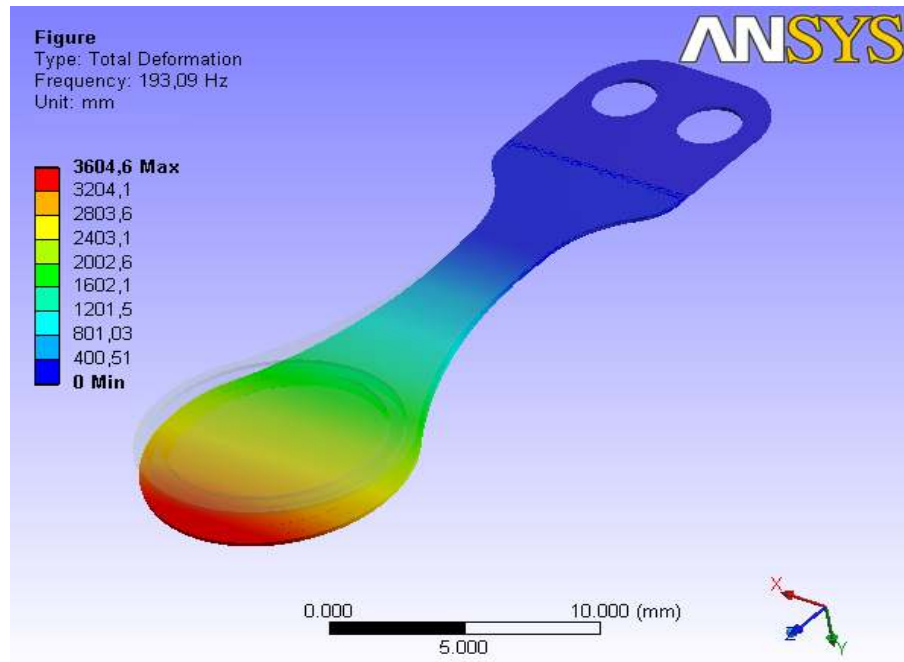


Figure 4.5. Simulated resonance frequency

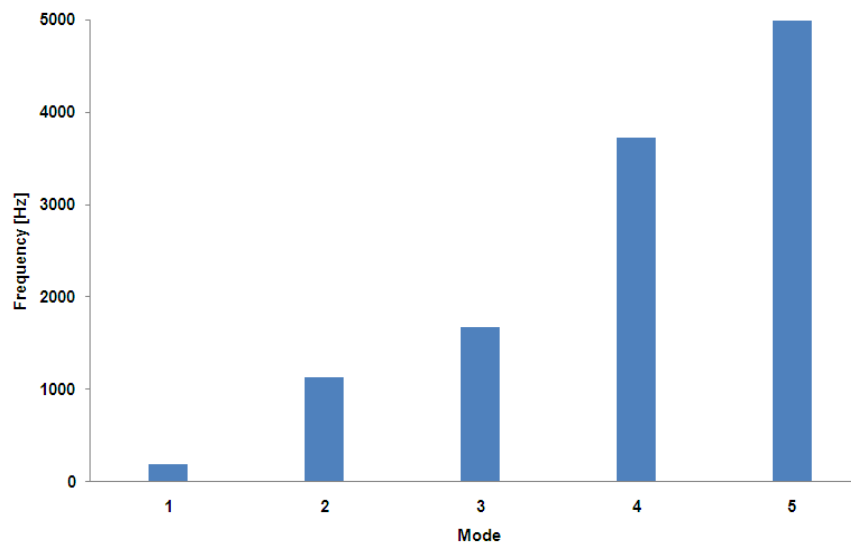


Figure 4.6. Modes and corresponding frequencies

### 4.2.3. Stiffness:

Another important characteristic of the valve leaf is stiffness which related to the applied force on the leaf and the corresponding displacement. Stiffness was obtained both experimentally and simulation. Experimental stiffness value was determined by applying force on the center of the valve leaf impact region and the displacement values are measured with Laser Doppler Vibrometer. Simulation stiffness was calculated by applying force on the center of the valve leaf impact region. Applied force increments and the corresponding deflection were obtained through the ANSYS. Applied force was plotted versus displacement of the valve leaf and the slope of the plot was the stiffness of the compressor valve leaf. Experimental stiffness was calculated as  $k_{\text{exp}} = 0.1590$  N/mm from Figure 4.7, on the other hand the simulated stiffness was obtained from the simulation as  $k_{\text{sim}} = 0.1643$  N/mm from Figure 4.8. The calculated experimental stiffness and simulated stiffness were close.

$$k = \frac{m_a * g}{\delta} = \frac{P}{\delta}$$

(4.1)

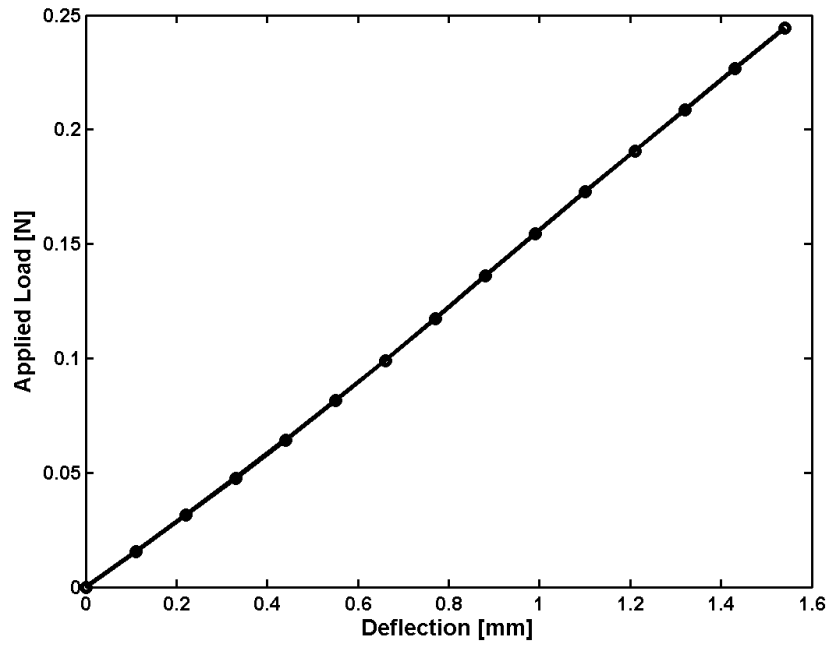


Figure 4.7. Experimental stiffness calculation

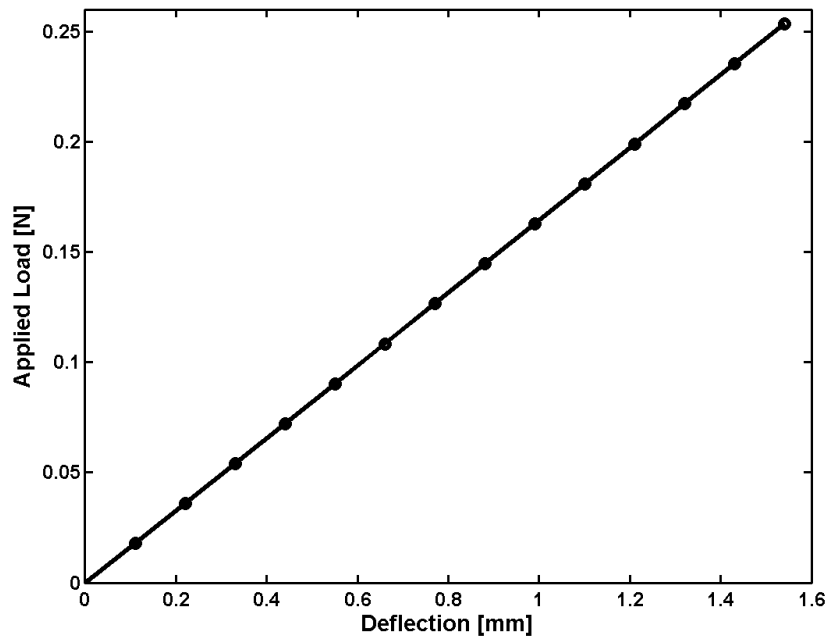


Figure 4.8. Simulation stiffness calculation

#### 4.2.4. Valve Leaf Impact Velocity Mapping:

Since the valve leaf and the valve plate are manufactured by fine blanking operation, tolerance values are defined for the parts. In addition to the tolerances the close fit part, which is fitted on the valve plate and used in assembling the valve leaf, contributed the tolerance scattering. Impact velocity mapping was done on the valve leaf impact region shown in Figure 4.9. In Figure 4.10, the velocity LDV measurement nodes were presented. Through the nodes, the valve leaf impact surface was meshed and the measured velocity data is represented as the z-direction height and colored as seen in Figure 4.12 and Figure 4.13.

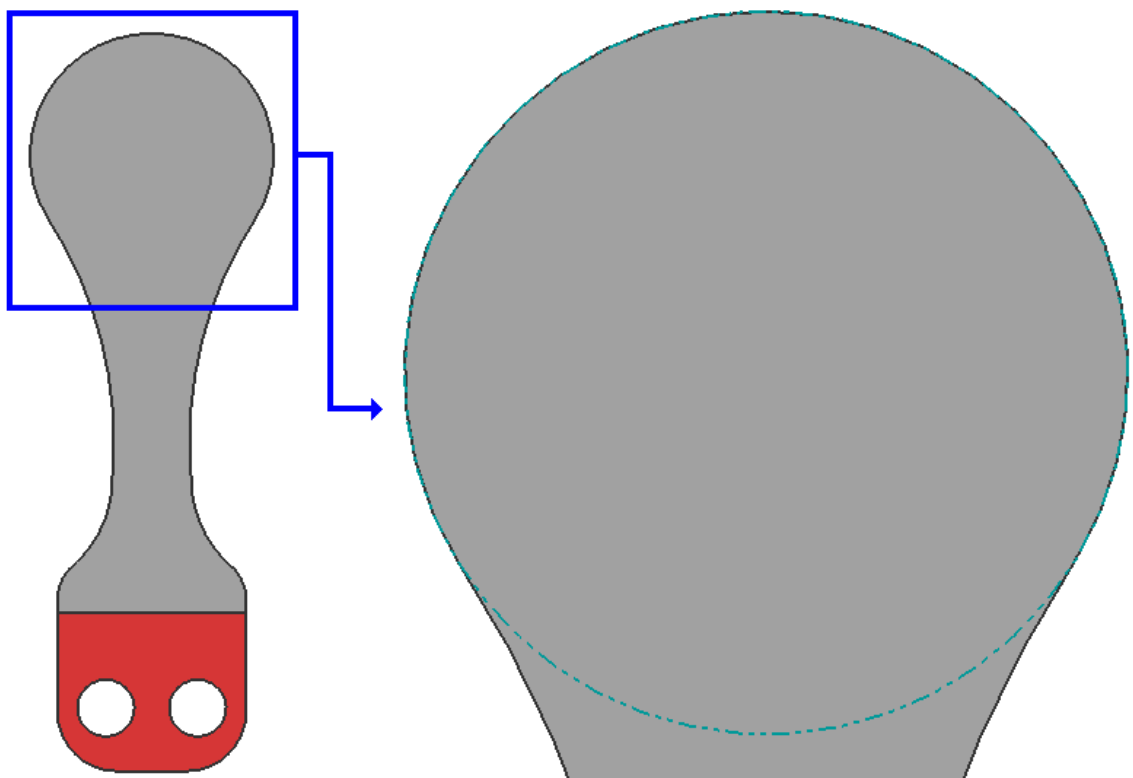


Figure 4.9 Valve Leaf impact region

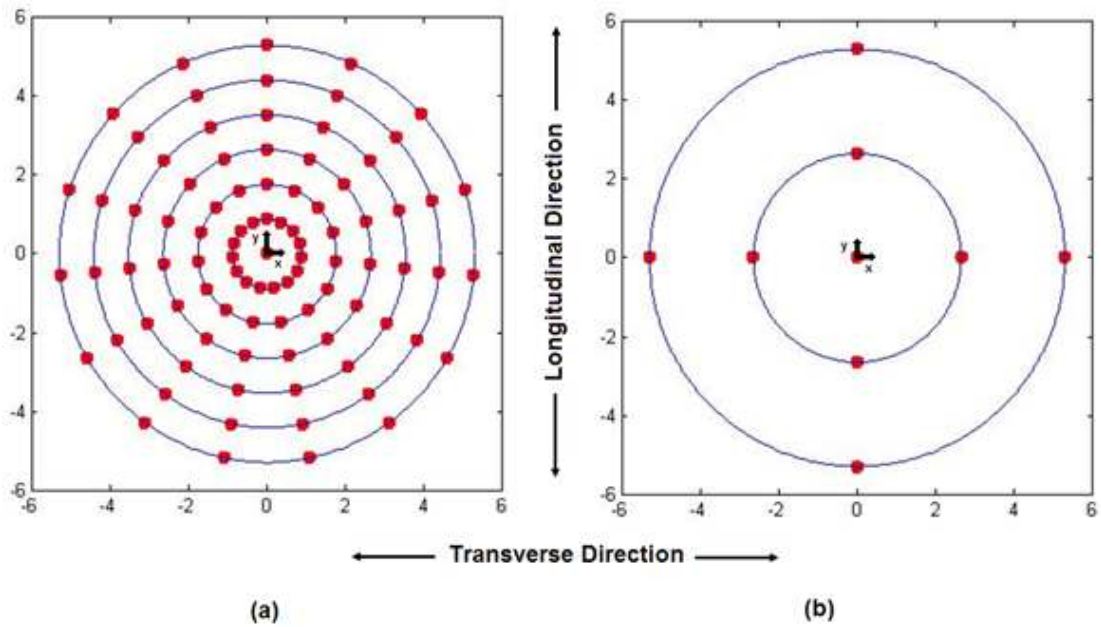


Figure 4.10. Valve Leaf (a) Impact region nodal representation (b) Measurement nodes (coordinates in [mm])

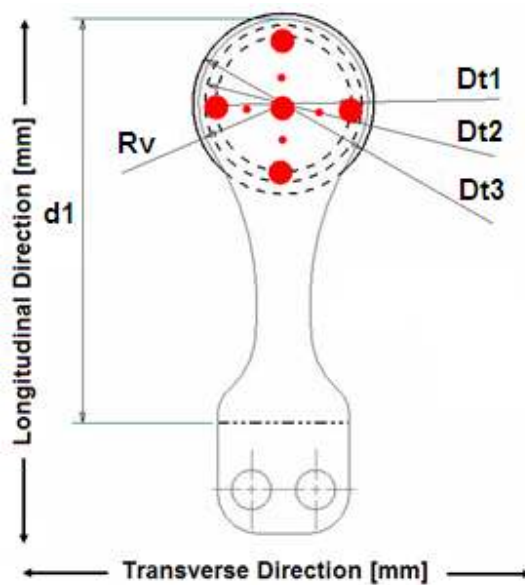


Figure 4.11. Impact velocity measurement on the valve leaf

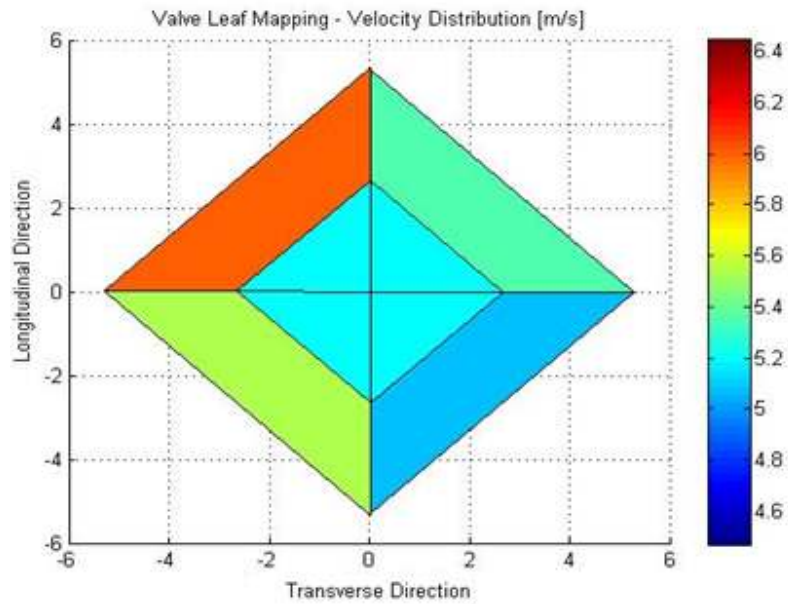


Figure 4.12. Valve leaf mapping - velocity profile

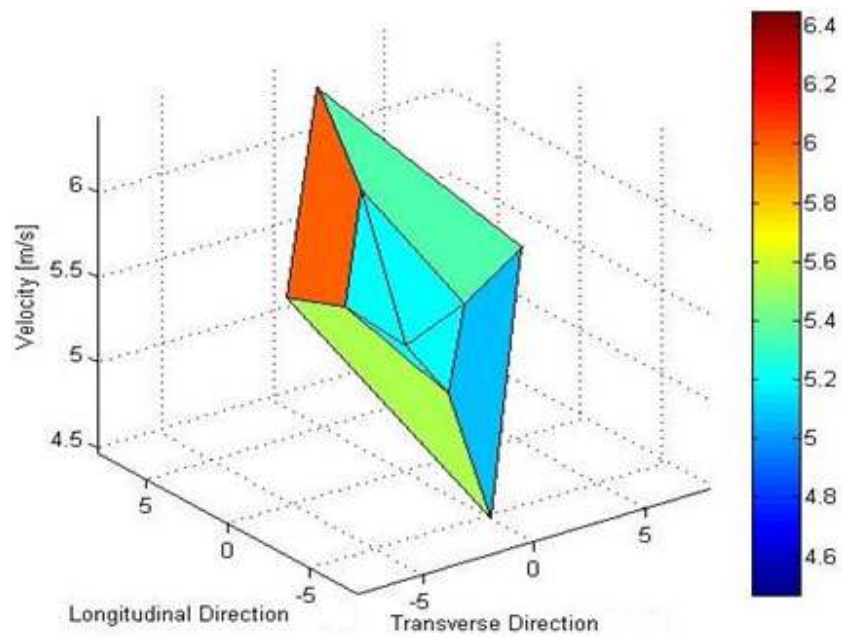


Figure 4.13. Valve leaf impact velocity mapping

#### **4.2.5. Stroboscopic Display of Impact:**

The impact motion of the valve leaf was stroboscopic displayed by using a stroboscope in order to make the cyclically motion of the compressor valve leaf appear to be slow-moving object. The approach offered a better understanding of the high frequency working of the valve leaf. The frequency of the stroboscope flash was adjusted to a unit fraction of the valve leaf working frequency and synchronization with the valve leaf is done. The illusion was a result of temporal aliasing (stroboscopic effect). The stroboscopic method provided an understanding in the motion of the valve leaf, crack initiation and propagation observations. The stroboscopic image frames are shown below for one cycle in Figure 4.14 and Figure 4.15.

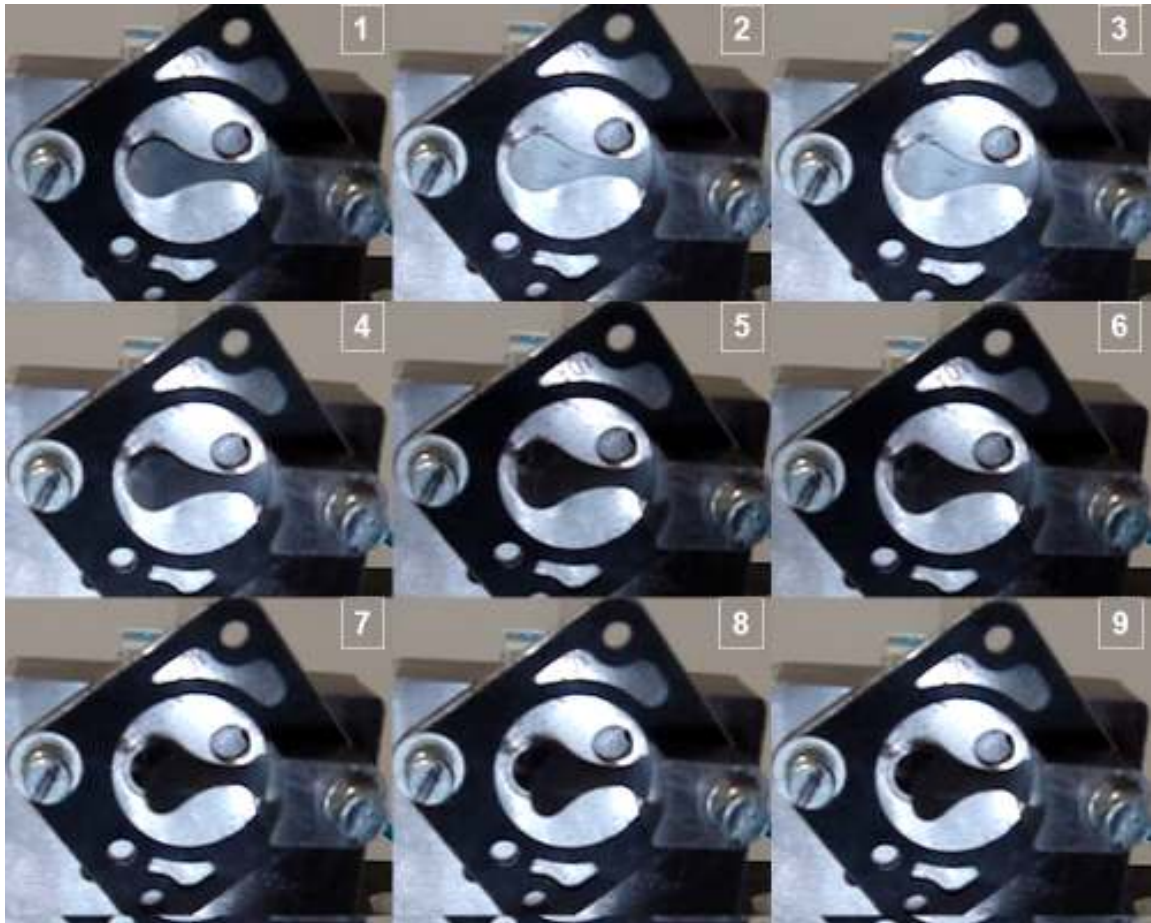
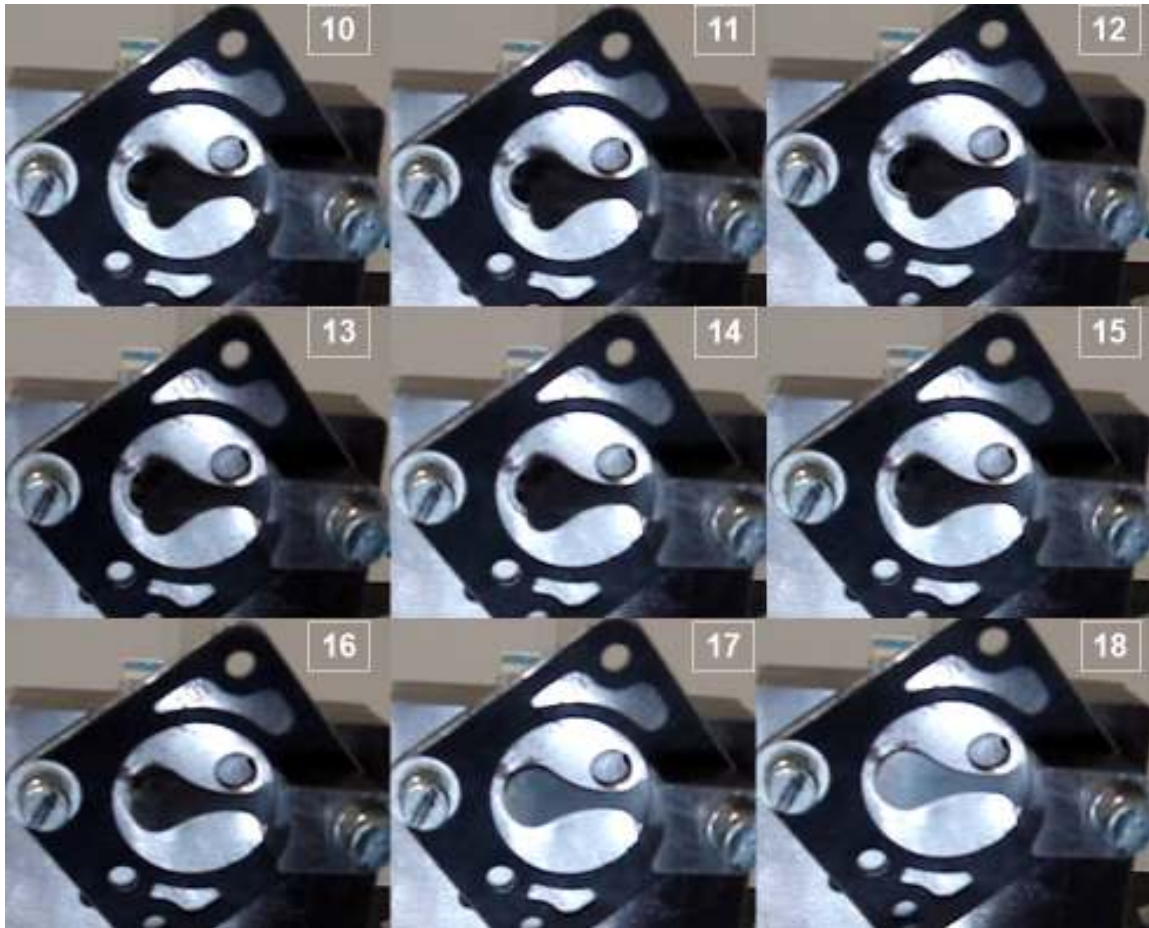


Figure 4.14. Stroboscopic image frames part (1)

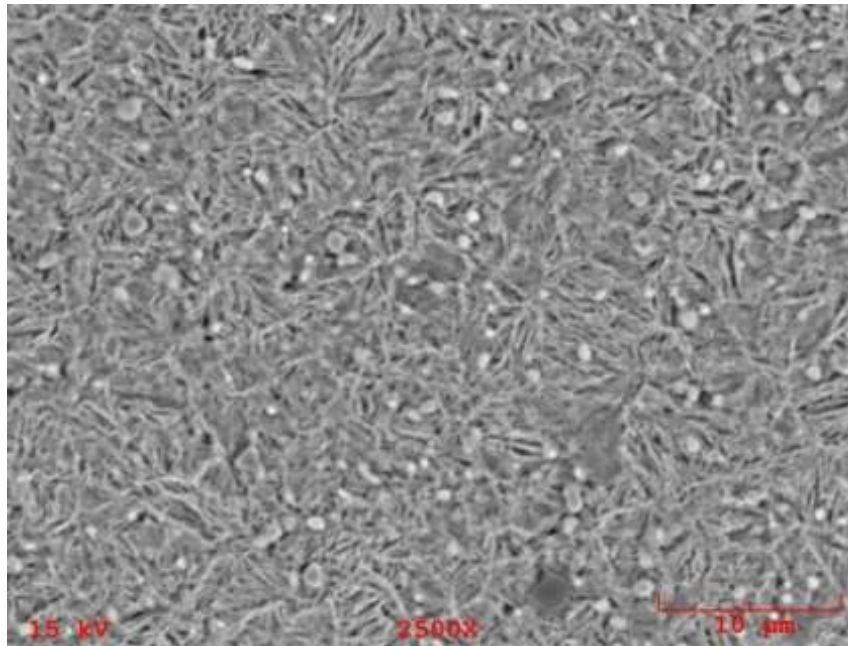


**Figure 4.15. Stroboscopic image frames part (2)**

#### **4.2.6. Microstructure Observation:**

Carbon strip steel was examined under the Scanning Electron Microscope (SEM) after the metallographic preparation. The microstructure of the material has a strong influence in the physical properties, such as strength, toughness, ductility, hardness, wear resistance. The microstructure of carbon strip steel was observed, shown in Figure 4.16. It can be seen

that the original microstructure consisted of a fine-grained martensitic matrix with smoothly distributed carbides.



**Figure 4.16. Microstructure of strip carbon steel**

### **4.3. Strip Carbon Steel Impact Fatigue Life:**

The impact fatigue life of strip carbon steel is determined in the experimental setup. Various impact velocities are examined and corresponding impact fatigue life is obtained. The purpose is to make a relationship between impact velocity of the valve leaf and the corresponding impact fatigue life in terms of number of cycles to failure. Impact velocity against lifetime plot provides a tool for designers to define the behavior of the specimen under specific impact fatigue conditions. Various impact velocities were investigated and the impact fatigue life of the specimens was averaged for each level of impact velocity. The

results of impact fatigue experiments for various impact velocities was presented in Figure 4.17. The impact fatigue limit, which the compressor valve leaf could withstand to the impact velocity while working without causing impact fatigue failure, is obtained.

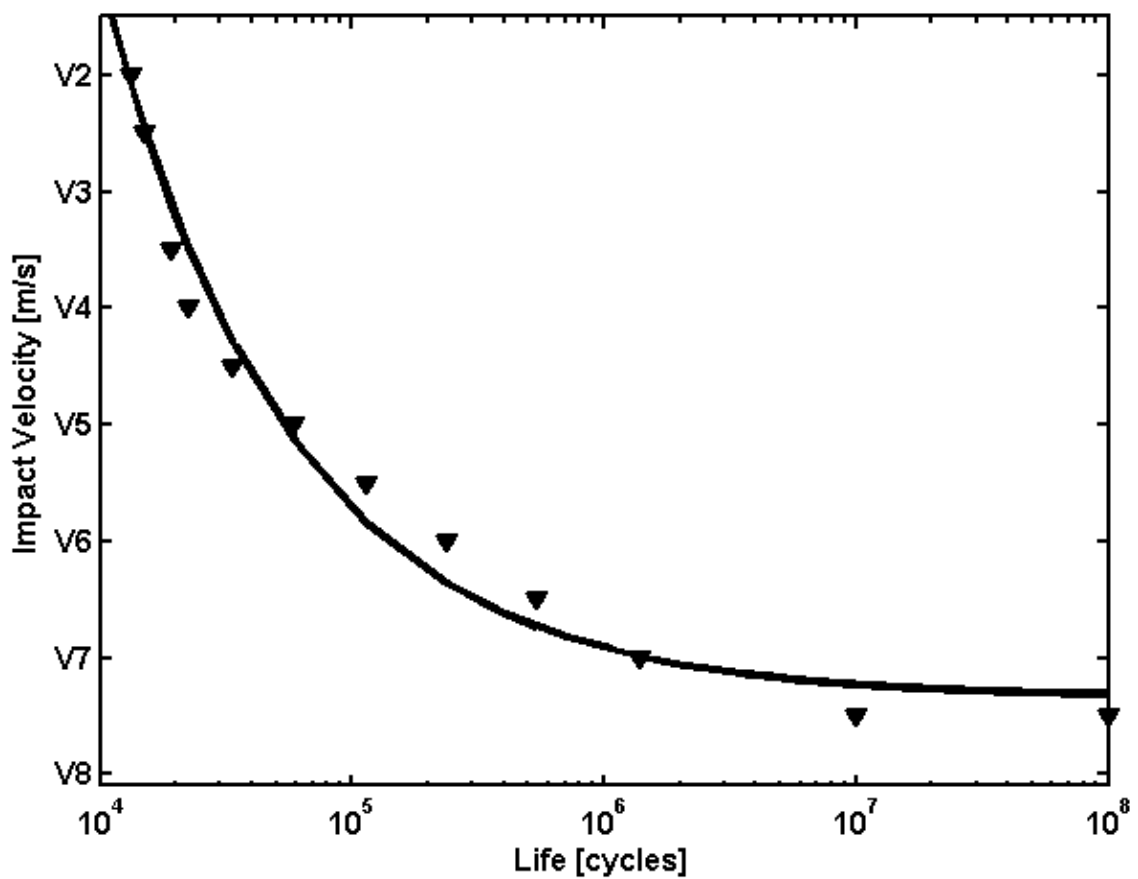


Figure 4.17. Endurance curve of strip carbon steel.

#### 4.4. Edge Radius Characterization and Correlation to Impact Fatigue Life

The influence of surface treatments were researched by Svenzon, M. (1976) and Soedel, W. (1984). Tumbling and shot peening were stated as the methods of surface treatments. On the surface of flapper valve steels, forming compressive residual stresses and reducing or eliminating the surface defect stress raisers by the surface treatments, significantly improved the bending fatigue strength [19, 20]. Chai, G., et al. (2004) emphasized that tumbling or tumbling and shot peening operation as a surface treatment, increased hardness near the surface by plastic deformation and introduce compressive residual stresses that leaded higher resistance to fatigue crack initiation [28].

Compressive residual stress introduced by shot peening operation was studied by Wang, S., et al. (1998) in steel and aluminum materials. Compressive residual stress distributions over the hardened layer from the surface were measured in an X-ray diffraction apparatus by 0 and 30° two-point method with step-by-step electrolytical dissolution. The depth of the compressive residual stress was increased with the peening intensity which was related with the velocity, harness, size and angle of the peening pellets and angle of the shot peening operation. Compressive residual stress within the surface layer formed compressive residual stress which forces the crack nuclei initiate at the tensile residual stress layer under the hardened layer. [35, 36].

After manufacturing of the valve leaves, a tumbling operation is performed to clean the burrs and eliminate possible fracture regions at the edges. Tumbling operation provides smooth and rounded edges and removes manufacturing defects which behave like stress raisers. The duration of the tumbling process, which affected edge radius and impact fatigue life of the valve leaves, was investigated for five levels. After manufacturing

process, the edge radius of the specimens was characterized (Figure 4.18) and tumbling duration was correlated with the impact fatigue life (Figure 4.19 and Figure 4.20). It can be clearly from the figures that tumbling operation had positive influence on the impact fatigue life of valve leaves. Besides, Figure 4.18 shows that the edge radius of carbon steel converged after T level tumbling operation, on the other hand stainless steel converged after 5T/4 operation. Alike the edge radius results, Figure 4.19 and Figure 4.20 shows that the impact fatigue life were directly proportional to the tumbling duration and tumbling operation enhances the impact fatigue life.

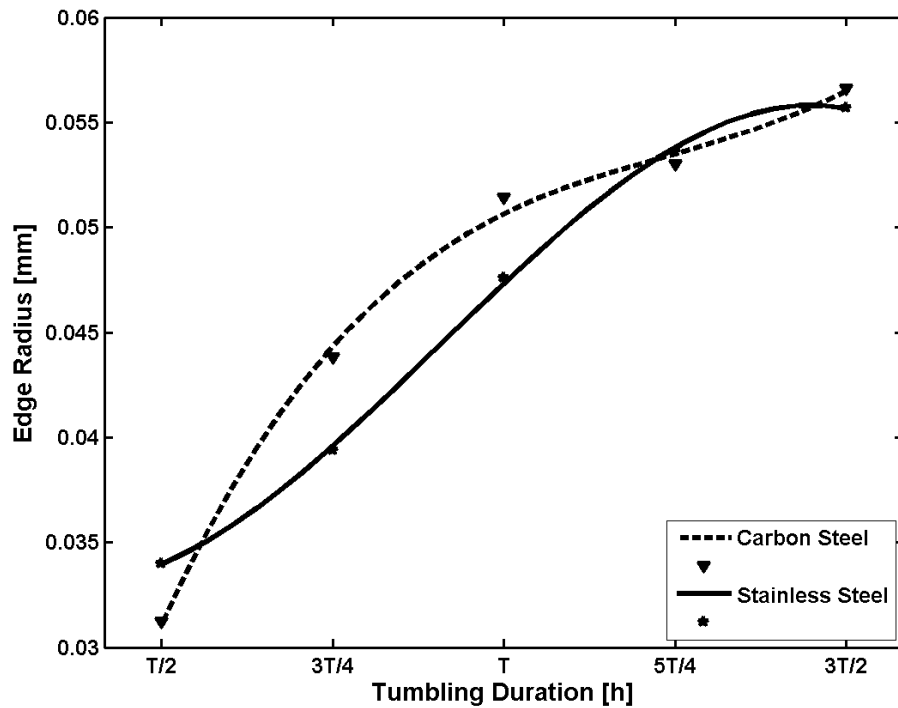


Figure 4.18. Edge radius characterization of carbon and stainless steel

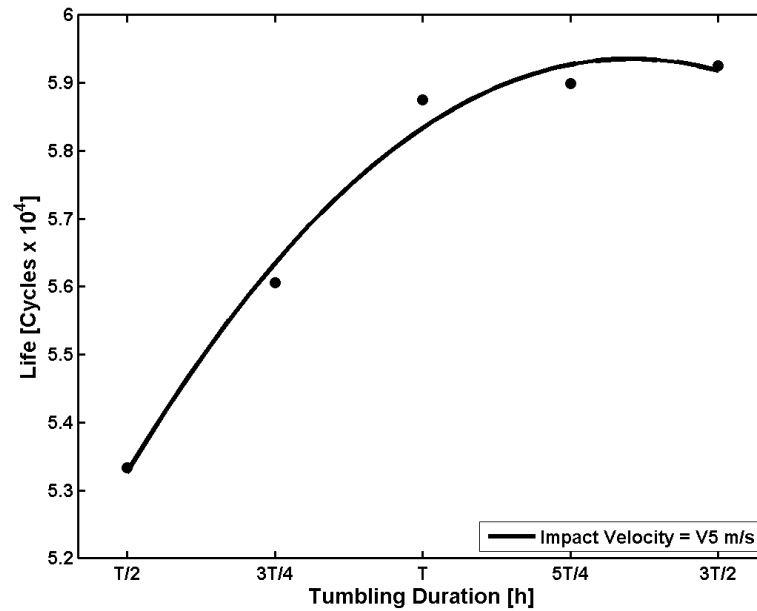


Figure 4.19. The effect of tumbling duration on impact fatigue life of carbon steel

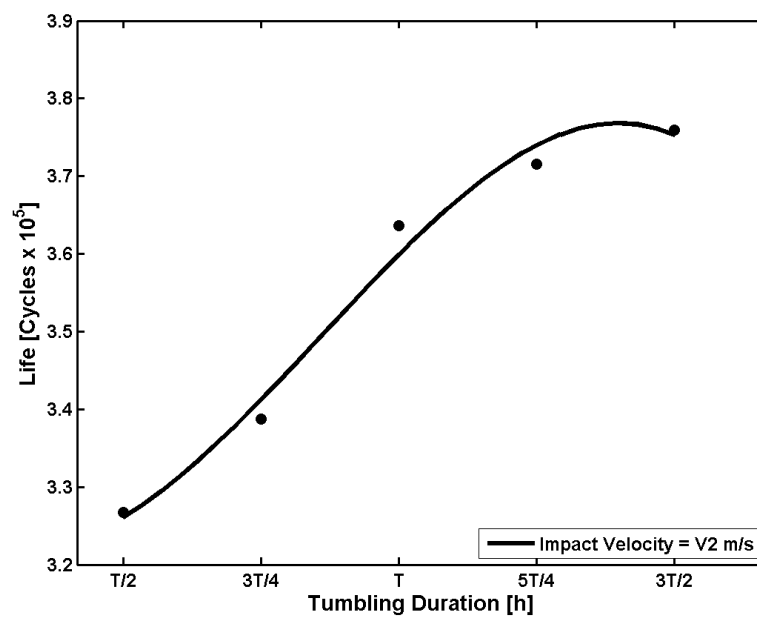
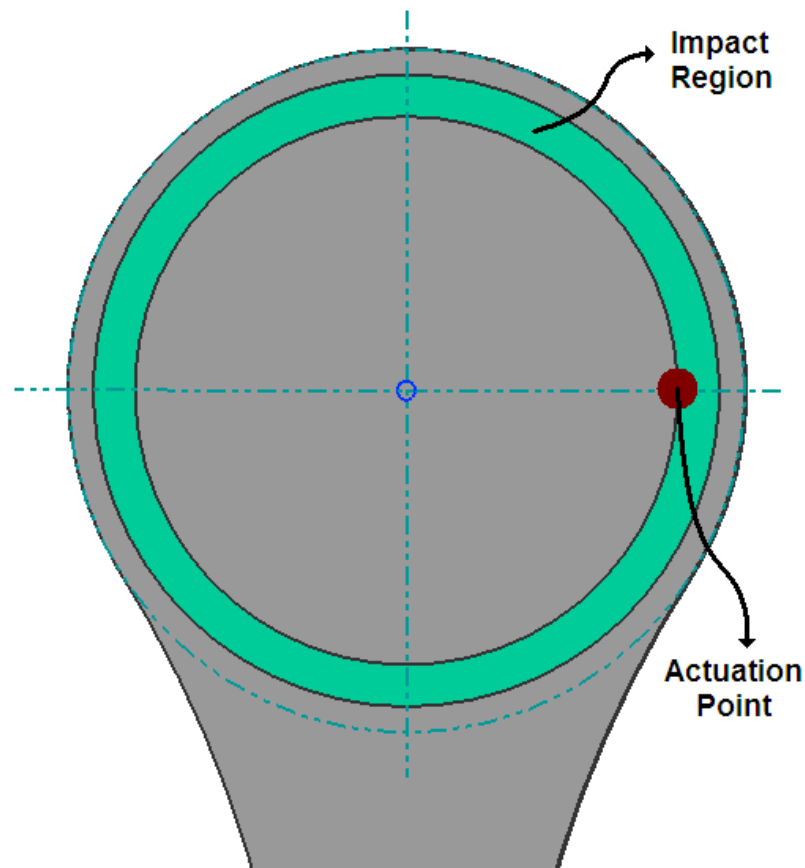


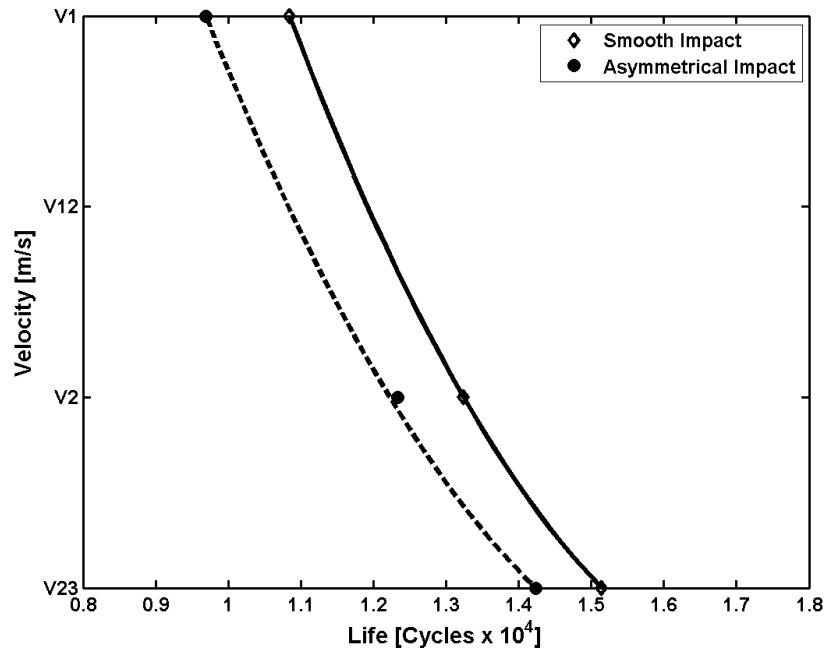
Figure 4.20. The effect of tumbling duration on impact fatigue life of stainless steel

#### 4.5. Asymmetrical Impacts

Although the impacts of valve leaves on the valve plate are predicted as smooth impacts, asymmetric impacts could be occurred due to the variation in working condition of compressor and the designs of other components. Asymmetrical tests were utilized by applying the air flow pulses on the edge of the valve leaf impact area shown in Figure 4.21. Asymmetrical impacts were investigated as working condition effect on the impact fatigue life and compared with the smooth impact lifetime in Figure 4.22.



**Figure 4.21. Valve leaf asymmetrical impact generation**



**Figure 4.22. Asymmetrical and smooth impact comparison**

#### **4.6. The Influence of Temperature on the Impact Fatigue Life:**

According to the information taken from the research/product & development, the valve leaves were experienced about T2 temperature level while working in the compressors. The experiments were performed around the working temperature and the influence of temperature on the impact fatigue lifetime was investigated. The tests carried out carbon steel with the original valve leaf design. Various impact velocities were tested at T1, T2, T3 levels and can be seen from Figure 4.23. The impact velocities were compared in terms of impact fatigue lifetime shown in Figure 4.27. Experiments showed that an increase in the temperature slightly decreased the impact fatigue life in the test temperature

range; in addition to that there was no clear difference between the impact fatigue lifetime at T1 level and room temperature.

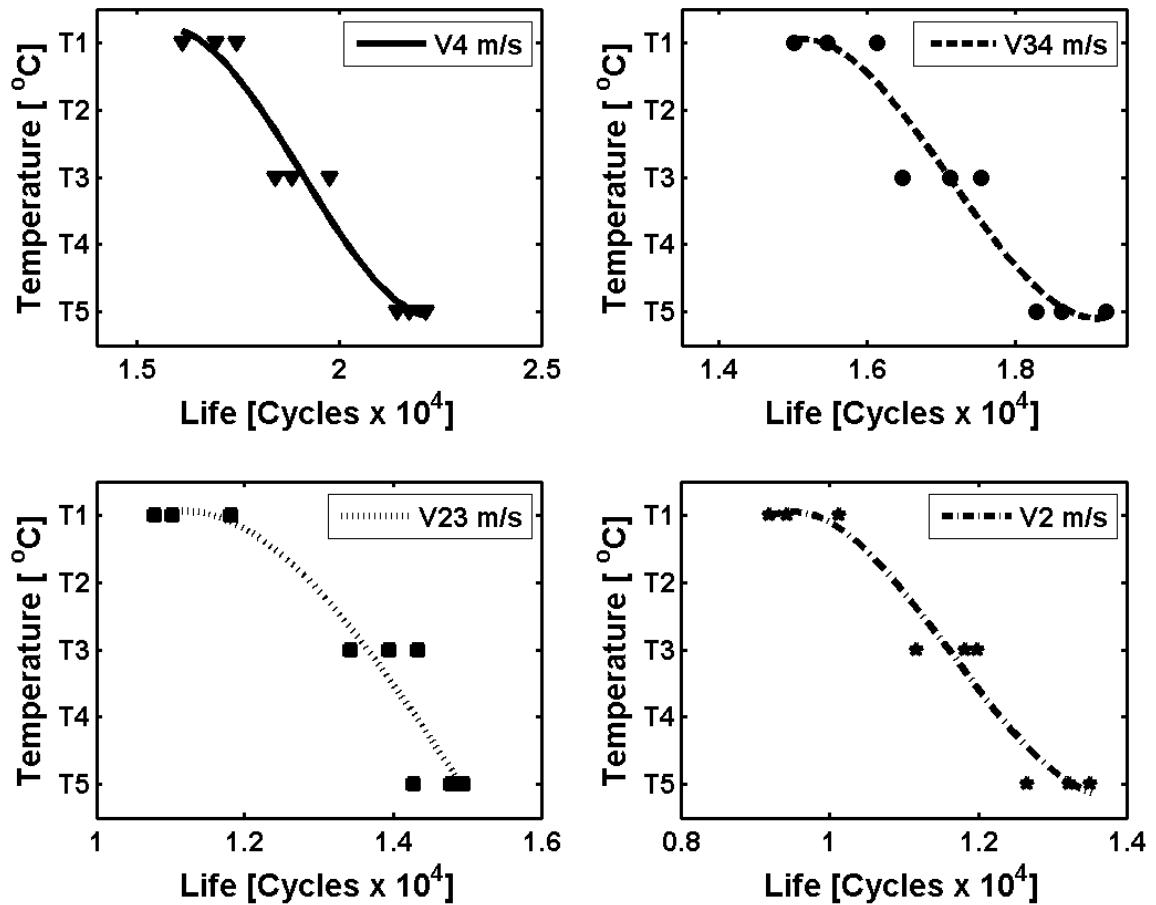


Figure 4.23. Temperature effect on the impact fatigue life of carbon steel

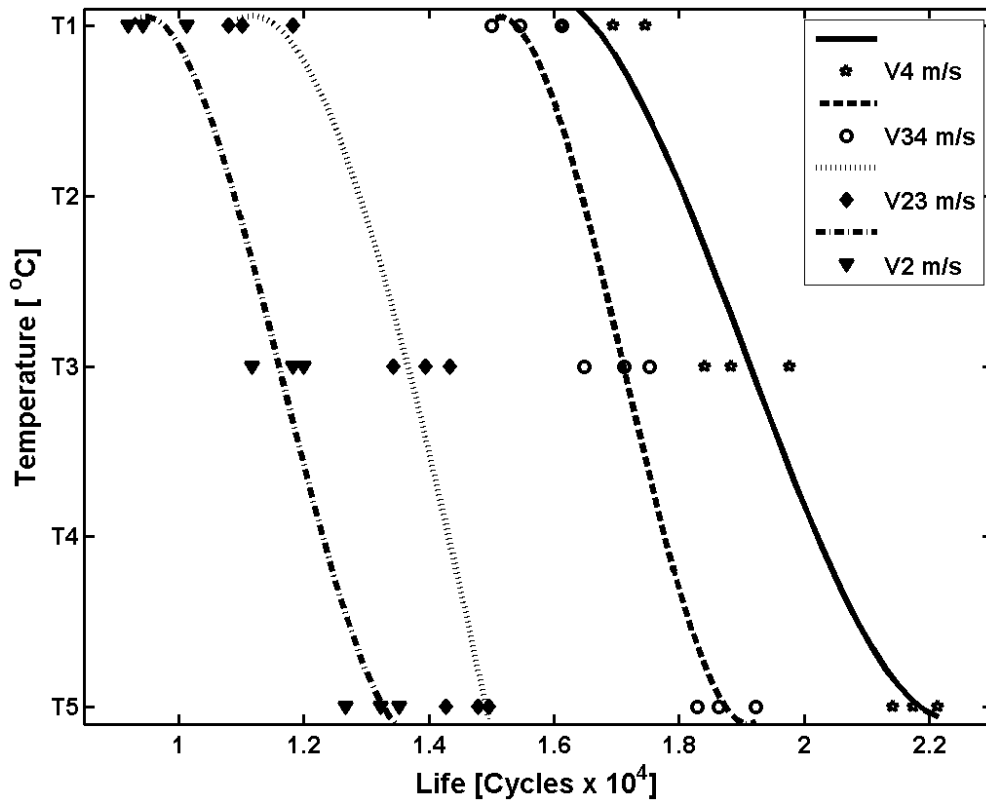


Figure 4.24. Temperature versus Lifetime for carbon steel

#### 4.7. Crack Length and Crack Growth Rate:

After an initial crack length was generated, the valve leaf was observed periodically under the optical microscope to visualize the possible crack initiation regions and crack propagations. The test performed at V1 impact velocity level. The crack length corresponded to the number of cycles were measured on the microscope. At the beginning of the test, three crack propagation paths were defined  $a_1$ ,  $a_2$ ,  $a_3$  shown in Figure 4.25. At the end of the observation, as it can be seen in Figure 4.26 a catastrophic final fracture was occurred in the path of  $a_1$ . The measured crack lengths versus corresponding number of

cycles were shown in Figure 4.27. The crack propagation rates were calculated and presented in Figure 4.28, crack path  $a_2$  had higher rate than  $a_1$  while  $a_3$  had a relatively low rate. It can be easily seen from Figure 4.28 that although the magnitude of cyclic plastic deformation due to impact fatigue loading intensified in the plastic zone at the crack tip of crack path  $a_2$  was higher, the final fracture occurred on the path of  $a_1$ . It is observed that the edge of the valve leave where the final fracture occurred exposed a highly plastic deformation while the chip was torn away. The region can be seen from Figure 4.28 that was marked a dashed circle. Since manufacturing tolerances cause a non-smooth and varying occupation of the valve leaf and valve plate, it can be said that the crack propagation rate presented below was unique for this sample.

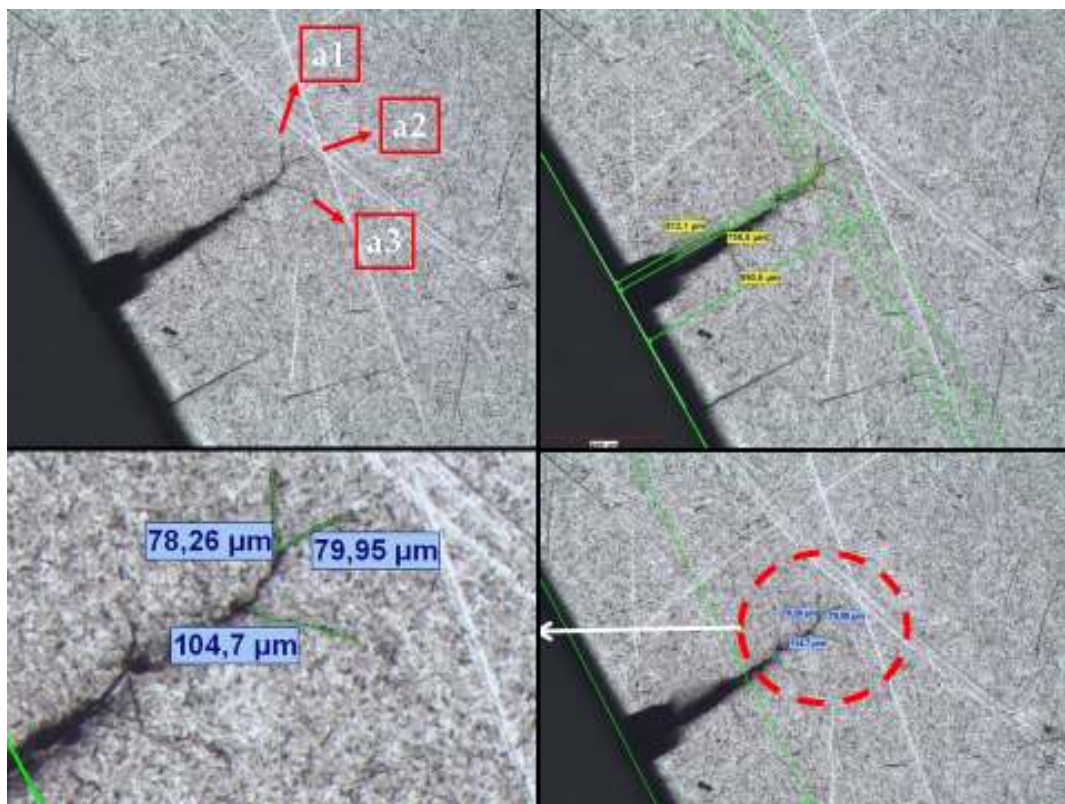


Figure 4.25. Crack length microscopic observation (50X).

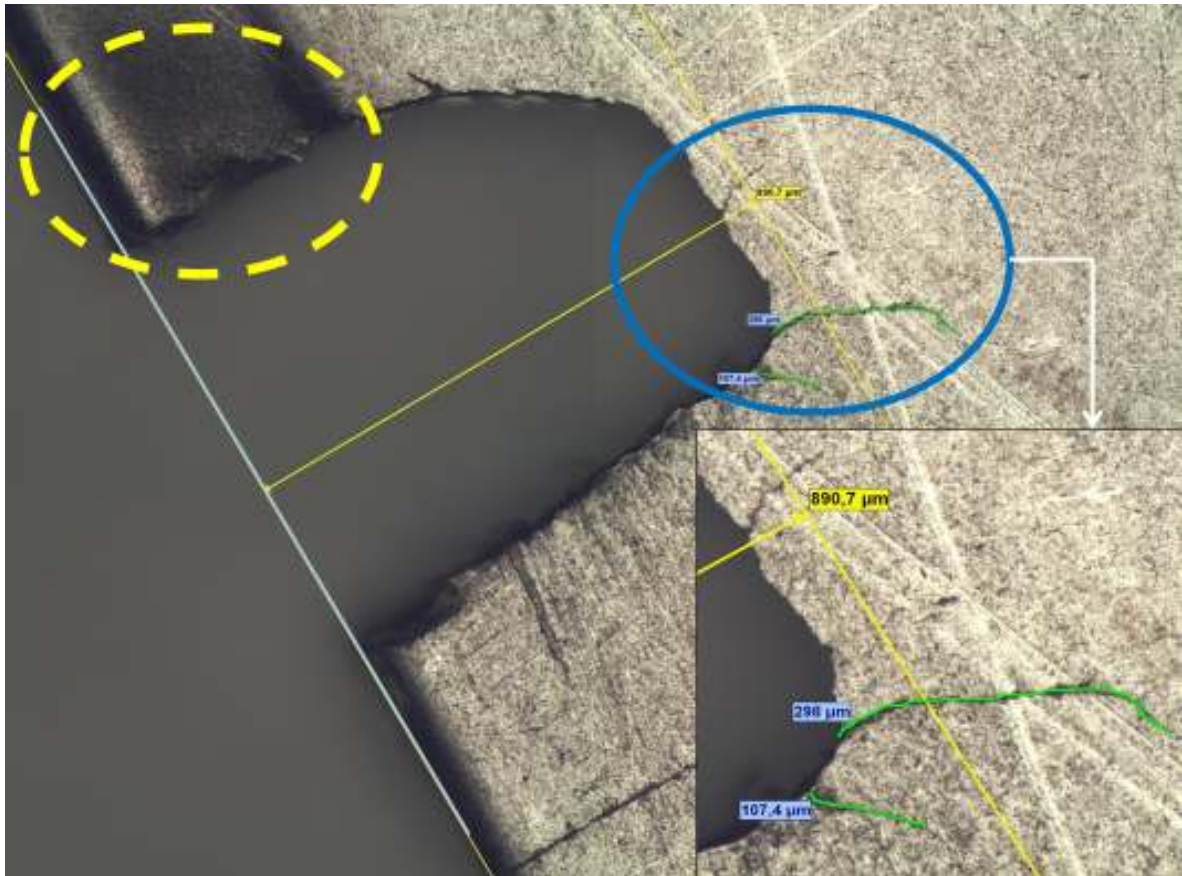


Figure 4.26. Microscopic observation of final fracture at the edge (100X).

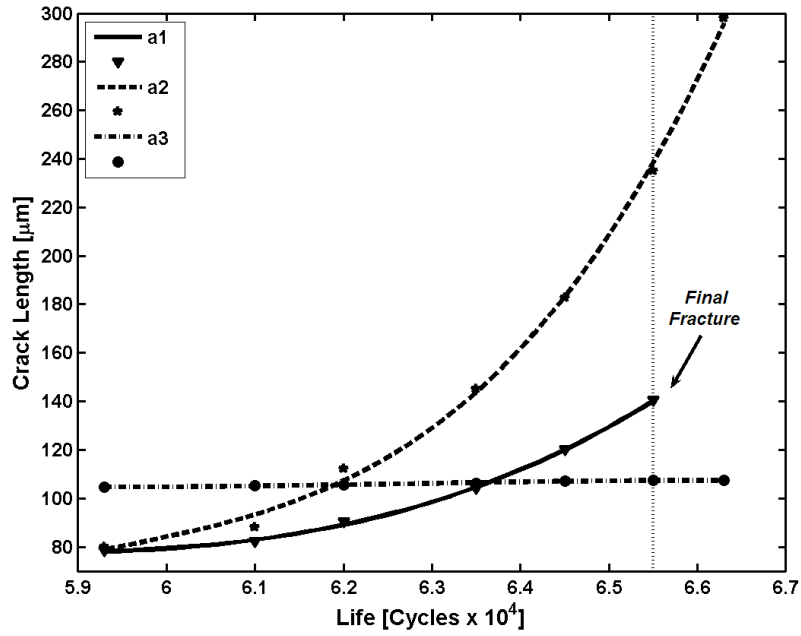


Figure 4.27. Crack length measurements for  $a_1$ ,  $a_2$ ,  $a_3$

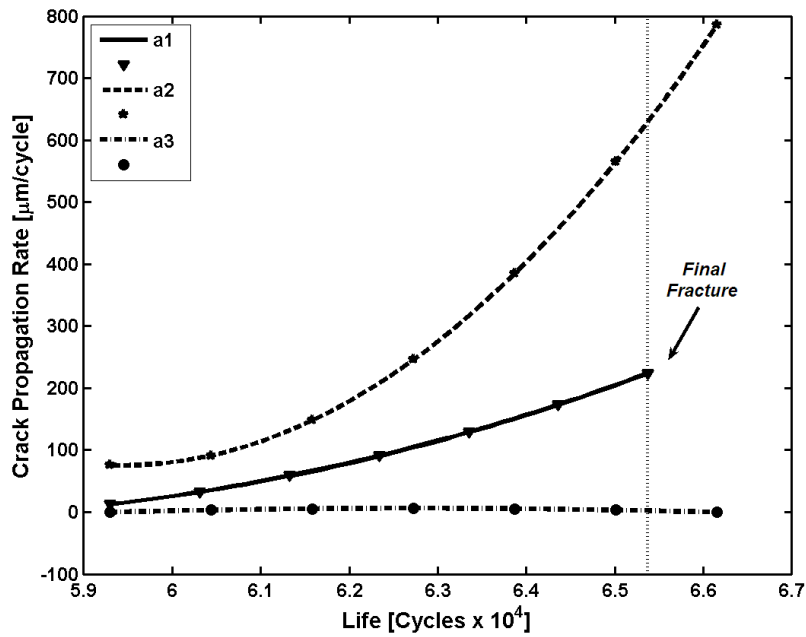


Figure 4.28. Crack propagation rates of  $a_1$ ,  $a_2$ ,  $a_3$

#### 4.8. Comparison of Impact Fatigue Life (Carbon Steel, Stainless Steel, New Stainless Steel Grade):

The tests were performed so that the influence of the strip steel used in compressor valve leaves was investigated in terms of impact fatigue life. Three types of material were tested; carbon steel, stainless steel and new stainless steel grade. The lifetime of three different strip materials were compared at V2 impact velocity level and presented in Figure 4.29. It can be easily seen from figure that stainless steel and new stainless steel grade were superior to carbon steel. In addition, stainless steel and new stainless steel grade were compared at three different impact velocity levels, at V1, V2 and V23 impact velocity levels. New stainless steel grade impact fatigue strength was higher than stainless steel. The difference between the lifetimes of the two types of materials decreased as the impact velocity increased. The results were presented in Figure 4.30 and Figure 4.31.

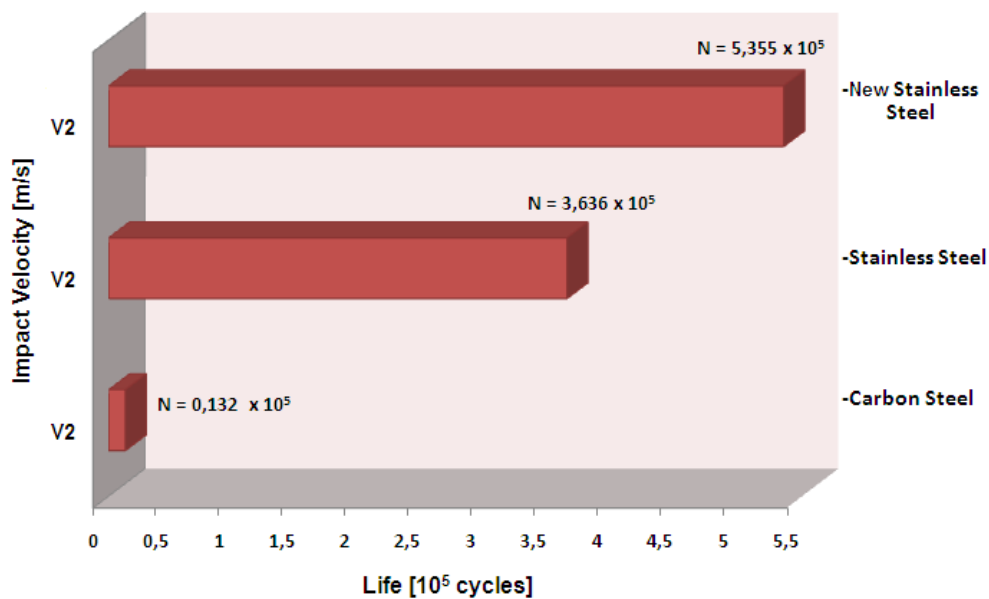


Figure 4.29. Comparison of impact fatigue life

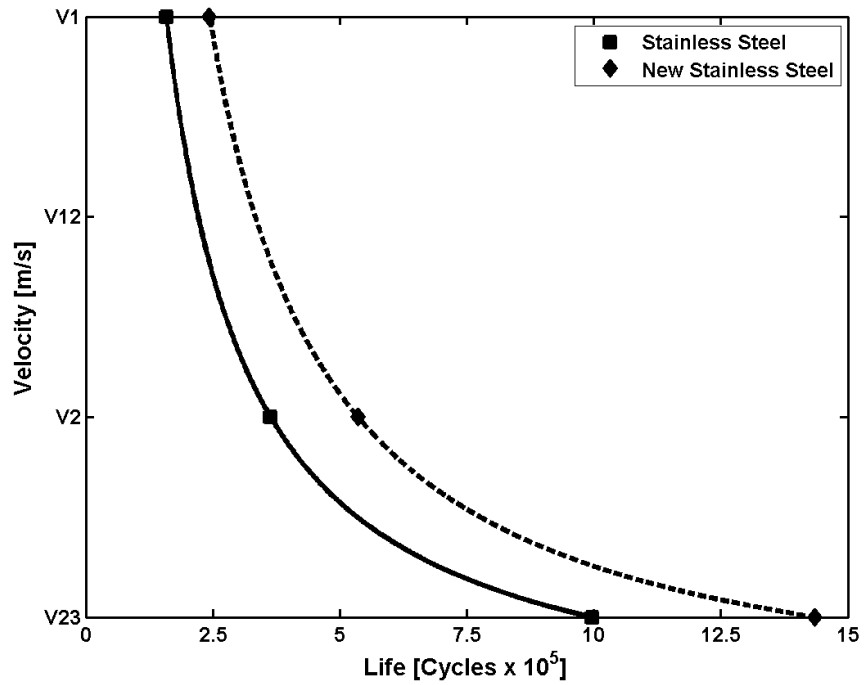


Figure 4.30. Comparison of Stainless Steel and New Stainless Steel Grade

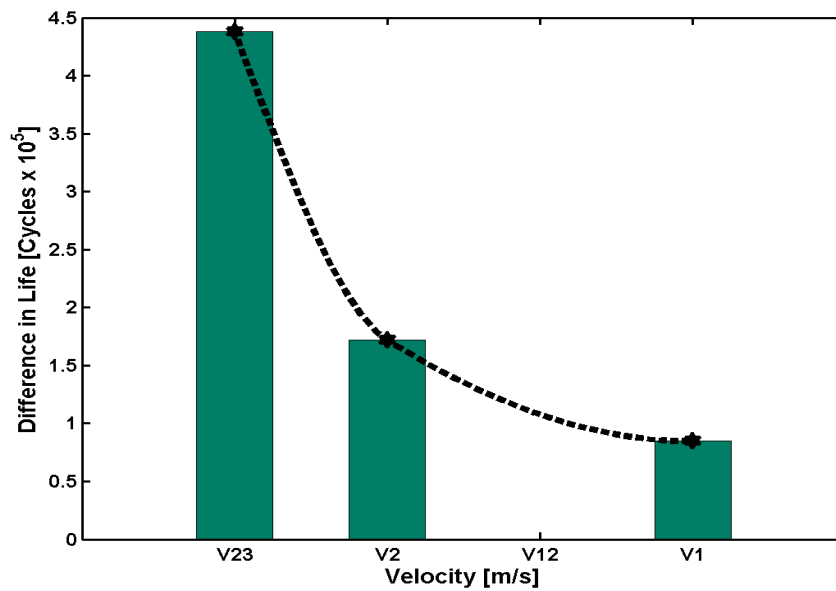
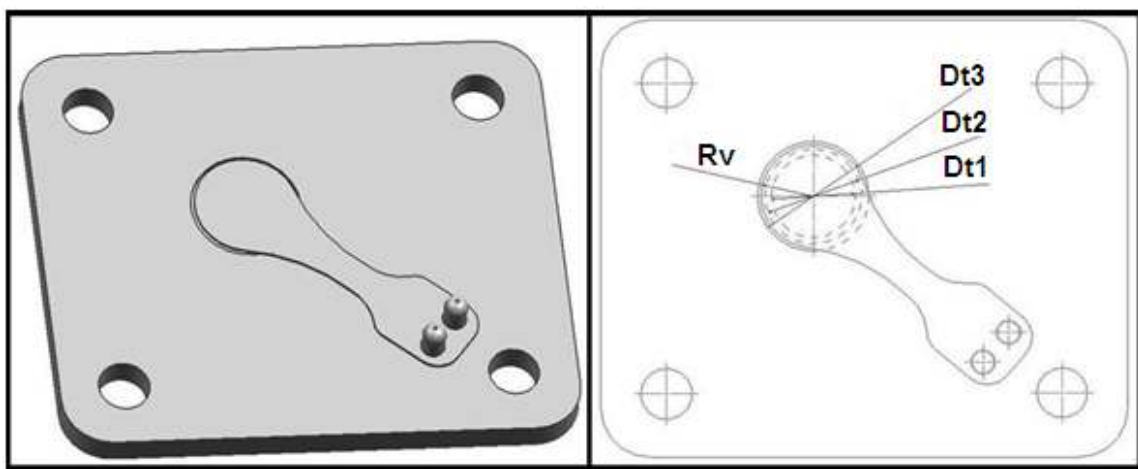


Figure 4.31. Difference in lifetime (Stainless Steel and New Stainless Steel Grade)

#### 4.9. Microscopic Surface and Fractographic Observations

The suction valve leaves which went into failure in the compressors were supplied from Arcelik A.S. and both microscopic surface and fractographic observations were utilized. The aim of the observation was to understand the mechanism of failure in the compressor.



**Figure 4.32. Valve leaf & plate assembly solid model and drawing**

In Figure 4.32, the solid model of the valve leaf & plate assembly was shown. The valve leaf contacts the valve plate in two valve plate dimension. These are cylinder diameter which  $R_v$  and the inner diameter of the groove on the valve plate presented in Figure 4.33, Figure 4.34 and Figure 4.35.

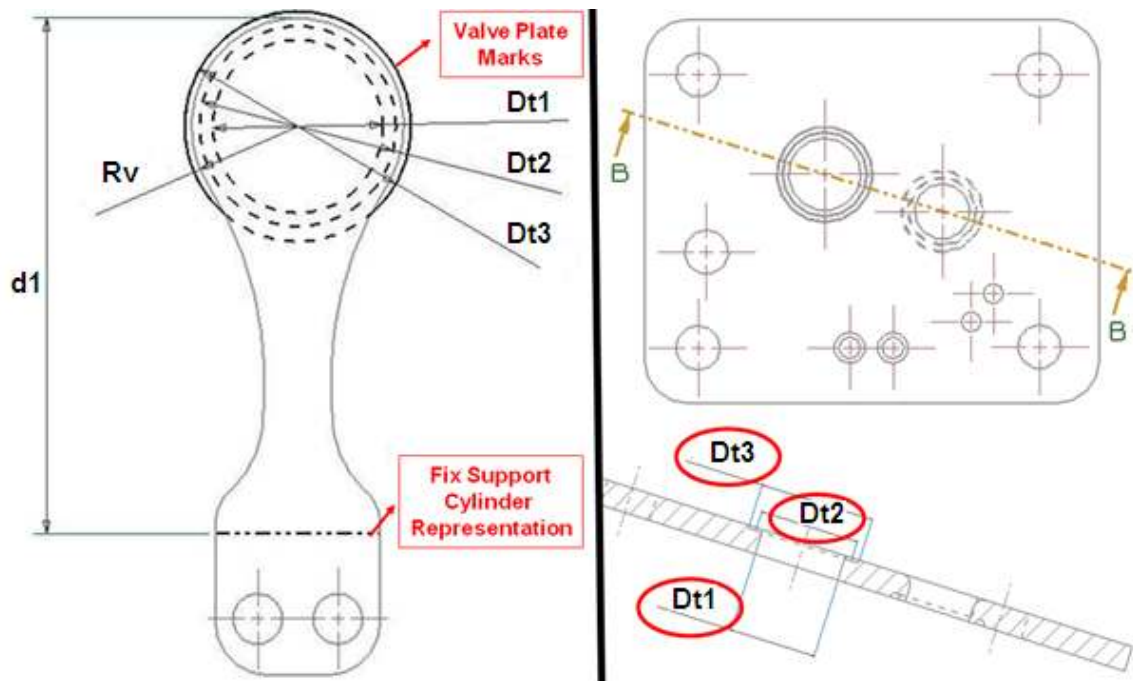


Figure 4.33. Critical regions on the valve plate

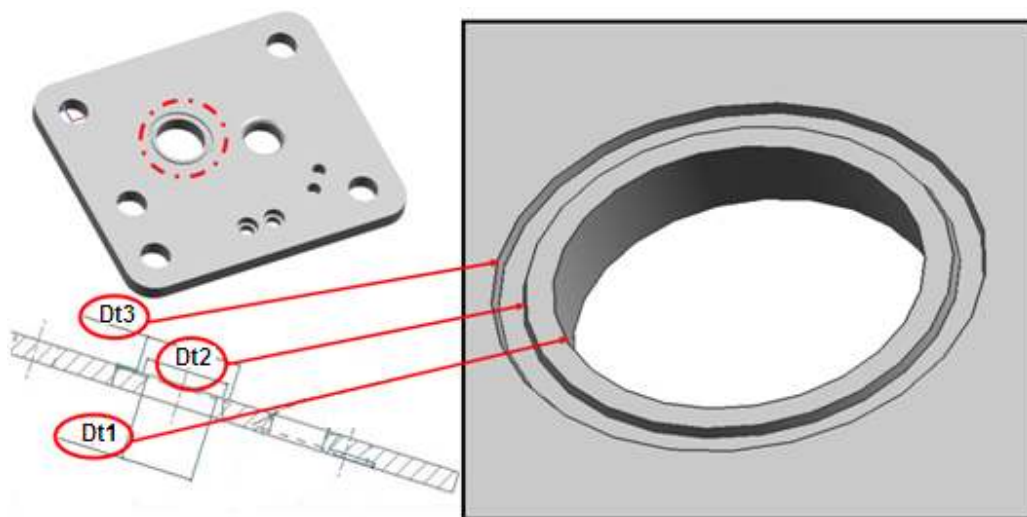
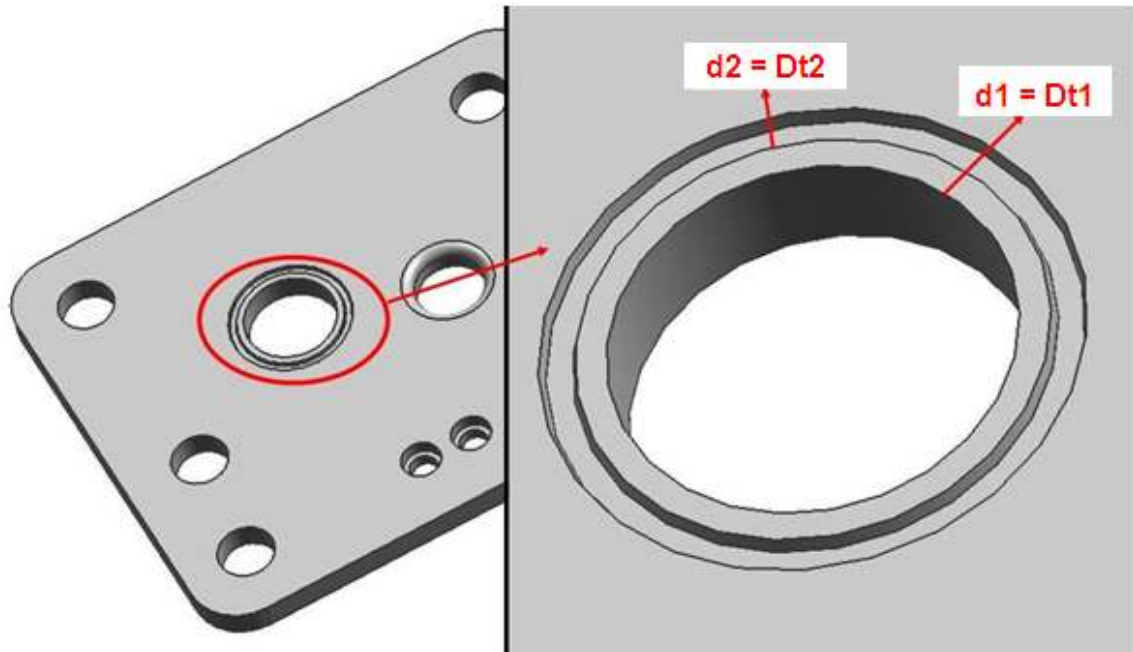
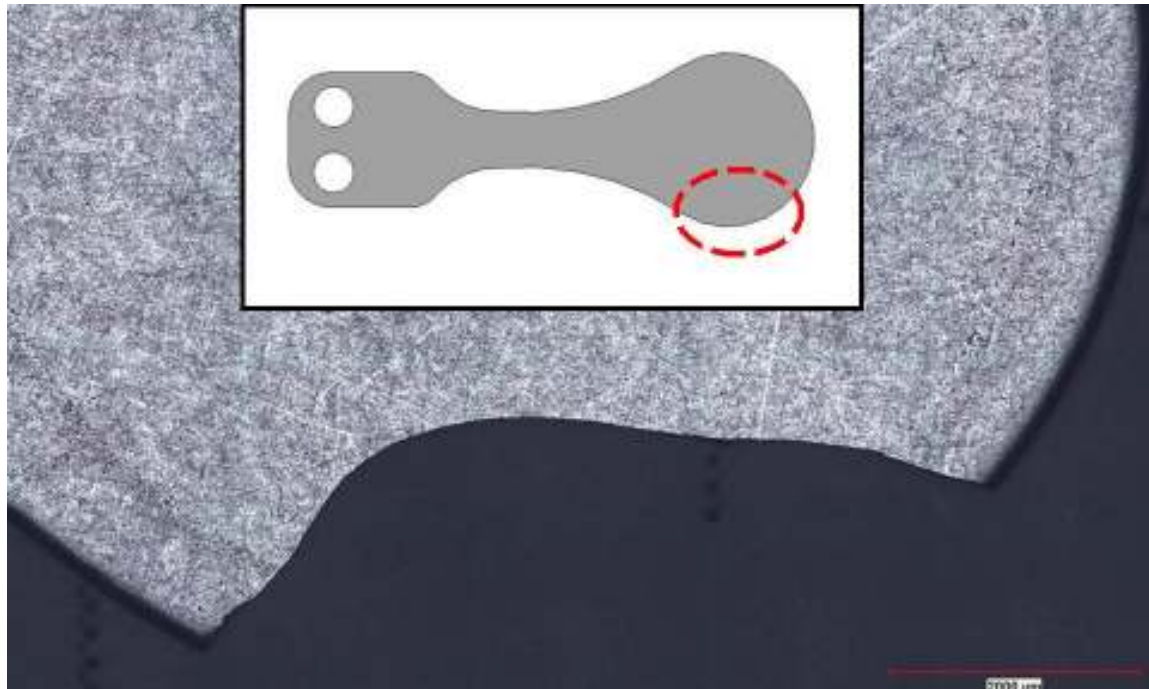


Figure 4.34. Valve plate critical regions

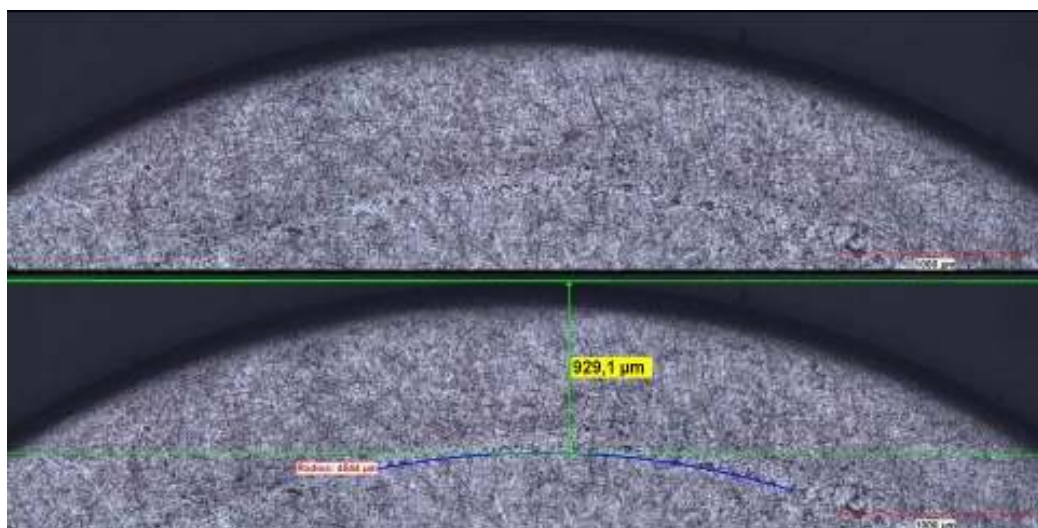


**Figure 4.35. Valve leaf contact diameters on the valve plate**

The valve leaf failure was investigated under the optical microscope to define the failure mechanism. The observation was utilized on the valve leaf shown in Figure 4.36. It can be clearly seen from the figure that there were wear marks on the valve leaf caused by the impacts on the valve plate. From Figure 4.37, the distance between the wear mark and edge of the valve leaf was measured. The wear mark diameter was calculated as 8.7 mm which almost corresponded to the cylinder diameter of the valve leaf. The slight difference could be caused by the design tolerances both valve leaf and valve plate.

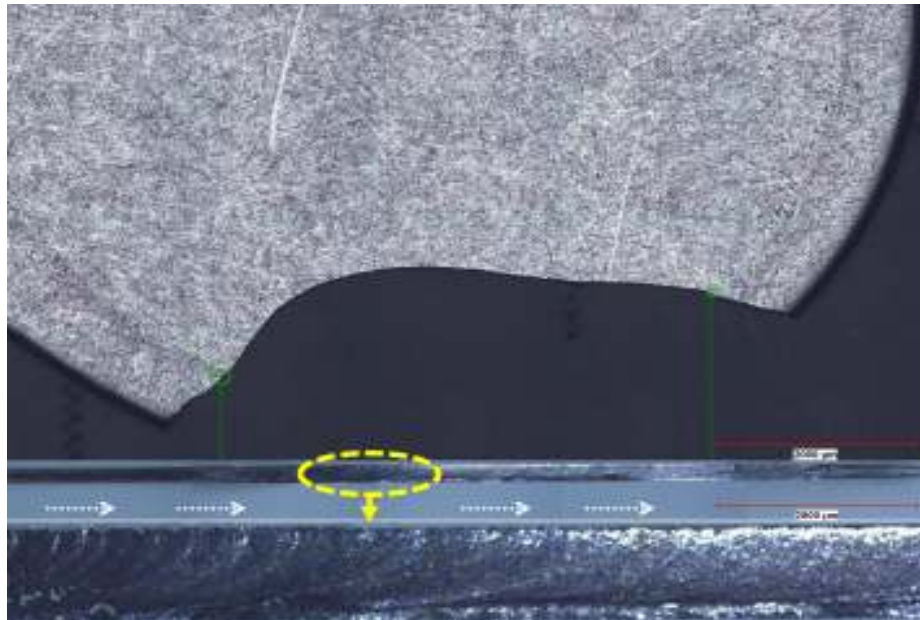


**Figure 4.36. Valve leaf microscopic observation**



**Figure 4.37. Valve leaf tip wear mark radius**

The fractographic observations were executed in order to interpret the features observed on the fracture surface topography and understand the crack mechanism caused by the impact fatigue failure. The initial fractographic observation was presented in Figure 4.38, the main purpose was to find a relation between the wear mark and fracture edge. For that reason, the intersection points were remarked and matched on the fracture surface. Since the beach marks direction were from the left side to the right side, the observation focused on the left intersection to find out the crack origin. The left side could not be clearly seen from figure because free-form surface resulted in microscope out of focus problem. Another observation was shown in Figure 4.39, which the fractographic observation was carried out perpendicular to the failure surface. The intersection point of wear mark and fracture was marked and fractographic observation was carried out which was presented in Figure 4.40. It can be concluded that, a catastrophic failure had been occurred between the edge of the valve leaf and the interaction point, in addition the crack propagated from the intersection point.



**Figure 4.38. Valve leaf fractographic observation case (1)**

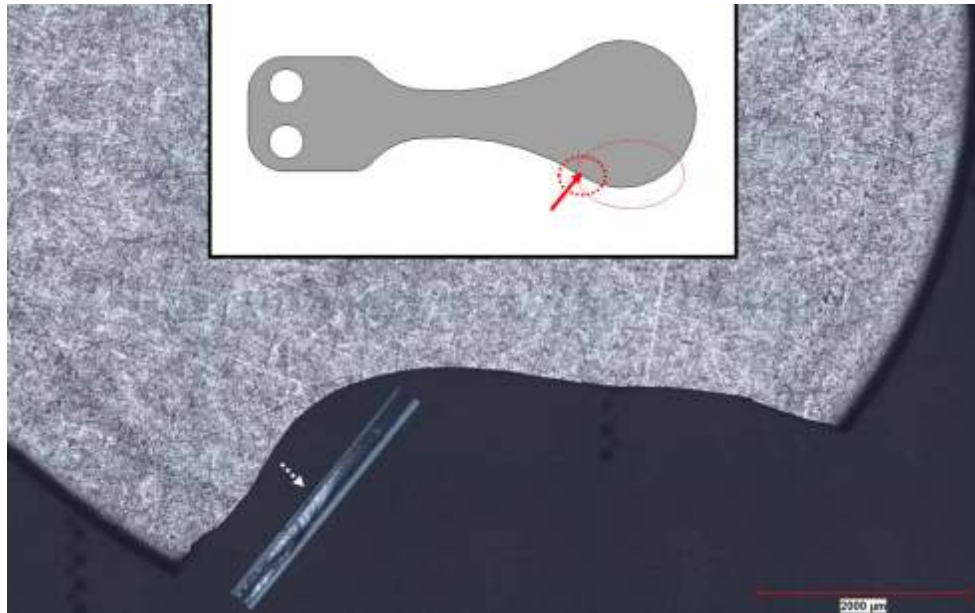


Figure 4.39. Valve leaf fractographic observation case (2)

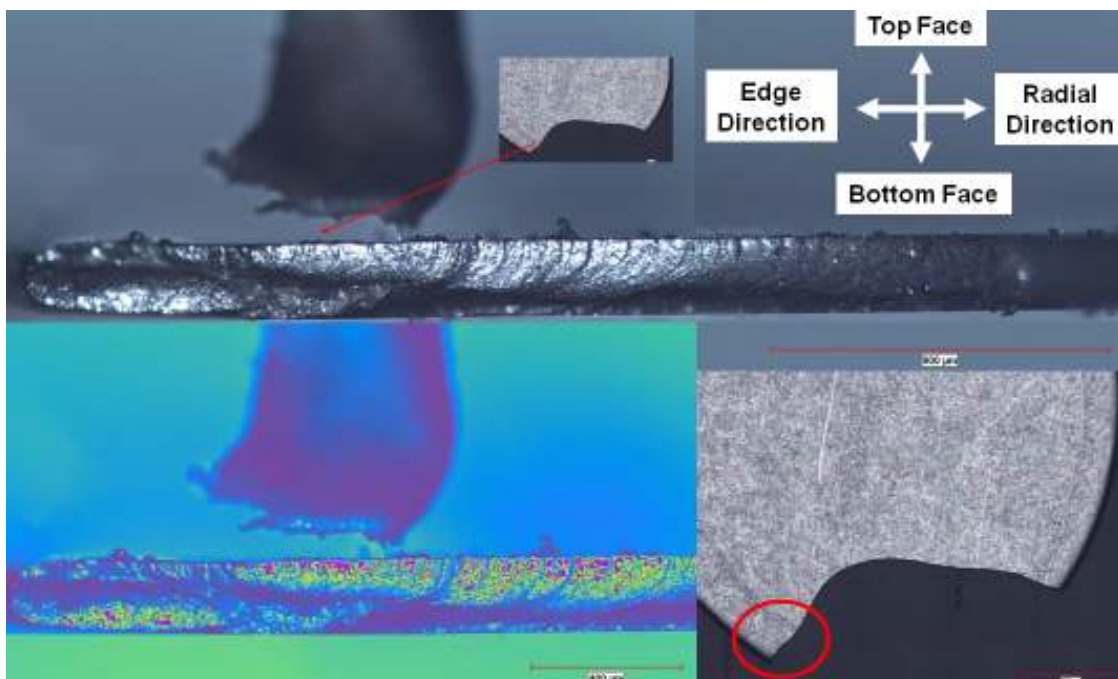
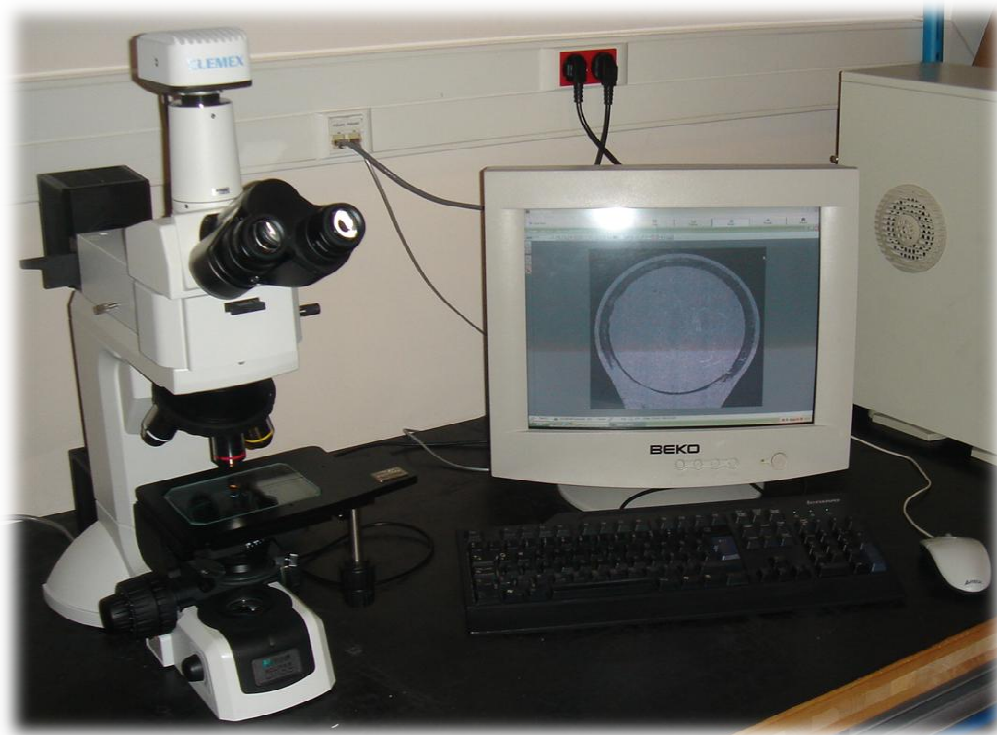


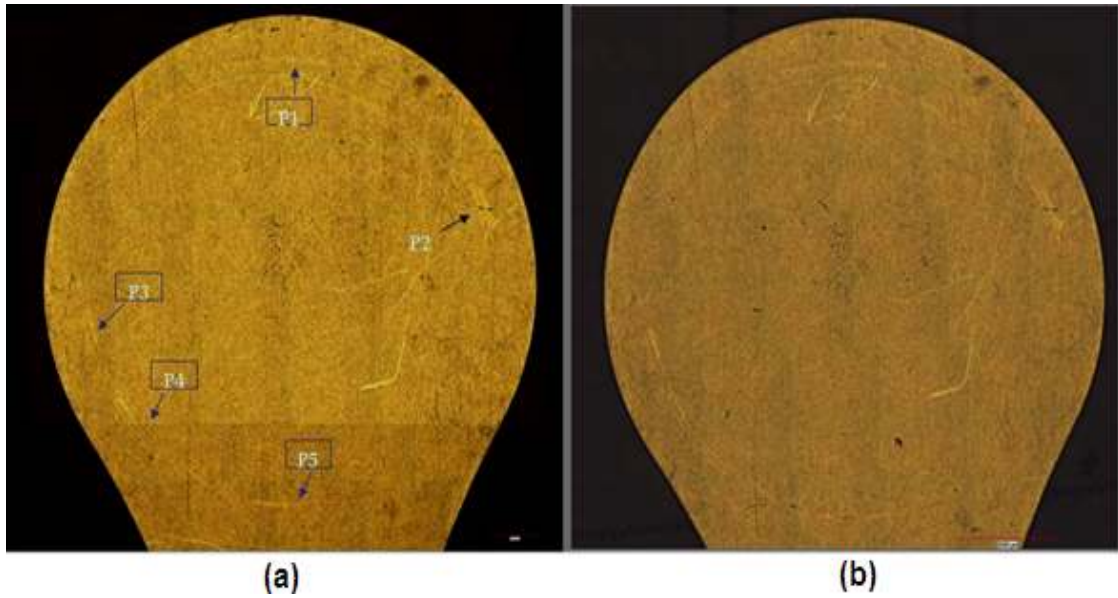
Figure 4.40. Fractographic Observation case (2)

#### 4.10. Wear Mark Evolution Microscopic Observation (Electromagnetic Setup):

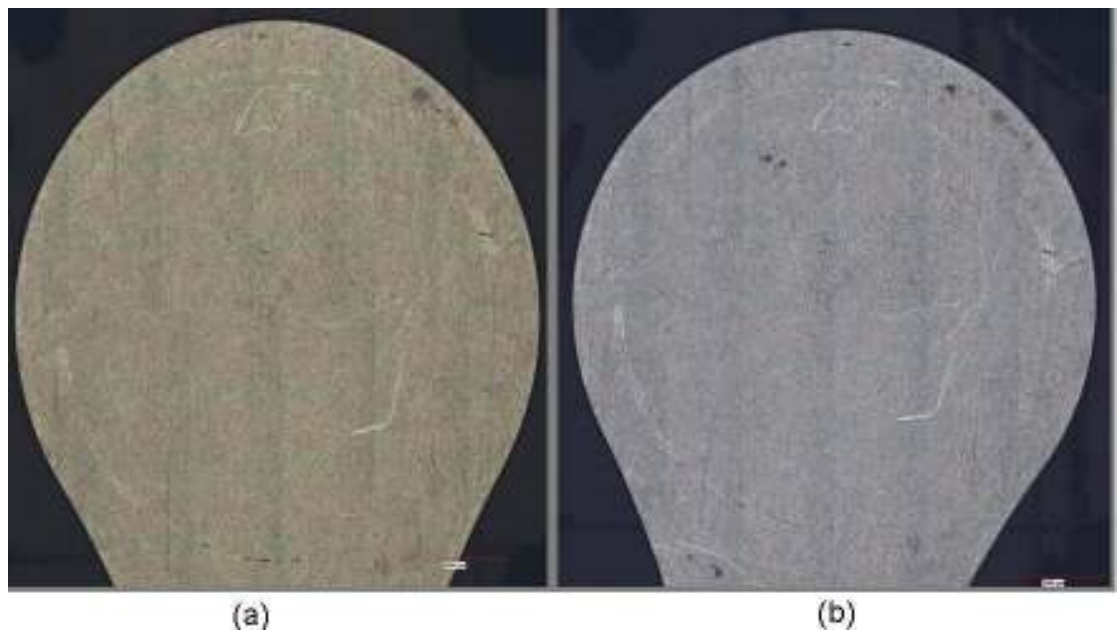
During the experiments in electromagnetic test system, the valve leaf was investigated periodically under the microscope (Figure 4.41) to visualize the possible crack and wear evolution mechanism. The microscopic images were presented at  $14 \times 10^7$  cycles and  $22 \times 10^7$  cycles in Figure 4.42, at  $25 \times 10^7$  cycles and  $32 \times 10^7$  cycles in Figure 4.43, at  $37 \times 10^7$  cycles and  $40 \times 10^7$  cycles in Figure 4.44 and at  $47 \times 10^7$  cycles and  $69 \times 10^7$  cycles in Figure 4.45. The experiments were carried out 5 m/s impact velocity at 200 Hz actuation frequency.



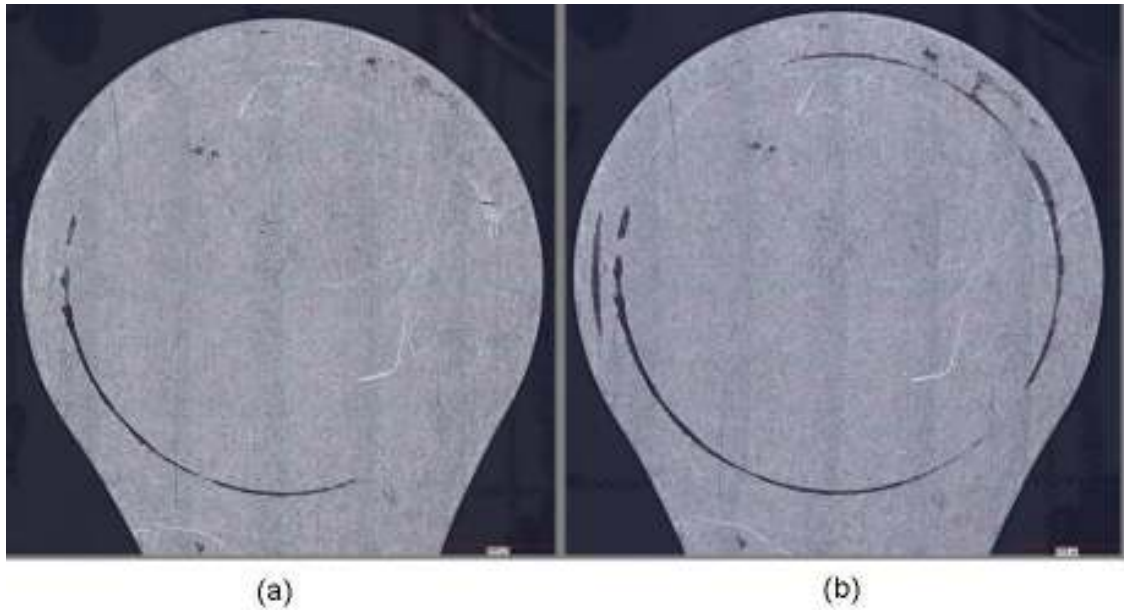
**Figure 4.41. Microscopic observation setup**



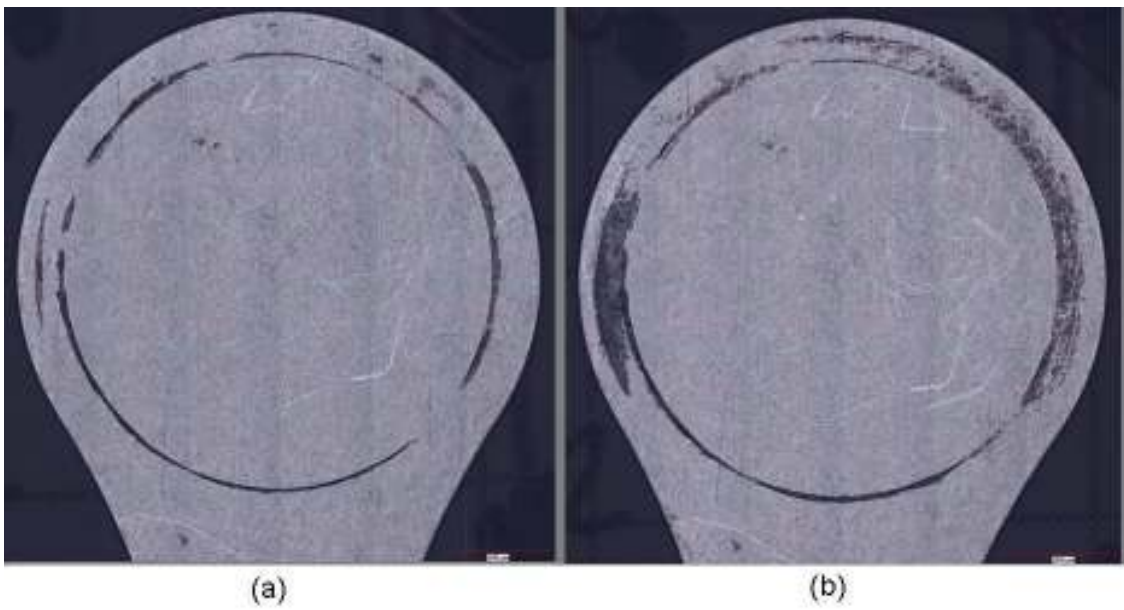
**Figure 4.42. Microscopic observations (a)  $14 \times 10^7$  cycles and (b)  $22 \times 10^7$  cycles**



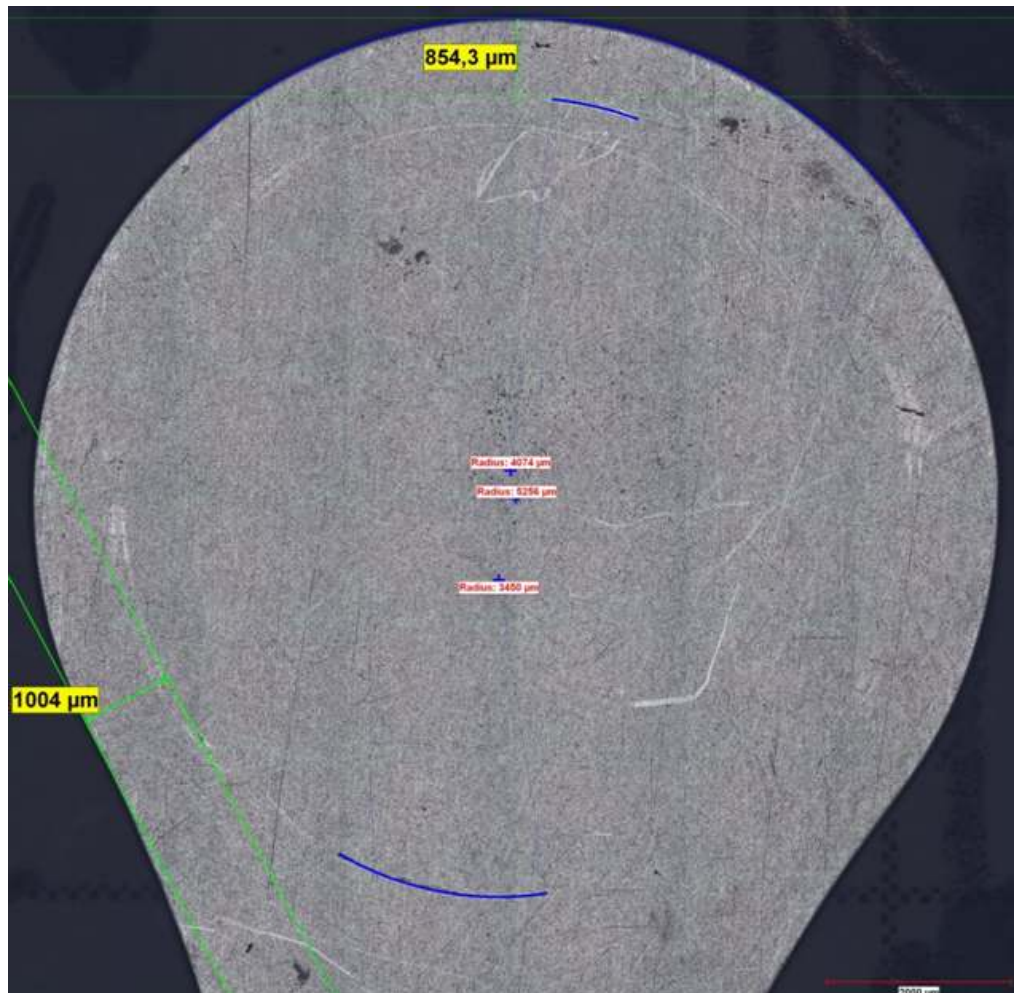
**Figure 4.43. Microscopic observations: (a)  $25 \times 10^7$  cycles and (b)  $32 \times 10^7$  cycles**



**Figure 4.44. Microscopic observations: (a)  $37 \times 10^7$  cycles and (b)  $40 \times 10^7$  cycles**



**Figure 4.45. Microscopic observations: (a)  $47 \times 10^7$  cycles and (b)  $69 \times 10^7$  cycles**



**Figure 4.46. Microscopic observation: wear marks  $32 \times 10^7$  cycles**

The inhomogeneous assembly of the valve leaf on the valve plate caused by the design and manufacturing tolerances resulted in different contact regions for the valve leaf. The different distances between the edge of the valve leaf and the wear marks can be seen in Figure 4.46.

#### 4.11. Scanning Electron Microscope (SEM) and Optical Microscope Observations:

The SEM observations were performed in order to clarify the crack initiation and propagation mechanism. The SEM (Figure 4.47) observations were executed in Materials Technologies department in Arcelik A.S., Istanbul, Turkey.

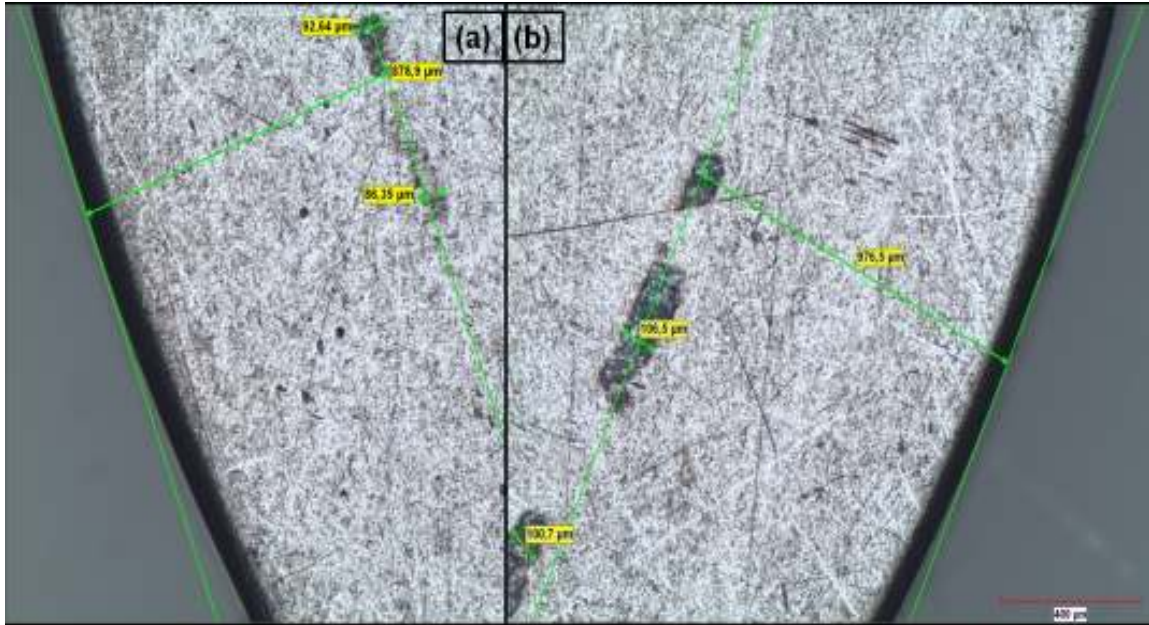


**Figure 4.47. Scanning Electron Microscope (SEM)**

A two crack originated valve leaf specimen was observed. The specimen stroboscopic image and microscopic image was shown in Figure 4.48. The distances were measured between the edge of the valve leaf and the wear mark from symmetrical regions of the valve leaf shown in Figure 4.49. The difference in the distances was a remark for unsmooth assembly, therefore various damage mechanisms were generated due to the unsmooth occupation caused by the design and manufacturing tolerances.

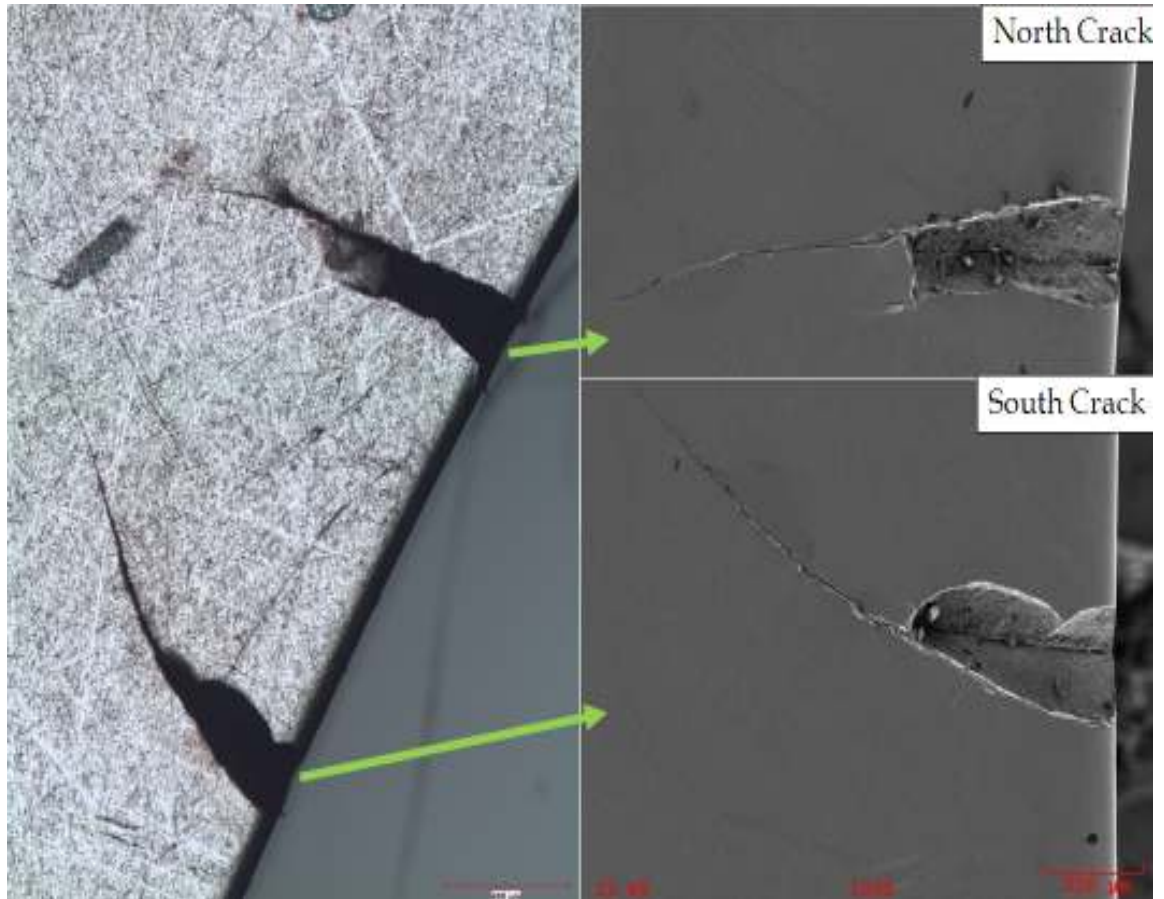


**Figure 4.48. Valve leaf double crack origin (a) stroboscopic image of top face and (b) microscopic display of impact face**



**Figure 4.49. Microscopic observation: wear marks of symmetrical regions (a) and (b)**

The microscopic observation was matched with the SEM observations and shown in Figure 4.50. The north crack impact surface in Figure 4.51 and non-impact surface with crack origin in Figure 4.52 were presented. In addition, the south crack impact surface in Figure 4.53 and non-impact surface with crack origin in Figure 4.54 were presented. Fracture surface topology was investigated for both north and south cracks in Figure 4.55 with fractographic observation.



**Figure 4.50. Microscopic and SEM observation**

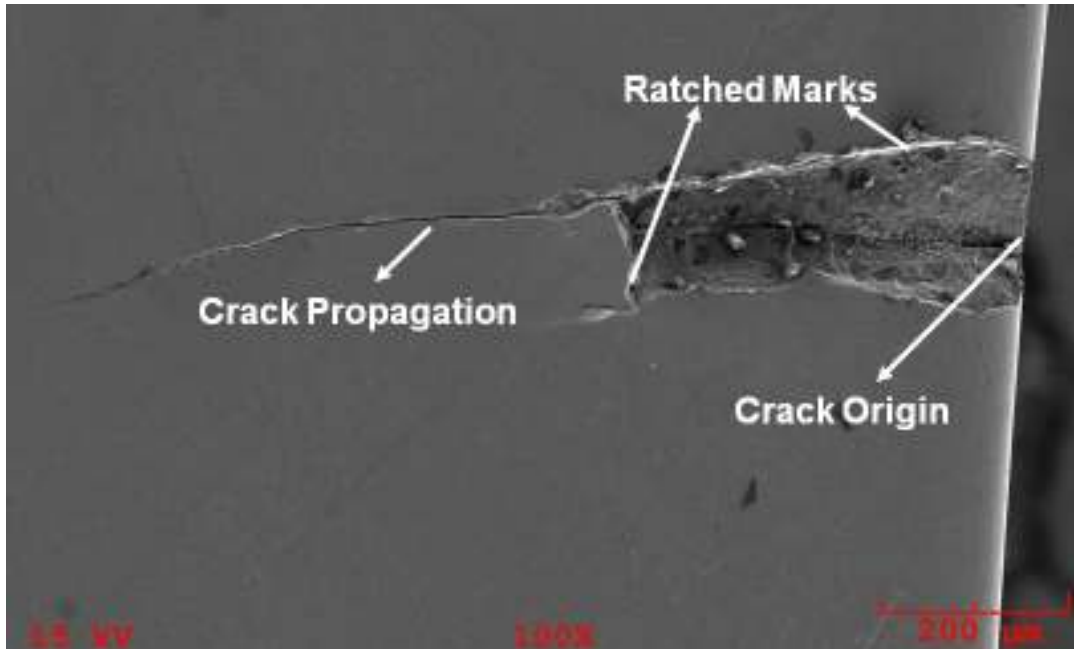


Figure 4.51. SEM observation: north crack

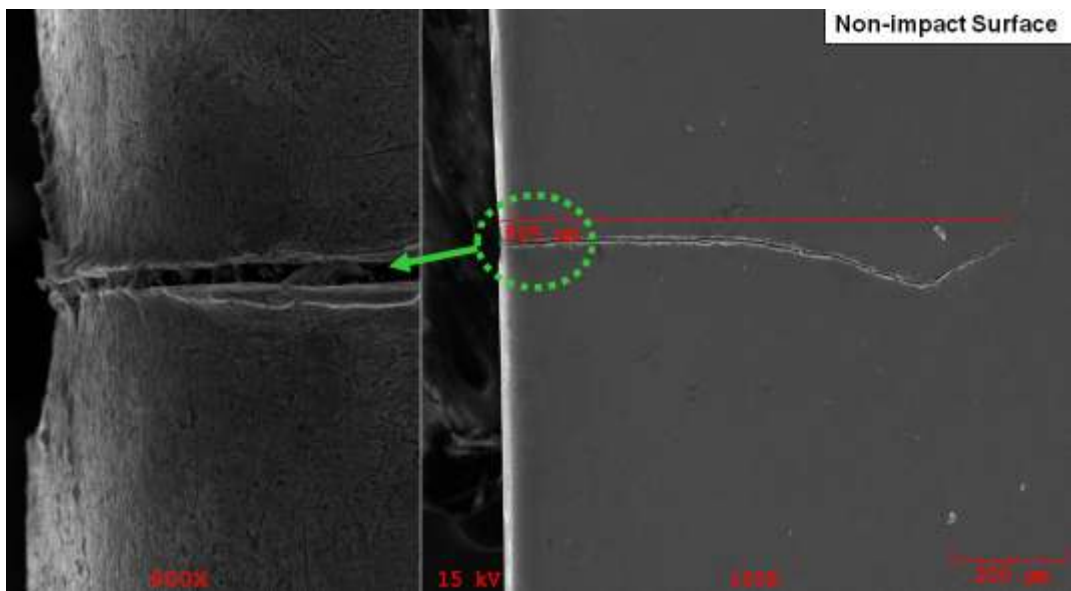


Figure 4.52. SEM observation: north crack origin

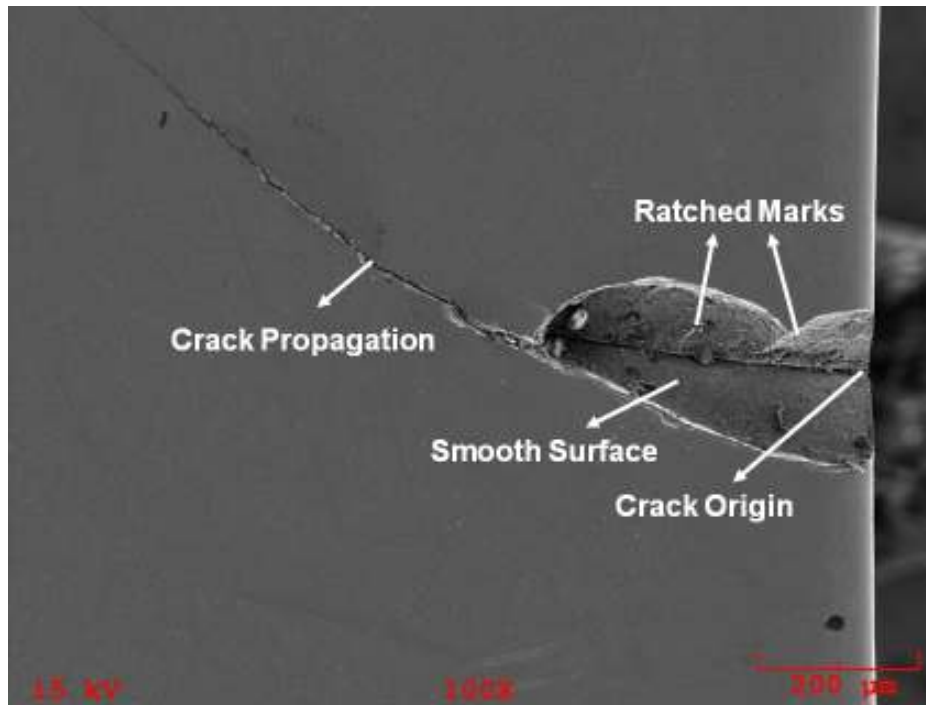


Figure 4.53. SEM observation: south crack

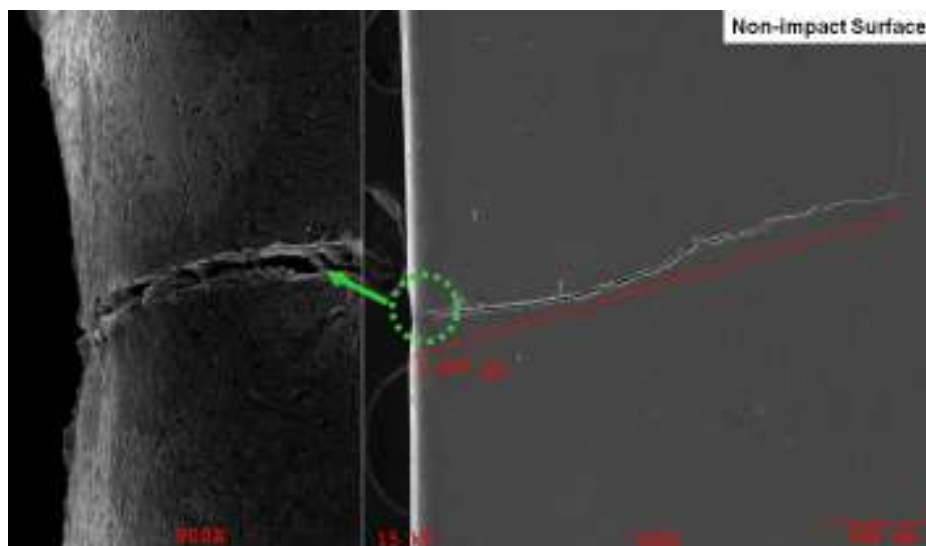
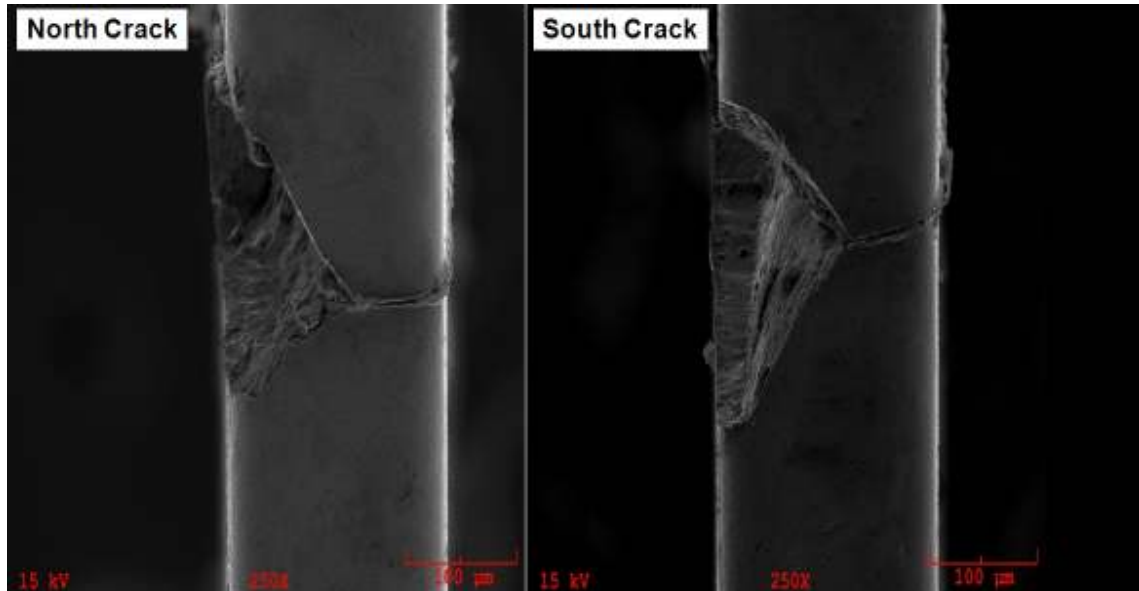


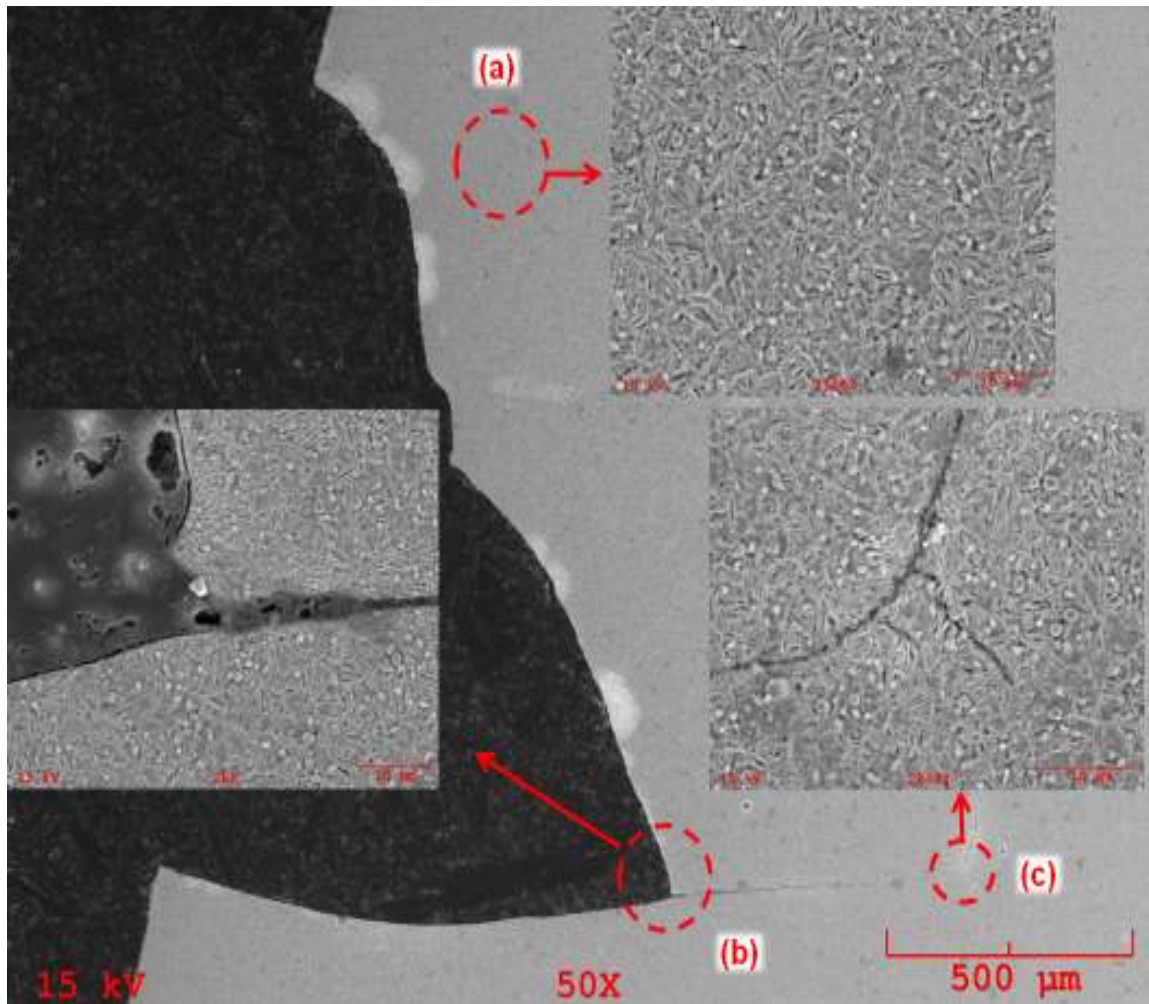
Figure 4.54. SEM observation: south crack origin



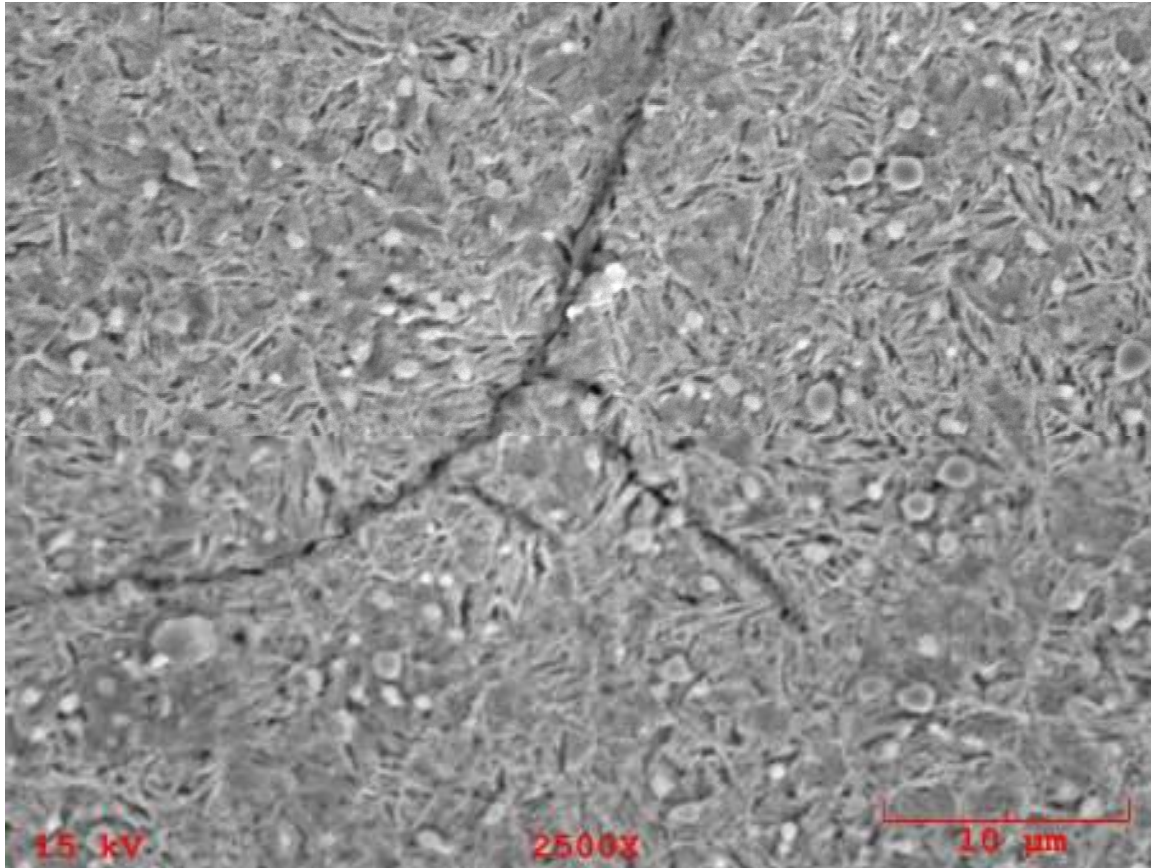
**Figure 4.55. SEM observation: Fractography**

#### **4.12. Metallographic Observations:**

The metallographic observation was performed to define the regional microstructure around crack and non-cracked region of the valve leaf. After metallographic preparation and etching operation, carbon strip steel microstructure could be seen in Figure 4.56 and branching in Figure 4.57. The observations were executed on SEM and it could be seen from the figures that the original microstructure consisted of a fine-grained martensitic matrix with smoothly distributed carbides. In Figure 4.56, three regions were examined in terms of microstructure. Regional microstructures crack origin (a), branching point (b) were compared with original microstructure (c) in order to understand the influence on the crack mechanism.



**Figure 4.56. Regional microstructure by SEM (a) crack origin, (b) branching point, (c) original microstructure**



**Figure 4.57. Branching along the crack path by SEM, Region (c)**

#### **4.13. High Speed Camera Observations:**

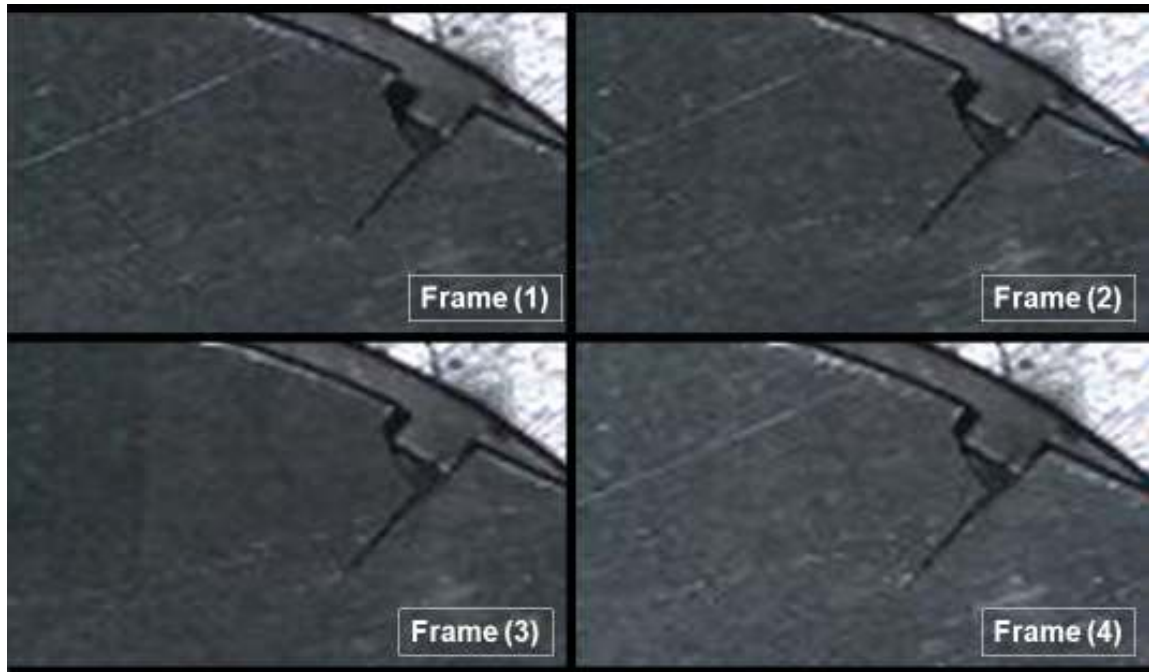
The high speed camera observations were performed on smooth specimen at 10000 fps (Figure 4.58) and 16000 fps (Figure 4.59). In addition a pre-cracked specimen was observed at 40000 fps for the crack propagation characteristics and presented in Figure 4.60 while the test actuation frequency was 200 Hz.



Figure 4.58. High speed camera display at 10000fps



Figure 4.59. High speed camera display at 16000fps



**Figure 4.60. High speed camera display at 40000fps**

#### **4.14. Finite Element Transient Impact Analysis:**

Transient impact analysis is a technique that is used to determine the response of the compressor valve leaf under a time-varying pressure. In the compressor, the valve leaves are exposed to a sharp pressure change in a fraction of time, thus the case was simulated under an impulse loading condition. However, an ideal impulse force cannot be produced numerically, the pressure was applied over a discrete amount of time  $\Delta t$  shown in Figure 4.61. Simulation time was set to 5 ms which corresponds to 200 Hz actuation frequency and contact time was set to 0.5 ms as  $\Delta t$ . In the ANSYS simulation, the valve leaf was fixed at one end as fixed in the compressor shown in Figure 4.62. At the impact region, the valve leaf was impacted with an impulsive force distributed as pressure through the impact

area which is the corresponding valve plate impact area. In simulation, the response of the node shown in Figure 4.63 was calculated for x and z direction stress components. It can be concluded that z-direction stress component (Figure 4.64) was very higher than x-directional stress component (Figure 4.65) for the selected surface node.

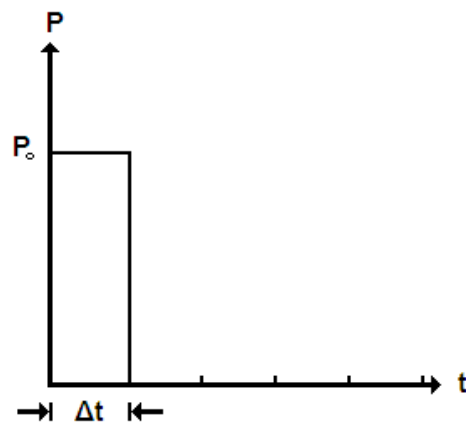


Figure 4.61. Simulation applied pressure

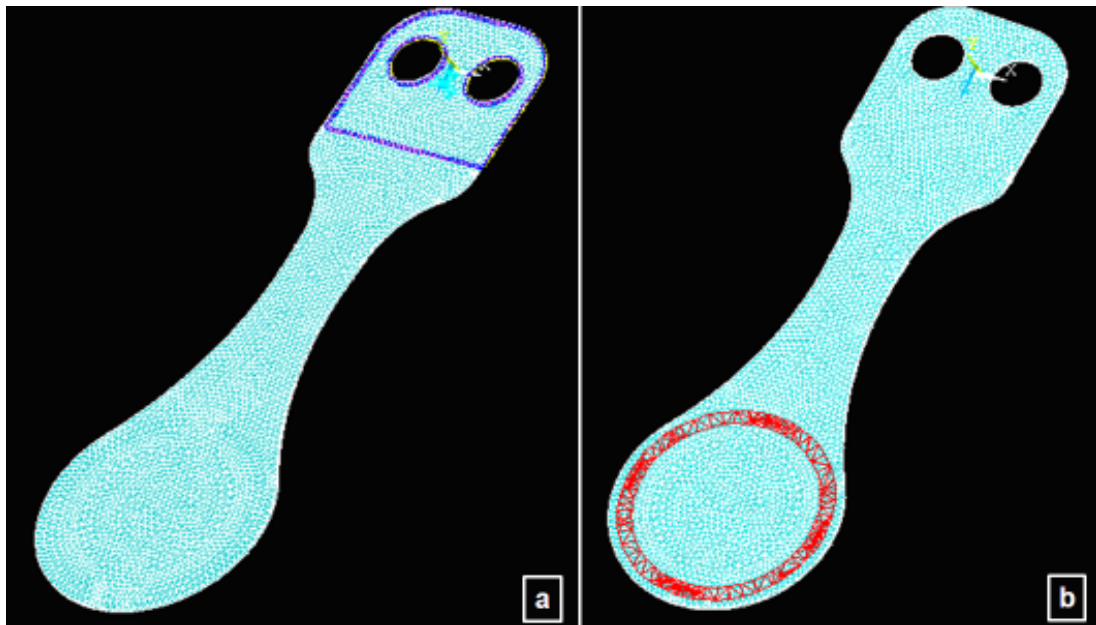


Figure 4.62. ANSYS (a) fixed support and (b) applied pressure region

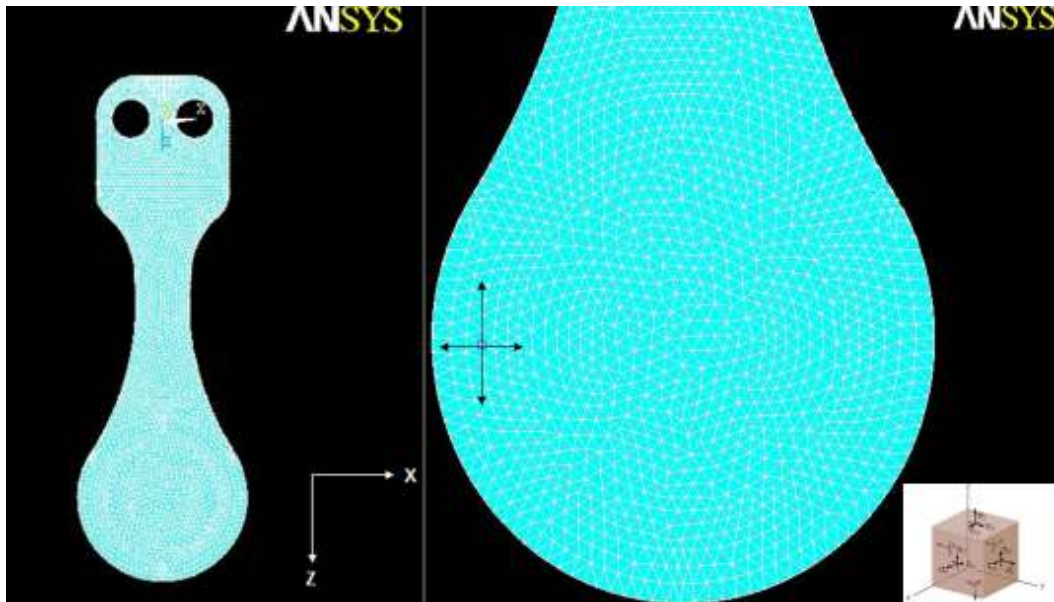


Figure 4.63. ANSYS analysis node selection

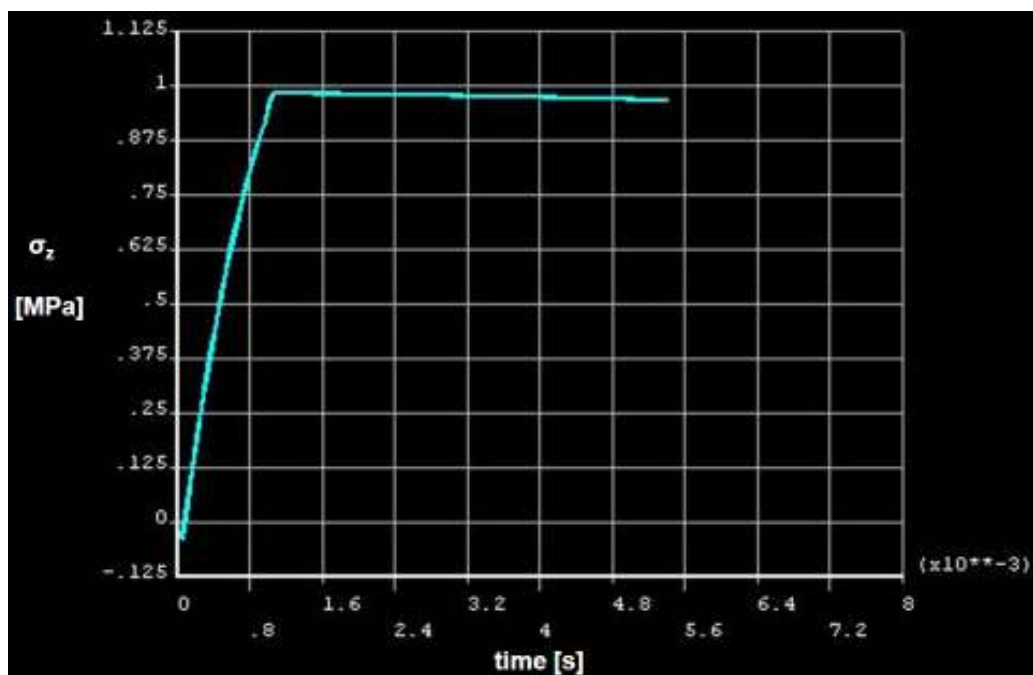


Figure 4.64. Stress along z-direction

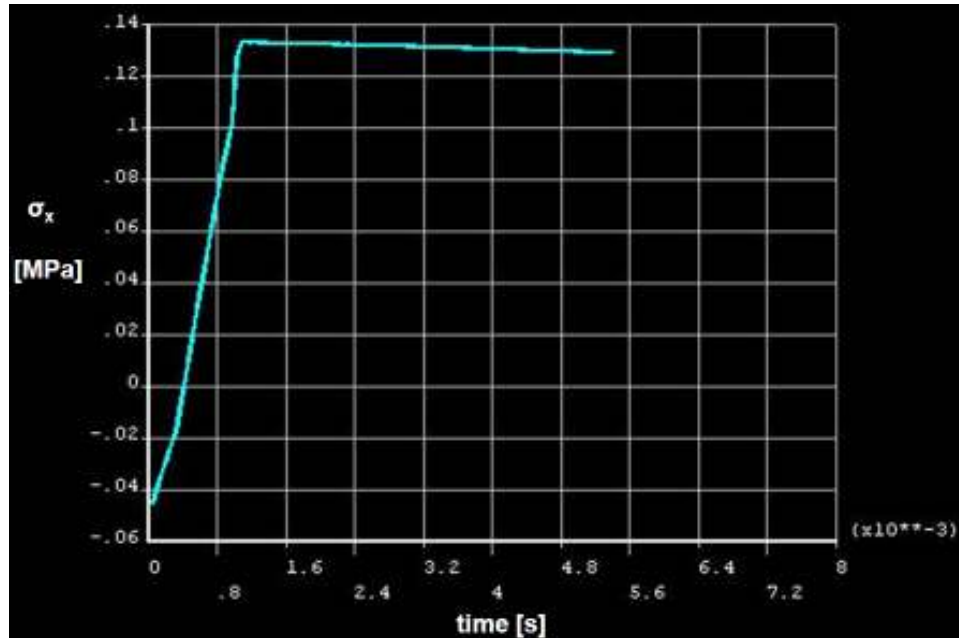


Figure 4.65. Stress along x-direction

#### 4.15. Finite Element Crack Propagation Modeling Analysis:

In compressor valve leaves when the crack initiated at the edge, the crack tends to propagate in the direction of the dominant stress wave formed during impacts. It is desired that the crack propagation rate is low and the crack occupies at the edge regions rather than travelling to the inner part of the impact region that cause a serious damage. For that reason, a finite element crack propagation modeling analysis in ANSYS was described. The model procedure was based on the duplicating nodes along crack path and separation of the nodes as the crack propagates (Figure 4.66). The meshed impact region of the valve leaf can be seen from Figure 4.67 (a) and the model application region with mesh refinement was shown in Figure 4.67 (b). In simulation, the crack path was pre-defined and the nodes along the crack path were duplicated for modeling. In figure, it can be seen that

tensile loads were applied to the nodes along the crack propagation path in the mesh refined region. The nodes along the crack path were separated as the formed directional stress at the nodes was higher than the defined threshold stress. The crack propagation provided in the pre-defined crack path and the Von-Mises stress at nodes was presented in Figure 4.68 as an order of magnitude. The crack propagation model approach should be enhanced by failure criteria and the crack path should be determined by that failure criteria.

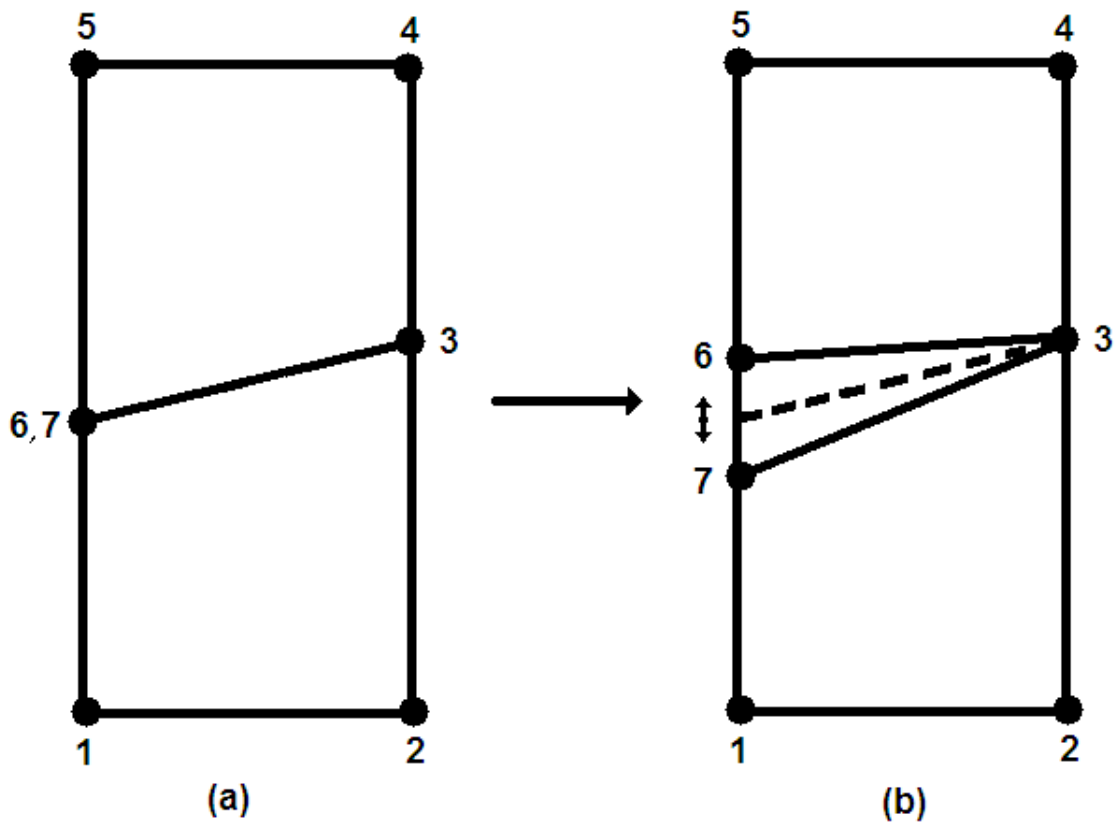


Figure 4.66. ANSYS crack propagation analysis procedure

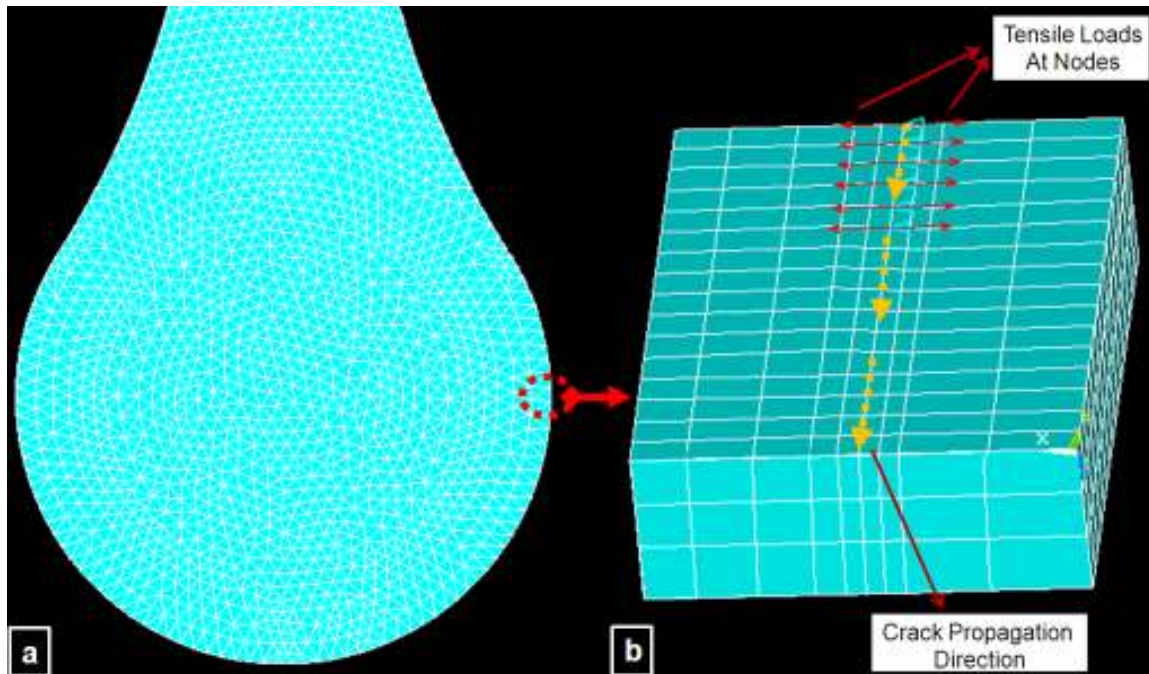


Figure 4.67. ANSYS (a) meshing and (b) mesh refinement of selected region

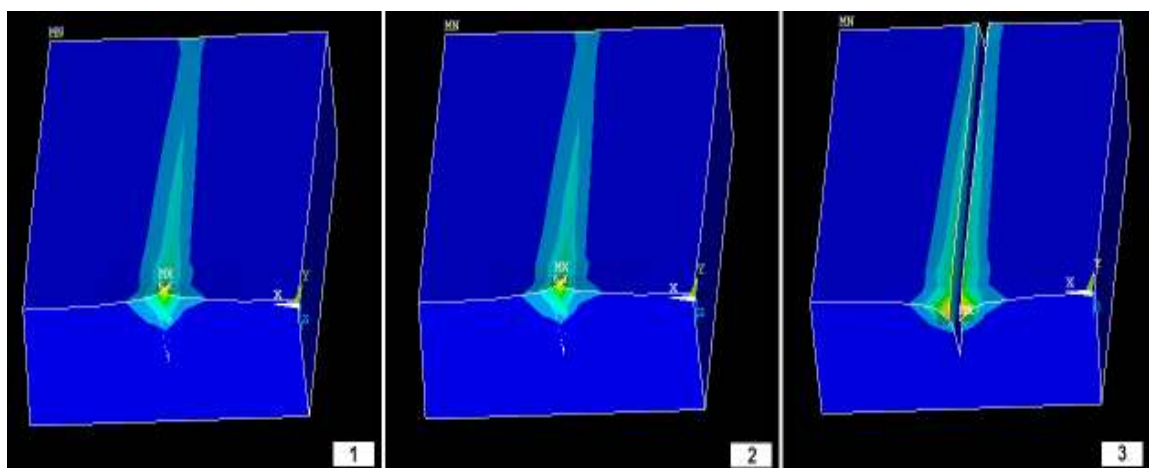


Figure 4.68. Crack propagation steps along the pre-defined crack path

### Chapter 5: Conclusions

- (1) The thesis introduced a new automated impact fatigue test apparatus which was designed and fabricated in order to enable extensive impact fatigue tests. The errors caused by operators were avoided by the automation system and provided reliable results. Impact fatigue tests were performed on carbon strip steel.
- (2) The form of the response curve exhibits a level off regime at  $10^7$  cycles and carbon strip steel had an endurance limit when subjected to impact fatigue loading when the real working behavior in compressor was simulated. As the impact velocity increased, the impact fatigue life of the specimens was decreased significantly.
- (3) As a surface treatment, tumbling duration was investigated on the impact fatigue life. The edge radius of carbon steel was almost leveled after T tumbling duration level and stainless steel leveled after  $5T/4$  level operation tumbling operation. Long enough tumbling operation enhances impact fatigue properties by smoothing the sharp edges of the valve leaves.
- (4) Asymmetrical impacts caused by corruptions of compressor proper working conditions and other component design effects, reduces the impact fatigue life of the valve leaf. It was observed that the cracks initiated at the region where air pulses were applied on.
- (5) The tests showed that there was a considerably difference in impact fatigue strength between carbon steel and two martensitic stainless grades. The difference between the

lifetimes of the two martensitic grades was decreased while the impact fatigue velocity was increased.

(6) The thesis introduced a reliable temperature control cabin which provides testing impact fatigue at various temperatures. Temperature effect on the impact fatigue life tests were performed on carbon strip steel. It was found that the impact fatigue life of the valve leaves was slightly decreased as the testing temperature was increased; however the tests showed that impact fatigue life at T1 temperature level and room temperature were almost same.

(7) Fractographic observations were performed on the suction valve leaves supplied from Arcelik A.S. which experienced failure in the compressors. It can be concluded that, a catastrophic failure was observed between the edge of the valve leaf and the interaction point of wear marks on the valve leaf and fracture edge. In addition in the light of the beach marks direction on the fracture surface, the crack propagated from edge to the inner part of the valve leaf.

(8) In the thesis, microscopic observations for crack initiation and propagation results were provided. When a crack occurred at the edge of the valve leaves, the crack propagation direction and forming new crack initiations by branching were a result of stress waves due to the geometrical shape and variations in the assembly of valve leaf caused by manufacturing tolerances.

(9) Microstructural observations showed that the regions around the crack origins, along crack paths and in branching points had same microstructure as the original microstructure of the valve leaf.

(10) Throughout the experiments, with the aid of stroboscopic displays and CCD camera it can be concluded that cracks initiated at the edge of the valve leaves and sometimes there were more than one crack origins at the edges. The origins could collapse each other or grew independently until one of them dominated over the other. In some situations the crack propagated to the tip direction, subsequently formed a fracture, after that the propagation mechanism reversed and propagated to the root direction. The travel of the crack, after nucleation at the edge, is strongly depended on the valve leaf geometry and occupation of the valve leaf and plate. Since crack origins were died away because of the inversely propagation mechanism, the final fracture contour misled the observers for diagnosing the failure of the valve leaves which experienced in the compressors.

(11) SEM observations showed that the crack propagated after a small part was broken away from the edge after the crack initiated. The crack nucleated at the impact area and some parts could be torn away from surfaces while the crack was travelling on the body.

(12) The combination of the three design and manufacturing tolerance values (valve leaf - valve plate - close fit) resulted in inhomogeneous occupation of the valve leaf on the valve plate. The inhomogeneous occupation of the valve leaf causes slightly asymmetrical impact velocity profile because of the different impact region generation of the valve leaf. Consequently the valve damage mechanism and the impact regions were changing due to the various occupations.

(13) Mode-I and Mode-III crack propagation was encountered during high speed camera observations. The mixed mode crack growth on the valve leaf was created by the impacts.

(14) Before and after manufacturing process, improper handling of the valve leaves result in mechanical surface defects. The defects, which were stress raisers on the valve surface, were critical to fatigue crack initiation and failure.

(15) In reciprocating test system, synchronous airflow pulses on the valve leaf were provided by the solenoid valves. Although the system was actuated at the highest level, any failure was not observed at  $5 \times 10^8$  cycles. Any failure occurred on the exhaust valves does not caused by the valve leaf and plate couple geometry, on the other hand external vibrations of the other components or disturbances caused by various working conditions of compressor could result in a failure.

---

### Bibliography

- [1] Xin R, Hatzikazakis P. Reciprocating Compressor Performance Simulation. International Compressor Engineering Conference at Purdue University, Vol. V-I, 2000, pp. 1-9.
- [2] Oguz E. An Investigation on the Effect of Transient Heat Transfer on the Performance of Hermetic Refrigerant Compressors. Mechanical Engineering Department, Istanbul Technical University 2006; Doctoral Thesis.
- [3] Tanaka T, Nakayama H. Studies on Impact Fatigue, Part I. Bulletin of the JSME 1973;16(102):1814-1828.
- [4] Tanaka T, Nakayama H. Studies on Impact Fatigue, Part II. Bulletin of the JSME 1974;17(113):1379-1388.
- [5] Tanaka T, Nakayama H. Studies on Impact Fatigue, Part III. Bulletin of the JSME 1975;18(126):1365-1374.
- [6] Iguchi H, Tanaka K, Taira S. Failure Mechanisms in Impact Fatigue of Metals. Fatigue & Fracture of Engineering Materials & Structures 1979;2(2):165-176.
- [7] Taira S, Iguchi H, Tanaka K. Development of impact fatigue testing machine and some test results. Proc 22nd Japan Cong Mater Res, Vol. 22, 1979, pp. 181-186.
- [8] Futakawa M, Kikuchik K, Muto Y, Shibata H. Impact bending fatigue and impact response behavior of a nuclear-grade graphite beam. Carbon 1990;28(1):149-154.
- [9] Dumitru I, Marsavina L, Faur N. Experimental study of torsional impact fatigue of shafts. Journal of Sound and Vibration 2007;308(3-5):479-488.
- [10] Wellinger K, Breckel H. Kenngrößen und Verschleiss beim Stoss metallischer Werkstoffe. Wear 1969;13(4-5):257-281.
- [11] Bayer RG, Engel PA, Sirico JL. Impact wear testing machine. Wear 1972;19(3):343-354.

- 
- [12] Sheldon GL, Kanhere A. An investigation of impingement erosion using single particles. *Wear* 1972;21(1):195-209.
- [13] Lapidés L, Levy A. The halo effect in jet impingement solid particle erosion testing of ductile metals. *Wear* 1980;58(2):301-311.
- [14] Cousens AK, Hutchings IM. A critical study of the erosion of an aluminium alloy by solid spherical particles at normal impingement. *Wear* 1983;88(3):335-348.
- [15] Studman CJ, Field JE. A repeated impact testing machine. *Wear* 1977;41(2):373-381.
- [16] Rice SL. Reciprocating impact wear testing apparatus. *Wear* 1977;45(1):85-95.
- [17] Rickerby DG, MacMillan NH. The erosion of aluminum by solid particle impingement at normal incidence. *Wear* 1980;60(2):369-382.
- [18] Mahoney NJ, Grieve RJ, Ellis T. A simple experimental method for studying the impact wear of materials. *Wear* 1984;98:79-87.
- [19] Svenzon M. Impact fatigue of valve steel. Uppsala, Sweden: Acta Universitatis Upsaliensis, 1976.
- [20] Soedel W. Design and mechanics of compressor valves. Office of Publications, Purdue University, 1984.
- [21] Glaeser WA. Failure mechanisms of reed valves in refrigeration compressors. *Wear* 1999;225-229(Part 2):918 - 924.
- [22] Libralato M, Contarini A. Impact Fatigue on suction valve reed: new experimental approach. In: International Compressor Engineering Conference at Purdue West Lafayette, USA, 2004.
- [23] Tekeli S. Enhancement of fatigue strength of SAE 9245 steel by shot peening. *Materials Letters* 2002;57:604-608.
- [24] Sonsino CM. Fatigue design of structural ceramic parts by the example of automotive intake and exhaust valves. *International Journal of Fatigue* 2003;25:107-116.

- [25] Sobiecki JR, Mankowski, P., Patejuk, A. Improving the performance properties of valve martensitic steel by glow discharge assisted nitriding. *Vacuum: Surface Engineering, Surface Instrumentation & Vacuum Technology* 2004;76:57-61.
- [26] Yu ZW, Xu XL. Failure analysis and metallurgical investigation of diesel engine exhaust valves. *Engineering Failure Analysis* 2006;13(4):673-682.
- [27] Reed J, Dadd M, Bailey P, Petach M, Raab J. Development of a valved linear compressor for a satellite borne J-T cryocooler. *Cryogenics* 2005;45(7):496-500.
- [28] Chai G, Zetterholm G, Walden B. Flapper valve steels with high performance. In: *International Compressor Engineering Conference at Purdue West Lafayette, USA, 2004*.
- [29] Johnson AA, Storey RJ. The impact fatigue properties of iron and steel. *Journal of Sound and Vibration* 2007;308(3-5):458-466.
- [30] Jin SH, Hwang GW, Cho KZ. Analysis of the 3-D Stress Wave in a Plate under Impact Load by Finite Element Method *International Journal of the Korean Society of Precision Engineering* 2001;2(2):5-9.
- [31] de los Santos MA, Cardona S, Sánchez-Reyes J. A Global Simulation Model for Hermetic Reciprocating Compressors. *Journal of Vibration and Acoustics* 1991;113:395-400.
- [32] Kwon YK, Lee GH, Lee TJ. The design of compressor valve to consider the flexibility and reliability. In: *International Compressor Engineering Conference at Purdue, 2004*, pp. 1-5.
- [33] Struers AS. *Metallography and Materials Testing*. In: *Technical Report, 2009*.
- [34] Bramfitt BL, Benschoter AO. *Metallographer's guide: Practice and Procedures of Iron and Steel*. 2002.
- [35] Wang S, Li Y, Yao M, Wang R. Compressive residual stress introduced by shot peening. *Journal of Materials Processing Technology* 1998;73(1-3):64-73.
- [36] Wang S, Li Y, Yao M, Wang R. Fatigue limits of shot-peened metals. *Journal of Materials Processing Technology* 1998;73(1-3):57-63.

**VITA**

Abdullah Can Altunlu was born in Istanbul, Turkey on August 31, 1985. He was received the B.S degree in Manufacturing Engineering in June 2007 from Istanbul Technical University, Istanbul, Turkey and the M.S. degree in Mechanical Engineering in June 2009 from Koc University, Istanbul, Turkey. Throughout the M.S. degree, research and teaching assistant duties were carried out. He was a member of Society of Manufacturing Engineering (SME) and Chamber of Mechanical Engineers, Turkey (TMMOB). He has been studying fatigue phenomenon specialized in investigation on the impact fatigue characteristics of compressor valve leaves; the project was supported by the Turkish Ministry of Industry and Commerce, and Arcelik A.S. Company.

Following M.Sc. studies he is going to pursue a Ph.D. degree in University of Twente, Netherlands.